Modulating antigen-specific humoral immunity with non-differentiating B cells

Ragan A. Pitner

A dissertation

submitted in partial fulfillment of the

requirements for the degree of

Doctor of Philosophy

University of Washington

2024

Reading Committee:

David J. Rawlings, Chair

Richard G. James

Andrew Oberst

Program Authorized to Offer Degree:

Immunology

University of Washington

Abstract

Modulating antigen-specific humoral immunity with non-differentiating B cells

Ragan A. Pitner

Chair of the Supervisory Committee:
David J. Rawlings
Department of Immunology

Antibody-derived inhibitors pose an ongoing challenge to the treatment of patients with inherited protein deficiency disorders, limiting the efficacy of both protein replacement therapy and corrective gene therapy. Beyond their central role as producers of serum antibody, B cells also exhibit many unique properties that could be exploited in cell therapy applications, notably including antigen-specific recognition and the linked capacity for antigen presentation. Here we employed CRISPR/Cas9 to demonstrate that *ex vivo* antigen-primed Blimp1-knockout "decoy" B cells, incapable of differentiation into plasma cells, participated in and downregulated host antigen-specific humoral responses after adoptive transfer. Following *ex vivo* antigen pulse, adoptively transferred high affinity antigen-specific decoy B cells were diverted into germinal centers *en masse*, thereby reducing participation by endogenous antigen-specific B cells in T-dependent humoral responses and suppressing both cognate and linked antigen-specific IgG following immunization with conjugated antigen. This effect was dose-dependent and, importantly, did not impact concurrent unrelated antibody responses. We demonstrated the therapeutic potential of this approach by treating factor VIII (FVIII)-knockout mice with antigen-pulsed decoy B cells

prior to immunization with a FVIII conjugate protein, thereby blunting the production of serum FVIII-specific IgG by an order of magnitude as well as reducing the proportion of animals exhibiting functional FVIII inhibition by 6-fold. Finally, we demonstrated that these Blimp1-deficient decoy B cells can be simultaneously gene-edited to enable constitutive secretion of the regulatory cytokine IL-10. Together, these results suggest that it will be possible to generate engineered regulatory B cells capable of modulating the activation and differentiation of antigen-specific CD4 T cells.

TABLE OF CONTENTS

LIST OF FIGURES

LIST OF TABLES

ACKNOWLEDGMENTS

I am incredibly grateful to my mentor Dr. David Rawlings for the guidance of his immense knowledge and experience, for encouraging my scientific creativity, for his patience when I was stubborn, for his reassurance when I was frustrated, and for his trust as I navigated a challenging and at times confounding project. I was fortunate to find a mentor who valued my independence and shared my excitement for immune engineering.

I thank Dr. Richard James for being a valuable secondary mentor and not only tolerating endless invasions of his office to discuss experimental design and exciting new results but also for engaging in reckless scientific speculation and sharing his bad NBA opinions.

I thank Drs. Jane Buckner, Brian Iritani, and Andrew Oberst for their uninterrupted support as I pursued my doctorate. I'm fortunate to have had such great scientists in my corner to provide rigorous and honest feedback with kindness. Without their help I would never have been able to publish the findings discussed herein.

I also thank current and former members of the Rawlings Lab that I have worked with during my training. Thanks to Kerri Thomas, Warren Anderson, Fahd Al-Quresah, Emma Suchland, Kelsey Roe, and Yuchi Honaker for helping me during the beginning of my graduate career. I would like to thank Noelle Dahl for always making time to assist with mouse experiments despite it delaying her plans more than once. Thank you to Socheath Khim and Anna Zielinska-Kwiatkowska for mouse colony maintenance and to Yu Chen for his early assistance with size exclusion chromatography. I thank Peter Cook for his assistance designing HDR editing templates. I have enormous gratitude to Jennifer Haddock for always coming through when I needed time

with David, Yumei Song for pushing through countless rushed orders, and Andrea Repele for expertly containing the madness inherent in a large lab.

Furthermore, I would like to thank our collaborators. Thank you to Drs. Michael Gerner and Jaime Chao for their crucial work putting together the imaging data for this project. I am also grateful to Drs. Carol Miao, Meng-Ni Fan, and Xiaohe Cai for providing hemophilic mice as well as their assistance designing and performing experiments. My gratitude extends to Dr. Clint Spiegel and Nathan Avery for providing the FVIII C2 domain used in this study.

I thank Daisuke Kitamura for sharing his 40LB cell line, Greg Hermanson for his advice generating the HEL-C2 conjugate, the CIIT Flow Cytometry Core for maintaining essential equipment, and the SCRI Office of Animal Care for technical support.

On a personal note, I am blessed to have the unending support of my fiancée, Hope Grandon. Pursuing a doctorate is the hardest thing I have ever done and the daily joy you bring my life has made the stress of the past few years much more bearable. Thank you for reminding me to breathe and to drop my shoulders from my ears. I love you and cannot wait to spend the rest of my life with you.

This work was supported in part by the Children's Guild Association Endowed Chair in Pediatric Immunology (to David Rawlings), the Hansen Investigator in Pediatric Innovation Endowment (to David Rawlings), the National Center for Advancing Translational Sciences of the National Institutes of Health under award number TL1TR002318 (to Ragan Pitner), and the NIH T32AR007108 (to Jaime Chao). Thank you all, as this work would not have been possible without your support.

Finally, I thank the mice whose lives made this work possible. I do not take the privilege lightly.

DEDICATION

This work is dedicated to my parents, Dianne Irene Ramey Pitner and John Ragan Pitner.

Mom, your gentle determination and sheer grit despite limited mobility and constant physical pain has inspired me not only to search for solutions that might someday alleviate the suffering of those who share your illness, but also to put kindness first and be too damn stubborn to let any disappointments kill me.

Dad, your unfaltering devotion to us both is an example I hope that I can honor in my own life. Your integrity is the lodestar by which I set my moral compass. Thank you for both pushing and allowing me to pursue my dreams from a young age, even when I did not understand.

Above all, I am grateful to have had two people love me as completely and unconditionally as you both have.

Chapter 1: Introduction

The protection afforded by antibodies is a cornerstone of adaptive immunity and is essential to control infections by numerous pathogens. Central to the efficacy of antibody-mediated protection is the vast potential for binding specificities conferred by the combination of V(D)J recombination and somatic hypermutation[1] as well as the ability of antibody-producing plasma cells to provide long-term protection by secreting antibody for decades.[2] However, these same features that make antibodies so valuable for protection from infectious disease can also generate hurdles for the treatment of chronic illnesses, as anti-drug antibodies can be detrimental to the efficacy of multiple biological therapies. Inhibitors of recombinant interferon β are known to abrogate the therapeutic efficacy in the treatment of multiple sclerosis.[3,4] Similar antibody-derived inhibition has been severe enough to cause the termination of a clinical trial for a promising checkpoint inhibitor.[5] This is especially problematic in the treatment of protein deficiencies borne out of genetic disorders, as the adaptive immune response cannot enforce central tolerance to a protein that is accurately recognized as non-self.

One such example is hemophilia A, a monogenic disorder in which patients have a mutation in the gene encoding factor VIII (FVIII), an important member of the blood clotting cascade.[6] To date, the only FDA-approved approaches for treating hemophilia A involve either provision of recombinant FVIII as an injected therapy or, in severe cases, gene therapy utilizing an adeno-associated virus (AAV) to introduce a functional FVIII secretion cassette into the patient.[7] A frequent problem limiting the efficacy of either approach is the generation of inhibiting antibodies. Since individuals with congenital hemophilia A do not express native FVIII, they also lack central immune tolerance for the protein and, in about 30% of cases,[8] repeated long-term

treatment with recombinant FVIII results in the generation of FVIII-specific antibodies that inhibit the drug. Gene therapy approaches that leverage viral vectors do not entirely avoid this problem; although liver-targeted gene therapy may prevent or reduce the generation of FVIII-specific inhibitors,[9] patients will certainly generate neutralizing antibodies specific for the viral vectors used to deliver the corrected gene.[10] This means that most gene therapy approaches that leverage *in vivo* delivery of viral vectors are "one-shot" options due to antibody neutralization. Therefore, an antigen-specific prophylactic therapy that could prevent the generation of drug inhibitors without requiring broader immune suppression would have significant value.

1.1 Antibody-Derived Drug Inhibitors

B cell receptor (BCR) V(D)J recombination during B cell development and somatic hypermutation (SHM) during T-dependent antibody responses yield up to an estimated 1 quintillion different possible antibody sequences,[1] meaning that it is theoretically possible for the humoral immune system to generate an antibody capable of binding to any macromolecule with at least moderate affinity. In adaptive immune responses however, the breadth of permissible antibody specificities is circumscribed by mechanisms of central and peripheral tolerance that lead to deletion or enforced anergy of B cells encoding BCRs specific for self-antigen.[11–13] While such vast potential is crucial for host defense against pathogenic infection, it can become a hurdle for patients requiring therapy with macromolecules that are accurately recognized as non-self.

FVIII is an essential member of the coagulation cascade and is absent or significantly mutated in patients with hemophilia A.[14] For most patients, replacement therapy with recombinant FVIII is an effective prophylactic for preventing dangerous bleeding events. In patients with major nonsense mutations or deletions of FVIII, therapeutic FVIII is recognized as non-self and 20-40%

generate serum antibody specific for critical regions of FVIII that greatly reduce its efficacy.[8] Presently, the only accepted clinical method to attempt to eliminate inhibitors is immune tolerance induction (ITI), the basic premise of which is long-term treatment with high doses of recombinant FVIII until serum inhibitors are no longer detectable by clotting assays.[15–17] Although ITI is effective in generating tolerance approximately 70% of the time,[18] it is expensive, time-consuming, and still leaves 10-20% of FVIII-treated hemophilia A patients with incurable FVIII inhibitors. Such patients must rely on some combination of bypassing agents such as recombinant activated factor VII, activated prothrombin complex concentrate, and emicizumab, a bispecific antibody that bypasses FVIII by binding to factors IX and X to mediate clotting.[19] These limit adverse bleeding events, but are limited by poor half-life and a potential for thrombotic events and thrombotic microangiopathy.[20]

Gene therapy is a promising alternative approach to protein deficiencies such as hemophilia A. Delivery of FVIII expression cassettes to the liver using AAV is a particularly intriguing approach, as the low turnover of hepatocytes in healthy liver tissue limits the dilution of episomal DNA and access to the circulatory system supports systemic distribution of secreted FVIII. [21,22] There is also evidence that FVIII secreted from an immune privileged site such as the liver may not only induce tolerance,[23] but it also may eradicate pre-existing inhibitors.[24] Unfortunately, neutralizing antibodies specific for the AAV vectors used to deliver corrected genes are a major obstacle to wider application of gene therapy. The seroprevalence of pre-existing antibody specific for AAV serotypes investigated for the transfer of repaired genes varies from 6% for AAV5 in the United Kingdom to 95% for AAV2 in South Korea[25,26] and the high degree of sequence conservation between AAV serotypes results in significant cross-neutralization.[27,28] Furthermore, the humoral immune system has evolved to be acutely responsive to viral infection and so repeat

administration of AAV is greatly limited by the generation of neutralizing antibodies following primary exposure. Although some AAV-mediated gene therapies have demonstrated continued efficacy 15 years after treatment,[29] acquired inhibitors prevent re-administration and so are problematic in cases where a patient first receives gene therapy early in life[30] or where repeat administration of a low dose of vector is needed to limit immunogenicity of the gene product or toxicity of the viral vector.[31,32] Coadministration of AAV with immunosuppressive drugs[33] such as rapamycin[34–38] and rituximab[34–36,39] has shown some promise preventing the generation of AAV-targeted antibodies, and one approach using rapamycin-loaded nanoparticles even demonstrated potential tolerance that allowed repeat administration of mice with AAV8.[40] There will, however, always be risks associated with even transient nonspecific immune suppression and there presently exists no truly antigen-specific therapy for preventing the generation of antibody-derived drug inhibitors. Rather than transiently dampening the adaptive immune response in general, we aimed to exploit germinal center (GC) biology to blunt T-dependent antibody responses in an antigen-specific manner.

1.2 T-Dependent Antibody Responses

Antibodies arises from both T-independent and T-dependent pathways. Although T-independent B cell responses can yield long-term humoral protection,[41] most of these responses are low-affinity or polyreactive.[42] There is some evidence of affinity maturation occurring in extrafollicular responses[43] but the consensus is that a majority of long-lived high-affinity antibody responses derive from long-lived plasma cells (LLPCs) that emerge from T-dependent GC responses.[44] As these antibodies are those most likely to cause problematic long-term inhibition of protein replacement and gene therapies, we focus here on antibody responses arising from pre-GC

plasmablasts (PBs) and GC-derived plasma cells (PCs), collectively referred to as antibody-secreting cells (ASCs).

1.2.1 GC Initiation and Dynamics

Initiation of a GC begins when antigen-specific $CD4^+$ helper T cells are first activated by antigen presenting cells (APCs), primarily dendritic cells (DCs). This occurs when their T cell receptor binds to cognate antigen peptide presented on major histocompatibility complex class II (MHC-II) on the surface of the DC in combination with CD28 co-stimulation. These signals in conjunction with DC-derived IL-6 direct the activated T cell to an intermediate pre-T follicular helper (Tfh) phenotype.[45] This results in expression of the transcription factor B cell lymphoma 6 (BCL6), followed by downregulation of CC-chemokine receptor 7 (CCR7) in favor of C-X-C chemokine receptor type 5 (CXCR5), drawing the activated pre-Tfh out of the T cell zone and migration to the T-B border. Antigen-specific B cells, in turn, also migrate to the T-B border by upregulating CCR7 following antigen stimulation following engagement of the BCR. These B cells present antigen on MHC-II to cognate pre-Tfh cells, maintaining stable, motile conjugates for up to hours at a time.[46,47] CD40 stimulation from cognate pre-Tfh drives Epstein–Barr virus-induced G-protein coupled receptor 2 (EBI2) expression in the interacting B cells,[48] directing migration of those conjugates along the T-B border, into the interfollicular region, and nearer to the follicles. Following this extended conjugation, activated B cells proliferate, disengage, and 1) differentiate into pre-GC memory B cells (MBCs),[49] 2) differentiate into short-lived pre-GC PBs,[50] or 3) upregulate their expression of BCL6 and migrate into the follicle where they seed a GC.

Reciprocally, B cells provide signals to their cognate pre-Tfh which appear to complete their differentiation into effector Tfh, driving increased expression of CXCR5 and subsequent

recruitment into the follicle.[45] Once in the follicle, ongoing inducible costimulatory (ICOS) stimulation from ICOS ligand (ICOSL) on cognate and non-cognate B cells drives increased CXCR5 and decreased CCR7, which is thought to allow fully differentiated Tfh to overcome suppressive signals that keep other activated T cells out of the follicle.[51] A subset of Tfh then downregulates EBI2 in favor of even greater CXCR5, driving them deeper into the follicle where they will serve as GC Tfh.[45,52] Shortly after, GC precursor B cells will have moved towards the center of the B cell follicle and formed an early GC.[52] Here they rapidly divide over the next 2-3 days until a fully established GC has formed, polarized into a light zone (LZ) and dark zone (DZ).[52] While proliferating, GC B cells within the DZ undergo SHM that diversify BCR affinity before trafficking into the LZ, where B cells compete for access to antigen presented on follicular dendritic cells (FDCs). Those B cells expressing higher-affinity BCR outcompete B cells expressing lower-affinity BCR to capture and present more antigen to GC Tfh also localized to the LZ. These B cells then receive differing degrees of CD40 stimulation and cytokine instruction signals that guide them to alternative fates, including 1) GC exit as precursor MBCs, 2) GC exit as PCs,[52] or 3) recirculation into the DZ to undergo additional proliferation and rounds of SHM.

1.2.2 Affinity Dependency of B Cell Selection and Differentiation

Relative BCR affinity for cognate antigen appears to be a dominant driver of B cell fate in T-dependent antibody responses. Generally, the highest-affinity B cells preferentially differentiate into early PBs, those with intermediate affinity preferentially enter GCs, and those with relatively low affinity preferentially differentiate into pre-GC MBCs.[53] Initially this was believed to be due to direct competition for antigen depleting and sequestering antigen, thereby depriving lower-affinity B cells of necessary survival and differentiation signals triggered by BCR ligation.[52,54]

This was supported by observations that dampening initial BCR affinity by discretely mutating antigen selectively depleted the pre-GC PB response while leaving the GC response intact.[50] Subsequent work utilizing antigen conjugated to antibody that binds DEC-205, a cell-surface lectin expressed on GC B cells[55] that delivers antigen to antigen processing compartments,[56] demonstrated that competition for help from $CD4^+$ T cells is the limiting factor guiding selection of B cells for both entry into[57] and selection in[55] GCs. Since higher BCR affinity allows for greater endocytosis and presentation of antigen, BCR affinity and access to T cell help are highly correlated.

A later study utilized a limiting dilution approach to transfer single naïve antigen-specific B cell clones and track their fates 7 days after immunization.[58] In mice receiving polyclonal B cells containing at most one antigen-specific clone, roughly half of these generated only one B cell subset (PB, GC B cells, MBCs, or activated precursors (APs)). MBC clones that also generated PBs bound roughly twice as much antigen as those clones that only generated MBCs, suggesting that the tendency to form early PBs was correlated with increased affinity. This was supported in dilution experiments with transgenic B cell lines of defined affinity as well. 58% of hen egg-lysozyme (HEL)-specific single MD4 B cells produced only pre-GC PBs and GC B cells following stimulation with HEL whereas only 12.5% of MD4 B cells repeated this pattern when stimulated with duck egg lysozyme (DEL), for which MD4 B cells have only limited affinity. HEL-stimulated clones also generated more PBs and fewer MBCs than DEL-stimulated clones. Another study[59] utilized single-cell transcriptomics and fate mapping to demonstrate that immunization yielded antigen-specific APs that generate a short wave of PBs followed a day later by the generation of GC B cells, while the majority of APs exited the cell cycle to become pre-GC MBCs. This pre-GC wave of PBs could be augmented at the expense of AP and GC B cell subsets with a secondary

immunization 3.5 days later. This suggests that differential access to limited antigen signaling over time, exacerbated by differential affinity, is a major driving force in the trifurcation of antigen-specific B cells into pre-GC PBs, pre-GC MBCs, or GC B cells following immunization.[59]

The general mechanics of B cell selection within GCs has been understood for some time.[60] When a B cell has received sufficient activation to enter a GC, it undergoes rapid proliferation in the DZ. This proliferation allows cytoplasmic activation-induced cytidine deaminase (AID) to access genomic DNA when the nuclear membrane breaks down during early mitosis, resulting in random mutations to the BCR.[61] B cells that undergo damaging mutations preventing BCR replacement apoptose in the DZ while those that retain a mutated BCR traffic into the LZ[62] where they compete for access to antigen presented on FDCs.[63,64] This competition is the crux of the affinity maturation that occurs in GCs, as B cells with higher-affinity BCRs receive more positive signaling through their BCR and endocytose more antigen for presentation to antigen-specific Tfh in the LZ. While access to T cell help via CD40 signaling appears to be the primary checkpoint driving B cell participation in GCs,[55] BCR crosslinking upon antigen acquisition appears to augment B cell selection when T cell help is subsaturating.[65] Similar to the extrafollicular pre-GC response, the fate of B cells participating in GCs may be linked with antigen affinity. In models utilizing high-affinity transgenic B cells, PCs emerging from GCs tended to be enriched for affinity-enhancing mutations at timepoints when these mutations were rare in GC B cells.[66,67] Loss of one copy of CD40 had no impact on B cell participation in GCs, although it inhibited their export from GCs as PCs.[68] This correlation is not without counter-evidence; another study utilizing transgenic B cells encoding a low-affinity germline-encoded precursor to a high-affinity BCR found no differences in affinity-enhancing mutations between GC B cells fated to return to the DZ and those that have initiated PC differentiation.[69] Both DZ- and PC-fated B cells, however, had

increased affinity-enhancing mutations relative to B cells that have initiated MBC differentiation. Furthermore, differentiation into MBCs appears to require a cessation of proliferation and BCL6 expression,[67,70] factors that are driven by access to T cell help and are necessary for either ongoing participation in the GC or differentiation into PCs.

In summary, in T-dependent humoral responses, relative low BCR affinity (and therefore limited T cell help) appears to favor B cell differentiation into MBCs, relative intermediate affinity favors entry into GCs, and relative high affinity favors differentiation into antibody-secreting PBs and PCs (Fig 1.1). Consequently, the presence of very high-affinity B cells can impact GC entry and differentiation by lower-affinity B cells following immunization. In one key study, Schwickert et al. showed that in the presence of high-affinity transgenic B cells, lower-affinity B cells received reduced activation and proliferation signals and that both pre-GC PB differentiation and GC entry were greatly reduced.[57] This at least partially explains the results from an earlier study[71] that demonstrated that the adoptive transfer of 10^6 high-affinity nitrophenyl (NP)-specific B cells greatly reduced both the amount and affinity of NP-specific antibody produced by host B cells following immunization with NP antigen. Because of both their affinity and their number, the transferred cells presumably endocytosed and presented more antigen, thereby acquiring preferential access to limiting help from activated T cells and reducing the efficiency of differentiation by lower-affinity endogenous B cells. Total NP-specific serum antibody, however, remained unchanged, since the transferred high-affinity B cells leveraged the superior access to T cell help to differentiate into ASCs and secrete their own NP-specific antibody. If it were possible to leverage the ability of transferred high affinity B cells to impair lower-affinity host B cell access to differentiation signals while preventing ASC differentiation of those transferred B cells, it may be possible to specifically blunt total production of antibody with that specificity.

1.3 Transcriptional Antagonism of GC and ASC Differentiation

In T-dependent GC responses, both GC recycling and ASC differentiation require simultaneous signals from antigen-engaged BCR and CD40 engaged with CD40 ligand (CD40L) on Tfh[70] (Fig. 1.2). Tfh-secreted IL-4 and IL-21 are also important *in vivo*, though less is understood as to how their balance and timing differentially impact GC and ASC fates. Naïve B cells are activated by BCR ligation and CD40 signaling, both of which drive the phosphatidylinositol 3-kinase/protein kinase B (PI3K/Akt) pathway and the nuclear factor kappa-light-chain-enhancer of activated B cells (NF-κB) transcription factor. Upon GC entry, BCR ligation ceases to induce NF-κB and CD40 signaling ceases to drive the PI3K/Akt pathway, disentangling activation of these signals and rendering GC B cells dependent on both BCR and CD40 ligation.[72] These collaborate to drive phosphorylation of ribosomal protein S6 (pS6) through mammalian target of rapamycin complex 1 (mTORC1) as well as expression of MYC.[73] pS6 supports the expression of forkhead box O1 (FOXO1)[73] and MYC drives activating enhancer protein 4 (AP4).[74] These transcription factors support the development of DZ GC B cells[75] and proliferation[74], respectively. BCL6, already highly expressed in GC B cells,[76,77] induces expression of BTB domain and CNC homology 2 (BACH2) which represses B lymphocyte-induced maturation protein 1 (Blimp1) expression.[78] Together, FOXO1, AP4, and BCL6 support ongoing B cell cycling in the GC.[70]

The PI3k/Akt pathways and NF-κB also collaborate to induce transient expression of the transcription factor interferon regulatory factor 4 (IRF4),[79,80] which further promotes expression of BCL6.[81] However, high and maintained levels of CD40 stimulation increases IRF4 expression both by direct means[80] and by repression of the ubiquitin ligase CBL, which targets IRF4 for degradation.[82] High levels of IRF4 suppress rather than promote expression of BCL6.[80] BCR

ligation also engages the tyrosine kinases SYK and LYN and the adaptor protein BLNK to engage the GTPase KRAS, activating the kinase ERK and repressing BCL6.[70] This combined suppression of BCL6 leads to an increase in Blimp1 expression that further represses BCL6.[83] Blimp1 in turn initiates the transcriptional program enabling ASC differentiation, which is marked by significantly reduced proliferation, the loss of antigen presenting capability due to the combined loss of MHC-II and surface BCR, and massive secretion of antibody.[84]

IRF4 and Blimp1 stand out as the most promising targets for ablation in a B cell to prevent ASC differentiation in the presence of strong BCR and CD40 ligation. IRF4 is essential not just for ASC differentiation, but also for initiating the GC program[81] as well as survival after differentiation;[85] Blimp1 expression, stimulated by IRF4, suppresses B cell-defining transcription factors to enable mature ASC differentiation[85,86] but is not known to be required for survival of any particular B cell state.[85] Previously published work demonstrated that although knockout of IRF4 prevented ASC differentiation, it also resulted in substantial defects in B cell proliferation such that over time, the $IRF4^{KO}$ cells were outcompeted in culture by $IRF4^{WT}$ cells.[87] Knockout of Blimp1, by comparison, appeared to prevent ASC differentiation without the same extreme loss of proliferative potential. Together, these factors imply that high-affinity Blimp1-deficient B cells may be able to compete favorably with low-affinity Blimp1-sufficient B cells for access to limiting T cell help in GCs.

1.4 Regulatory B Cells

There is increasing recognition that some B cells play an important role in suppressing immune responses and maintaining immunological tolerance through the secretion of regulatory cytokines such as interleukin-10 (IL-10) and transforming growth factor beta-1 (TGF-β1).[88,89]

These regulatory B cells (B_{Regs}) can limit T cell activity indirectly through other APCs,[90–93] but some of the induced tolerance appears to be antigen specific. Adoptively transferred B_{Regs} have been found to be protective in the murine multiple sclerosis model experimental autoimmune encephalomyelitis (EAE), but this protection disappears when the transferred B_{Regs} are MHC-II-deficient.[94] In another study, IL-10-producing B_{Regs} isolated from collagen-immunized mice were able to prevent collagen-induced arthritis but not ovalbumin (OVA)-dependent hypersensitivity upon adoptive transfer; *in vitro*, these B_{Regs} inhibited the differentiation of interferon-gamma (IFNγ)-producing $CD4^+$ T cells in the presence of irradiated APCs and collagen (but not OVA) antigen.[95] In humans, it was found that B_{Regs} isolated after but not prior to flu vaccination suppressed the *in vitro* proliferation of $CD8^+$ T cells in the presence of flu antigen.[96]

These antigen-specific effects make induced B_{Regs} a potentially attractive therapeutic option. However, there are presently multiple challenges to their application as an immune modulating therapy. B_{Regs} appear capable of arising from almost any B cell subset in response to toll-like receptor (TLR) signaling, cytokine signaling, CD40 ligation, and/or BCR activation during infection or autoimmune dysregulation.[89,97] This variability of origin means that a regulatory phenotype is likely not associated with any single gene expression pattern. Furthermore, no lineage-defining transcription factor has been defined and multiple experiments have found that the secretion of regulatory cytokines is transient.[98] Other investigations have shown that B_{Regs} frequently differentiate further into PCs,[99] thereby downregulating their expression of surface BCR and MHC-II and losing their ability to act as efficient APCs.[84] Thus, unlike T_{Regs}, natural B_{Regs} likely exist as an activation state rather than a permanent lineage. If existing gene editing technology can be optimized to induce constitutive secretion of regulatory cytokine while maintaining the antigen presentation capability of non-differentiated activated B cells, it may be

possible to precisely tolerize antigen-specific $CD4^+$ T cells with engineered regulatory B cells (eB_{Regs}).

1.5 Central Hypothesis: T-dependent humoral responses can be blunted with high-affinity non-differentiating "decoy" B cells

High-affinity B cells have a competitive advantage for acquiring, endocytosing, and presenting antigen relative to lower-affinity B cells following immunization, and differential access to early T cell help is known to result in a competitive advantage for both GC entry and PB differentiation.[57] When high-affinity antigen-specific B cells are delivered to naïve mice prior to immunization, this competition results in a large reduction in host-derived antigen-specific antibody.[71] However, this reduction is buttressed by antibody secreted by ASCs that differentiate from the transferred high-affinity B cells, resulting in no net change in total antigen-specific antibody circulating in the serum. Upon acquiring sufficient activation signals to drive differentiation, master transcription factor Blimp1 orchestrates both massive antibody secretion and simultaneous repression of the GC transcriptional program.[70,100] B cell-intrinsic deletion of Blimp1 has been shown to increase the number, size, and duration of GCs after immunization.[86] This, paired with the reduced capacity of ASCs to act as antigen-presenting cells (APCs) after reduction of surface BCR and MHC-II, suggest that Blimp1 deficiency confers an advantage in the competition for access to help from GC Tfh. These factors combine to suggest that it may be possible to specifically suppress the generation of undesired antibody-derived inhibitors via prophylaxis with Blimp1-deficient, antigen-specific, high affinity "decoy" B cells. Furthermore, it may also be possible to augment the anticipated decoy effect by enabling constitutive regulatory

cytokine secretion. Outcomes from these studies will enable us to explore the potential of engineered antigen-specific B cells to serve as precise regulators of the adaptive immune response.

1.5.1 Hypothesis #1: Adoptively transferred high-affinity B cells reduce the host humoral response to linked antigen.

In the case of hemophilia A, antibody-derived inhibitors typically target multiple domains of FVIII, with multiple domains often targeted in the same patient. One study found that 83% of patients with measurable FVIII inhibitors had serum antibodies that targeted two or more different domains.[101] As previously established, it is known that adoptively transferred high affinity B cells reduce host-derived antibody specific for cognate antigen. B cells are able to receive help from T cells specific for both cognate and linked antigen,[102] suggesting that competition for access to a rate-limiting pool of T cell help may also impact antibody specific for linked antigen. This would be a great advantage for clinical translation, as the ability to reduce the generation of host antibody specific for both the C2 and A2 domains of FVIII using engineered B cells that encode a single high-affinity BCR specific for the C2 domain would greatly broaden the potential scope of application. To investigate this possibility, we immunized immune competent mice with HEL-OVA conjugate antigen and measured the impact of adoptively transferring high-affinity HEL-specific MD4 B cells[103] on the generation of host mouse antibody specific for both cognate (HEL) and linked (OVA) antigen. If MD4 B cell treatment blunted the generation of host OVA-specific antibody following HEL-OVA immunization, this would suggest that B cell competition for limited T cell help might be leveraged to reduce polyclonal host-derived antigen-specific antibodies.

1.5.2 Hypothesis #2: Blimp1-deficient, antigen-specific "decoy" B cells blunt the host humoral response without secreting antibody.

Previous studies[55,57] strongly suggest that access to T cell help rather than antigen sequestration by higher-affinity B cells is the primary rate-limiting factor in generating T-dependent humoral responses. However, other studies have demonstrated that the transfer of high-affinity monoclonal antibody decreases antigen access in ongoing GCs, resulting in increased apoptosis in antigen-specific B cells and smaller GCs.[104] If the observed reduction in antigen-specific antibody following adoptive transfer of high-affinity B cells is dependent on such antibody feedback, then the adoptive transfer of Blimp1-deficient high-affinity B cells is unlikely to result in a net reduction in antigen-specific antibody. Using CRISPR/Cas9 to target the *Prdm1* gene, we knocked out Blimp1 in MD4 B cells and repeated the experiment described in 1.5.1 to determine whether high-affinity Blimp1-deficient B cells could serve as "decoys" that continue to blunt the generation of host-antigen specific antibody despite being unable to secrete antibody themselves.

1.5.3 Hypothesis #3: Decoy-mediated antibody suppression is antigen-specific.

It is possible that the adoptive transfer of large numbers of high-affinity antigen-specific B cells results in larger and more numerous GC following immunization, since greater numbers of activated B cells may drive increased Tfh differentiation while providing larger numbers of B cells to seed those GCs. This may be exacerbated by Blimp1 deficiency, as B cell-intrinsic deletion of Blimp1 has been associated with larger, more numerous, longer-lasting GCs.[86] Previous work has suggested that there is a fixed number of permissive GC niches containing preassembled FDC

clusters and that prohibitive cluster occupancy by competing GC reactions can compromise subsequent GC formation.[105] Therefore, although adoptively transferred high-affinity B cells appear to outcompete host antigen-specific B cells in nascent and established GCs, large numbers may transiently disrupt T-dependent humoral responses non-specifically. To test the antigen specificity of decoy-mediated suppression, we simultaneously immunized MD4 decoy-treated mice with HEL-OVA and the unrelated antigen NP-CGG; if suppression was antigen-specific, we expected to see no change in NP-specific IgG with MD4 decoy treatment.

1.5.4 Hypothesis #4: Decoy Blimp1 deficiency supports decoy and reduces host B cell participation in GCs.

Past studies suggest that Blimp1 deficiency favors rather than inhibits B cell participation in GCs[86] and these observations are supported by the discovery that Blimp1 reciprocally represses BCL6.[83] However, we are unaware of any experiments that have examined the behavior of adoptively transferred high-affinity Blimp1-deficient B cells in GCs following immunization with cognate antigen, nor their impact on the participation of host B cells in those GCs. Blimp1^{lo} B cells in the DZ are associated with higher rates of proliferation than Blimp1^{neg} B cells,[106] suggesting that low levels of Blimp1 expression may confer some advantage for GC competition. Using confocal microscopy and flow cytometry, we examined the impact of Blimp1 deficiency on decoy B cell dominance in GCs as well as the impact of this dominance on host B cell participation in GCs.

1.5.5 Hypothesis #5: Decoy B cells can be leveraged to reduce functional antibody inhibitors of clinically relevant therapeutic proteins.

Findings gleaned from earlier research suggest that decoy-mediated suppression may be an effective strategy for blunting the T-dependent humoral response to specific antigens. However, as described it is likely to have a more limited impact on antigen-specific IgM than on IgG, and FVIII-specific IgM antibodies are known to occasionally act as inhibitors both of FVIII[107] and AAV.[108] Furthermore, a reduction in antigen-specific antibody does not necessarily translate to a reduction of functional inhibition. To determine whether a reduction in antigen-specific antibody correlated with a reduction in functional antibody-derived inhibitors, we transferred HEL-specific decoy B cells into FVIII-deficient HemA mice[109,110] before immunizing them with an antigen composed of HEL conjugated to the immunogenic C2 domain of human FVIII. We then utilized Bethesda assays[111] to measure the impact of decoy-mediated suppression on the generation of FVIII inhibitors in immunized mice.

1.5.6 Hypothesis #6: Primary murine B cells can be dual-edited to simultaneously prevent differentiation and secrete regulatory cargo.

The therapeutic potential of immunosuppressive B cells has long been recognized.[97,112] If high-affinity decoy B cells were augmented to constitutively secrete regulatory cytokine(s), it may be possible to leverage their inherent advantages as antigen-specific APCs to confer enduring antigen tolerance by directly modulating the activation and differentiation of antigen-specific CD4 T cells. However, there is no known master transcription factor that confers a regulatory phenotype onto B cells and this instead seems to represent a transient phenotype exhibited by B cells across multiple stages of their development and activation.[89] It is, however, possible to directly force constitutive expression of secreted factors by inserting an expression cassette into a cell's genome. Since primary B cells are resistant to lentiviral transduction[113,114] and the insertion of genes via

lentivirus occurs at random loci,[115] multiple groups have begun editing the genomes of primary human and murine B cells at precise loci by introducing gene cassettes via AAV transduction immediately following electroporation with CRISPR/Cas9 ribonucleoprotein (RNP) targeting that gene locus.[116–118] This method utilizes homology directed repair (HDR) to insert homology arm-flanked cassettes of up to ~4.4 kb into the precise location surrounding the Cas9 cut site. Using this approach, we endeavored to generate dual-edited Blimp1-deficient, IL-10-secreting eB_{Regs}.

1.5 Figures

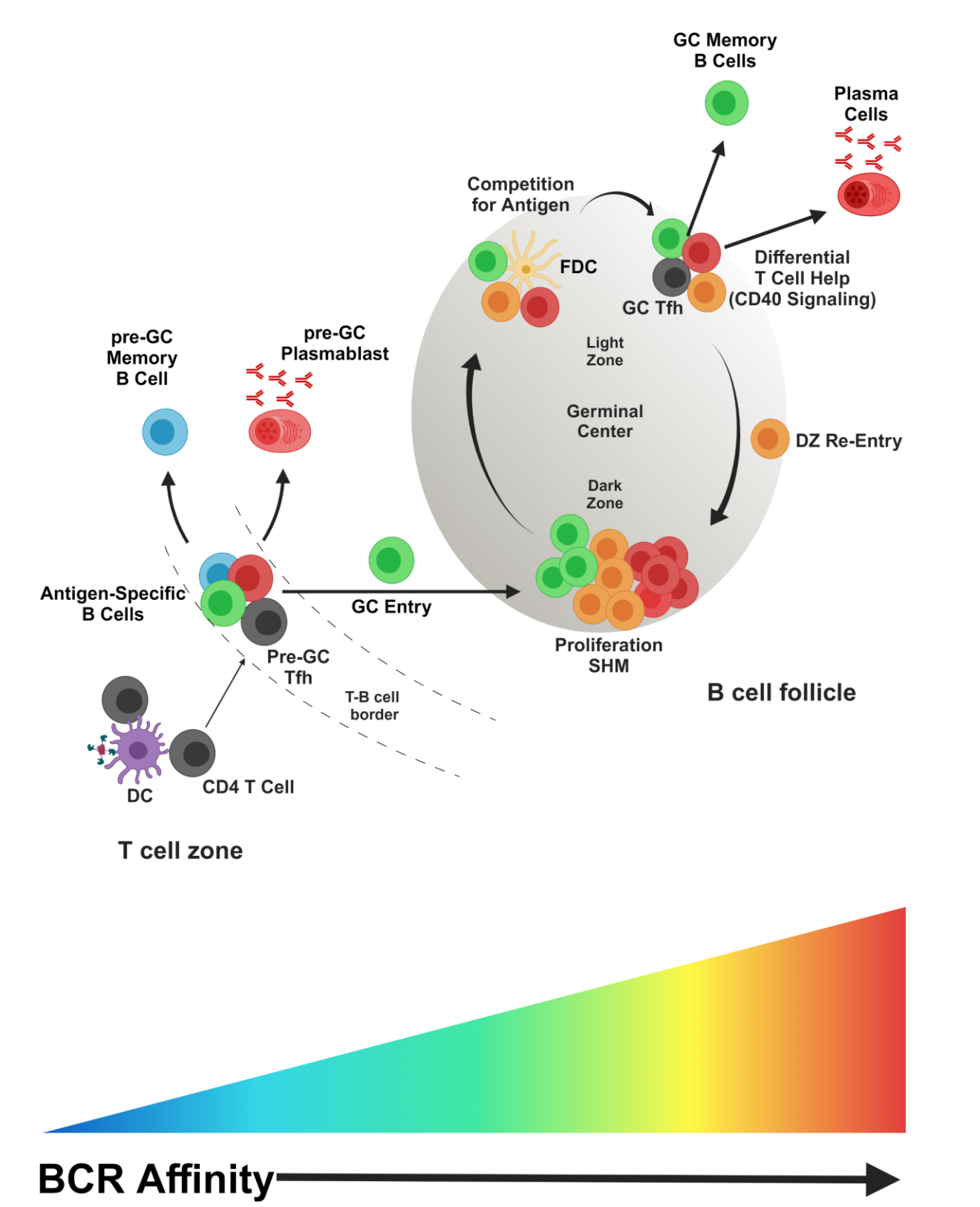
GC Memory
B Cells
Plasma
Cells
Competition
for Antigen
FDC
GC Tfh
Differential
T Cell Help
(CD40 Signaling)
pre-GC
Memory
B Cell
pre-GC
Plasmablast
Light
Zone
Germinal
Center
DZ Re-Entry
Dark
Zone
Antigen-Specific
B Cells
GC Entry
Pre-GC
Tfh
Proliferation
SHM
B cell follicle
T-B cell
border
DC
CD4 T Cell
T cell zone
BCR Affinity

Figure 1.1. BCR affinity partially guides B cell differentiation. Antigen-specific B cells of varying BCR affinity are activated following antigen stimulation, migrate to the borders between B cell follicle and T cell zone, and interact with pre-GC Tfh that have been activated by antigen presenting cells. B cells then take one of three paths: the lowest-affinity cells favor differentiation into pre-GC memory B cells, the highest-affinity cells favor differentiation into short-lived pre-GC plasmablasts, and the cells of intermediate affinity favor migration into the follicle to seed a GC. During the GC reaction, GC B cells enter the DZ where they proliferate and undergo SHM, then enter the LZ where they compete for antigen presented by follicular dendritic cells. This antigen is endocytosed, processed, and presented on MHC-II to GC Tfh cells and the degree of T cell help received is thought to play a role guiding subsequent B cell fate. Lower-affinity cells tend to emerge from GCs as memory B cells and higher-affinity cells either differentiate into plasma cells or re-enter the DZ to undergo further proliferation, SHM, and affinity-based selection in the LZ. Created with BioRender. *Adapted from the dissertation "Activated PI3Kδ signaling in humoral immunity" by Fahd Al-Quresah (2021).*

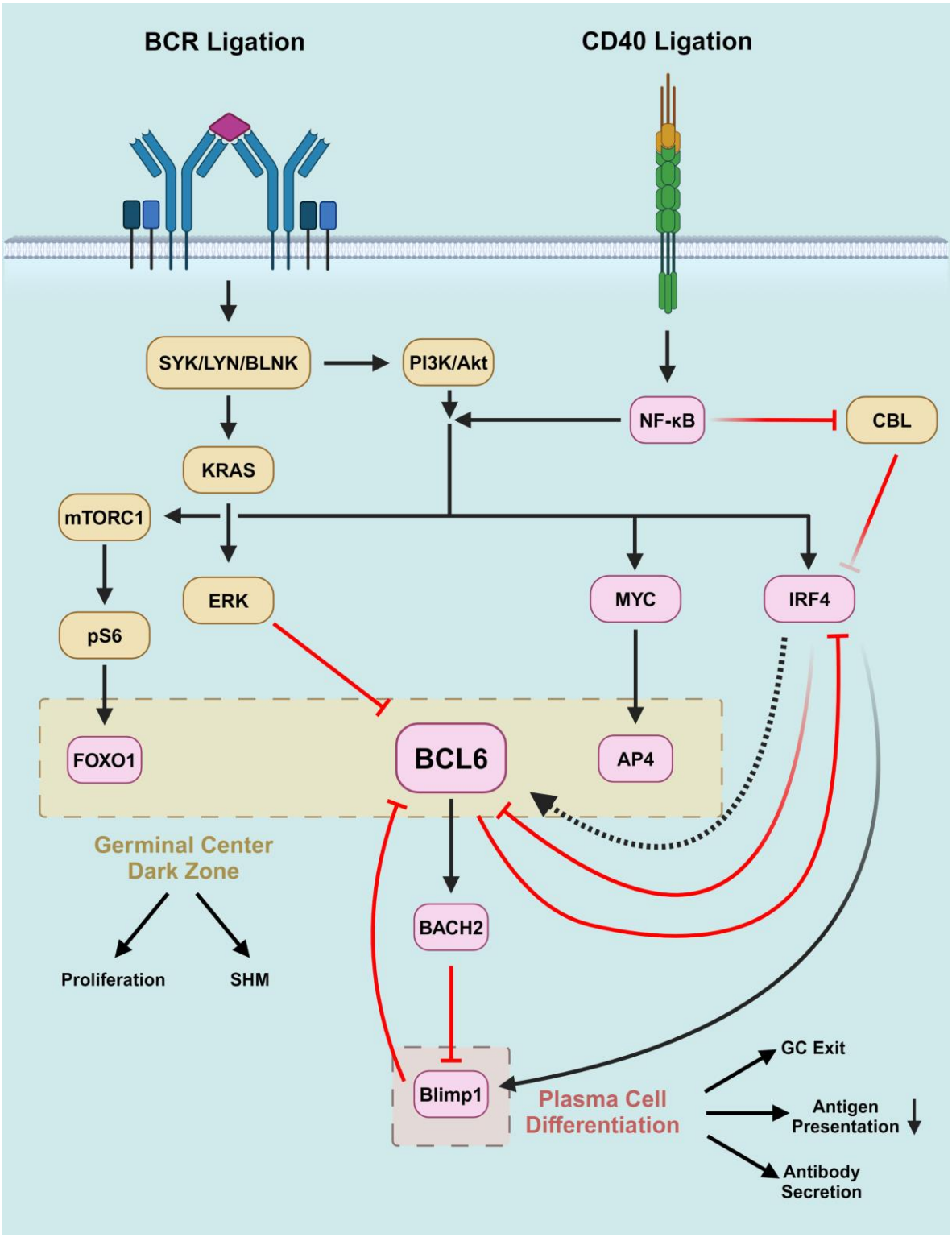
BCR Ligation
CD40 Ligation
SYK/LYN/BLNK
PI3K/Akt
NF-κB
CBL
KRAS
mTORC1
ERK
MYC
IRF4
pS6
FOXO1
BCL6
AP4
Germinal Center
Dark Zone
Proliferation
SHM
BACH2
Blimp1
Plasma Cell
Differentiation
GC Exit
Antigen
Presentation
Antibody
Secretion

Figure 1.2. Differential T cell help guides differentiation in GC B Cells. Ligation of the B cell receptor (BCR) results in activation of the phosphatidylinositol 3-kinase/protein kinase B (PI3K/Akt) pathway, and when paired with nuclear factor kappa-light-chain-enhancer of activated B cells (NF-κB) driven by CD40 signaling they collaborate to induce expression of MYC and to induce phosphorylation of ribosomal protein S6 (pS6) through mammalian target of rapamycin complex 1 (mTORC1). pS6 induces expression of forkhead box O1 (FOXO1), which supports proliferation and migration to the DZ, while MYC induces activating enhancer protein 4 (AP4) which also supports cell proliferation. Together, FOXO1 and AP4 support the transcriptional program necessary for proliferation and SHM in the DZ while BCL6 (highly expressed in GC B cells) inhibits plasma cell differentiation by inducing BTB domain and CNC homology 2 (BACH2) expression. BCR and CD40 ligation also support the expression of interferon regulatory factor 4 (IRF4), which transiently supports the expression of BCL6 (which in turn represses IRF4). However, strong NF-κB expression derived from CD40 represses the signal molecule ubiquitin ligase CBL, which represses IRF4. As CBL is depleted, IRF4 expression increases and instead represses BCL6, leading to increased expression of Blimp1. Further supported by BCR ligation-derived repression of BCL6 through SYK/LYN/BLNK, KRAS, and ERK, Blimp1 extinguishes the GC transcriptional program by directly repressing BCL6. Blimp1 initiates the transcriptional program associated with plasma cell differentiation, losing much capacity for antigen presentation in favor of massive antibody secretion. Signaling molecules are colored yellow while transcription regulators are red. Created with BioRender. *Adapted from Laidlaw et al.*[70]

Chapter 2: Blunting specific T-dependent antibody responses with engineered 'decoy' B cells

This chapter is adapted from the following manuscript:

Pitner, RA, Chao JL, Dahl NP, Fan MN, Cai X, Avery NG, Roe K, Spiegel Jr PC, Miao CH, Gerner MY, James RG, Rawlings, DJ. Blunting specific T-dependent antibody responses with engineered 'decoy' B cells. *Manuscript in review.*

2.1 Introduction

Despite being vital for immune defense against numerous pathogens, some antibody responses pose challenges to modern therapies. Of particular concern are monogenic diseases such as hemophilia A where the success of both recombinant FVIII therapy[119,120] and viral-mediated gene therapy[121,122] are limited by the generation of antibody-derived inhibition of the foreign therapeutic protein and/or immune responses targeting components of the viral vector. The only presently approved strategy to eliminate FVIII inhibitors is ITI, the basic premise of which is long-term treatment with large quantities of FVIII – a process that is time-consuming and often incompletely effective.[15,123] In the case of gene therapy, repeat administration of potentially therapeutic AAV is limited by the generation of antibody inhibitors to multiple components of the vector.[10] Strategies for preventing such unwanted immune responses might permit repeat vector administration, for example, in cases where a patient first receives gene therapy early in life[30] or where repeat administration of a low dose of vector is needed to limit immunogenicity of the gene product or toxicity of the viral vector.[31,32] Thus, a prophylactic therapy for preventing the generation of undesired antibody inhibitors without requiring broader immunosuppression[124,125] would be a valuable addition to existing strategies for treating genetic disorders.

Engineered B cells and plasma cells are emerging as a potential therapy to secrete pathogen-specific antibodies[117,118] or a broad range of other protein therapeutics.[116,126,127] These new therapy platforms leverage key properties of plasma cells including longevity and capacity for very high rates of protein secretion. Importantly, B cells also function as antigen-specific antigen-presenting cells (APCs) and can therefore shape specific immune responses without secreting antibodies. B cells alone are sufficient to prime Tfh responses to *Plasmodium* infection in mice[128] and in one model were found to be the dominant antigen APC following immunization

with virus-like particles.[129] Moreover, because GC entry is regulated by affinity-mediated access to limited CD4 T cell help,[57] it should be possible to influence the humoral output of specific T-dependent antibody responses with engineered high-affinity B cells. Consistent with this notion, adoptively transferred, naïve mature B cells expressing a defined, high-affinity BCR can enter GCs and compete with endogenous B cells recognizing the same antigen.[57] Importantly, in this competitive setting, high-affinity, antigen-specific B cells can out-compete lower-affinity B cells for access to antigen and receipt of activation, expansion and differentiation signals mediated by Tfh cells, thereby reducing the generation of ASCs[71] derived from the endogenous B cell populations.

In this study, we tested whether engineering competition for antigen could effectively regulate specific humoral responses. Importantly, we hypothesized that by eliminating the capacity of antigen-specific B cells to differentiate into plasma cells, we could exploit affinity-based selection to flood antigen-specific GCs with non-differentiating "decoy" B cells. To achieve these goals, we utilized *Prdm1*-targeted CRISPR/Cas9 gene editing to knock out Blimp1[86] in the decoy B cell population, thereby blocking plasma cell development. In parallel, we leveraged the APC activity of decoy B cells as a means to limit the host humoral response to a target protein antigen while leaving non-specific antibody responses intact. Strikingly, we show that *Prdm1*-edited primary B cells enter and dominate GCs in an antigen-specific fashion, and that these antigen-specific, Blimp1-knockout decoy B cells can suppress humoral responses to both cognate and cis-linked antigen. We demonstrate the therapeutic potential of this approach by preventing the generation of FVIII-specific clotting inhibitors in a murine model of hemophilia A. Finally, we show that primary B cells can be dual-edited to simultaneously knock out Blimp1 and insert a

constitutive IL-10 secretion cassette, suggesting that it may be possible to generate non-differentiating eB_{Regs}.

2.2 Results

2.2.1 Adoptive transfer of antigen-primed, antigen-specific B cells reduces the humoral response to both cognate and cis-linked antigen

We hypothesized that adoptively transferred, high-affinity B cells specific for one protein antigen might be able to outcompete lower-affinity host (endogenous) B cells specific for the same and/or linked antigens. We predicted that transferred B cells might achieve this dominance by competing more effectively for access to antigen, subsequent peptide presentation on MHCII, and/or access to T cell help sufficient to mount a robust antibody response. Further, we predicted that the competitive advantage conferred by high affinity B cells could be amplified by exposing activated, antigen-specific B cells to cognate antigen ex vivo prior to adoptive transfer and subsequent immunization.

To begin to examine these ideas, we performed adoptive transfer studies shown schematically in Fig 2.1 A. To obtain primary B cells with a defined antigen-specificity, we utilized B cells from MD4 transgenic mice, in which ~95% of splenic B cells express a high-affinity BCR (HyHEL10) which recognizes HEL and is expressed on the B cell surface as non-switchable IgM and IgD.[103,130] Primary B cells were first enriched from the spleens of MD4 or control C57Bl6 (B6) mice. To drive B cell activation, these respective bulk B cell populations were cultured for 2 days in media supplemented with multimeric CD40 ligand (MCD40L) to mimic CD4 T-cell help[131] and α-CD180 to mimic Toll-like receptor 4 engagement[132,133] without driving cytokine secretion.[134] Next, to initiate cis-linked antigen presentation, activated B cell populations were exposed to HEL

conjugated to ovalbumin (HEL-OVA conjugate) in the presence of soluble IL-4 for 2 hours. IL-4 was utilized to promote B cell survival.[135,136] Activated HEL-OVA-pulsed B cells were then adoptively transferred into cohorts of antigen-naïve B6 mice and three days later these mice were immunized intraperitoneally (i.p.) with HEL-OVA antigen in Sigma Adjuvant.

To track antigen-specific humoral responses, serum was collected at days 7, 14, and 28. We found that α-HEL IgM was increased and, as predicted by prior reports,[57,71] that α-HEL IgG was decreased in mice receiving MD4 cells regardless of whether they had been primed *in vitro* (Fig. 2.1 B,C). Strikingly, we also found that MD4 cells primed with HEL-OVA significantly depressed OVA-specific IgG responses. This along with the increased inhibition of α-HEL IgG suggests that *ex vivo* antigen priming prior to adoptive transfer may confer an additional competitive advantage to the transferred B cells in T-dependent antibody responses. Collectively, these data show that transfer of B cells primed with cis-linked antigens can regulate subsequent humoral responses to both cognate and cis-linked antigen.

2.2.2 Blimp1-deficient, antigen-specific B cells blunt the host humoral response without secreting antibody

While antigen-primed MD4 B cells markedly reduced the production of both α-HEL and α-OVA IgG, the recipient mice exhibited significantly increased levels of serum α-HEL IgM. We predicted that differentiation of adoptively transferred MD4 B cells, rather than endogenous B cells, was responsible for the rise in serum HEL-specific IgM. The transcription factor Blimp1 plays an essential role in terminal differentiation of B cells into ASCs.[86,137] Therefore, to eliminate differentiation of adoptively transferred B cell populations we developed a strategy to knock out Blimp1 expression using CRISPR/Cas9 to target the *Prdm1* gene.[87]

We first assessed the efficiency of *Prdm1* disruption. Enriched splenic B cells were cultured for 2 days as in Fig 2.1 A and then electroporated with ribonucleoprotein complexes (RNPs) consisting of Cas9 bound to single guide RNA (sgRNA) targeting either a control locus (*Rosa26*) or *Prdm1*. Electroporated cells were expanded in IL-4 on a fibroblast line (40LB feeder cells) expressing surface murine CD40L and secreting murine B cell-activating factor (BAFF)[138] for 8 days (Fig. 2.2 A). The *Prdm1* gene was PCR-amplified from genomic DNA (gDNA) purified from feeder-depleted, expanded B cells and submitted for Sanger sequencing. Trace files were analyzed via inference of CRISPR edits (ICE) to estimate *Prdm1* gene indel and knockout rates[139] of 98% and 93%, respectively (Fig. 2.2 B). Total antibody levels and the size of the $CD19^{lo}CD138^{+}$ ASC[60,84] population were greatly reduced following *Prdm1* targeting relative to mock or control edited populations (Fig 2.2 C,D), findings consistent with near complete loss of Blimp1-mediated ASC differentiation and antibody secretion.

To determine if Blimp1-deficient MD4 B cells lacking the ability to generate antibodies retain the ability to reduce antigen-specific IgG following immunization, HEL-OVA antigen-primed *Prdm1*-targeted B cells were adoptively transferred into B6 mice (Fig. 2.2 E). Relative to Rosa26-targeted B cells, transfer of Blimp1-deficient B cells led to a marked reduction in α-HEL IgM (Fig. 2.2 F). Together with *in vitro* data, these findings are strong evidence that the increase in α-HEL IgM in recipients of $Blimp1^{WT}$MD4 B cells is derived from the transferred B cells. Consistent with Fig 2.1, α-HEL IgG and α-OVA IgG responses were also markedly reduced in recipients of antigen-primed *Prdm1*-targeted MD4 B cells (Fig. 2.2 F).

MD4 B cells compete for binding to HEL-OVA during ongoing humoral responses via their specificity for HEL; they should not be able to compete for binding to unconjugated OVA. We observed no significant reduction in α-OVA IgG if mice were immunized with unconjugated

OVA following the transfer of HEL-OVA-primed Blimp1^{KO} MD4 B cells (Fig. 2.S1), suggesting that the reduction in antigen-specific antibody requires the ongoing ability to compete for antigen. Because antigen-primed, Blimp1^{KO} MD4 B cells can effectively blunt both cognate and cis-linked humoral responses without contributing to the humoral response, they are referred to hereafter as "decoy" B cells.

2.2.3 Decoy B cells exhibit cell dose-dependent antigen-specific suppression.

To examine the relationship between cell dose and decoy-mediated suppression, we transferred a range of doses of CD45.2^{+} antigen-pulsed MD4 decoy B cells into CD45.$^{1+}$B6 mice. Spleens were collected from a subset of host mice at Day 3 post-transfer to assess B cell engraftment and the remaining animals were immunized as above (Fig. 2.3 A). Flow cytometry-based cell enumeration showed a linear increase in B cell engraftment with an average splenic engraftment rate of ~1-2% of the total transferred decoy cell population (Fig 2.3 B). The reduction in α-HEL IgG following immunization was dose-dependent, with reductions observed at each decoy B cell dose. In contrast, a significant reduction in serum α-OVA IgG was present only at the highest dose of decoy B cells (Fig. 2.3 C).

As GC-dependent responses may be restricted by a finite number of FDC niches,[105] adoptive transfer of large numbers of antigen-specific B cells may limit the response to concurrent antigenic challenge. To examine this possibility, mice were treated with either polyclonal or MD4 decoy B cells and then immunized simultaneously with HEL-OVA and NP-CGG, another T-dependent antigen (Fig. 2.3 D). While α-HEL and α-OVA IgG were reduced with antigen-specific decoy treatment, α-NP IgG was unaffected across conditions (Fig 2.3 E). This suggests that

antigen-primed decoy B cells may outcompete endogenous antigen-specific B cells without limiting the humoral output from B cells specific for other antigens.

2.2.4 Blimp1^{KO}MD4 decoy B cells outcompete endogenous B cells in germinal centers.

To directly assess the impact of decoy B cells on GC responses *in vivo*, we next performed a series of imaging experiments and parallel flow cytometry studies evaluating the kinetics of GC formation and cellular distribution. Antigen-primed Blimp1^{WT} or Blimp1^{KO} B6 or HEL-specific MD4 B cells expressing the CD45.2 congenic marker were adoptively transferred into cohorts of CD45.1^{+}B6 recipient mice (Fig. 2.4 A). Following immunization with HEL-OVA, spleens were harvested and analyzed via confocal microscopy at multiple timepoints to examine the impact of antigen-specificity and Blimp1 expression on decoy B cell localization across the GC response. Immediately prior to immunization, transferred B cells appeared to be distributed throughout the splenic B cell follicles regardless of specificity or Blimp1 expression (Fig. 2.S2). Strikingly, five days after immunization, Blimp1^{KO}MD4 B cells dominated most GCs (Fig. 2.4 B,D, Fig. 2.S3 A). In contrast, while GCs were readily detected in immunized mice that received Blimp1^{KO}B6 or Blimp1^{WT}MD4 B cells, those GCs exhibited significantly reduced penetrance of transferred CD45.2^{+} B cells and were largely composed of endogenous B cells (Fig. 2.4 B,D, Fig. 2.S3A). By day 11, GC penetrance by both Blimp1^{WT}MD4 and Blimp1^{KO}MD4 was equivalent, and both conditions exhibited increased penetrance over Blimp1^{WT}B6 or Blimp1^{KO}B6 transfer conditions (Fig. 2.4 C,D, Fig. 2.S3A). Adoptive transfer of Blimp1^{KO} B cells appeared to increase the variance in GC size but did not appear to disrupt germinal center formation *per se*, as average GC size across mice across conditions was found to be comparable (Fig. 2.S3 B).

Next, we used flow cytometry to help further define the impact of Blimp1^{KO} antigen-specific decoy B cells on the host GC response, utilizing congenic markers and HEL and OVA tetramers to track and quantify endogenous and decoy B cells following immunization. Our experimental approach is shown schematically in Fig. 2.5 A with representative cell gating strategy displayed in Fig. 2.S4. Ten days after immunization, α-HEL and α-OVA serum IgG were similarly reduced in mice treated with Blimp1^{WT} or Blimp1^{KO}MD4 (Fig. 2.5 B). Importantly, the reduction in serum antibody correlated with a marked decrease in the proportion of endogenous antigen-specific GC B cell populations (Fig 2.5 C, shows representative data for one Blimp1^{KO}MD4 recipient). Specifically, in comparison to the no cell transfer control, at day 11, Blimp1^{WT} or Blimp1^{KO}MD4 recipient mice exhibited a significant reduction in both HEL- and OVA-specific GC B cells (Fig. 2.5 D) and HEL- and OVA-specific GC ASCs (Fig. 2.5 E). Surprisingly, despite not impacting day 14 serum concentrations of IgG in previous experiments, α-HEL and α-OVA serum IgG (Fig. 2.5 B), α-HEL and α-OVA GC B cells (Fig. 2.5 D), and α-HEL and α-OVA GC ASCs (Fig. 2.5 E) were also partially reduced in mice treated with polyclonal Blimp1^{KO} B6 B cells, though to a lesser extent than the reduction upon treatment with Blimp1^{WT} or Blimp1^{KO} MD4 B cells. Notably, in recipients of adoptively transferred Blimp1^{WT} and Blimp1^{KO} MD4 B cells, but not Blimp1^{KO}B6 B cells, transferred B cell populations present within the GC expressed increased LZ markers (CXCR4^{lo}CD86^{hi}) relative to endogenous HEL- or OVA-antigen-specific GC B cells (Fig. 2.5 F). Together, these results demonstrate that high-affinity antigen-specific B cells primed with antigen conjugate not only invade GCs but also inhibit participation of endogenous B cells specific for either antigen in GCs initiated following immunization. Interestingly, the increased dominance of early GCs suggests that this effect may be augmented by Blimp1 deficiency during the early GC response.

2.2.5 HEL-specific decoy B cells prevent the generation of factor VIII inhibitors in a murine model of hemophilia A.

To explore whether decoy B cells could be used to suppress an undesired antibody response to a clinically relevant therapeutic protein, we next performed studies assessing inhibitory responses to human FVIII. The C2 domain of FVIII contains binding sites for von Willebrand factor and phosphatidylserine[140,141] and may serve as a docking module to promote FVIII proteolytic activation by thrombin or activated factor X.[142,143] Its necessity for the proper function of FVIII paired with its immunogenicity makes the C2 domain a frequent target of inhibitory antibodies following FVIII therapy.[144,145] We therefore chemically conjugated the C2 domain of human FVIII to HEL in a 1:1 ratio and primed Blimp1^{KO}MD4 B cells with the conjugate. These antigen-primed decoy B cells, or alternatively, HEL-C2 primed, polyclonal B cells, were then injected into the FVIII exon 16-mutated HemA mouse strain[109,110] prior to immunization with the same HEL-C2 conjugate to model the generation of FVIII inhibitors with or without decoy B cell treatment (Fig. 2.6 A). Strikingly, transfer of HEL-C2 primed, HEL-specific, Blimp1-deficient decoy B cells significantly reduced the generation of α-C2 IgG following immunization relative to the antibody produced in untreated mice (Fig. 2.6 B,C). In contrast, mice treated with HEL-C2 primed, polyclonal B cells exhibited marginally increased α-C2 IgG. Importantly, the reduction in α-C2 IgG in Blimp1^{KO}MD4 B cell-treated mice translated to a stark reduction in functional inhibition of FVIII-mediated clotting 28 days after immunization (Fig 2.6 D). Collectively, our results show that antigen-specific decoy B cells can reduce not only host humoral responses to relatively weak cis-linked antigens such as OVA, but also functional inhibitors of immunogenic and clinically relevant antigens.

2.2.6 Primary murine B cells can be dual-edited to simultaneously disrupt Blimp1 and incorporate a constitutive IL-10 secretion cassette.

To determine whether decoy B cells could be augmented to constitutively secrete regulatory cargo, we adapted existing protocols for editing primary B cells via AAV-mediated HDR.[116–118] As in previous experiments, primary B cells were stimulated *ex vivo* for 2 days with MCD40L and α-CD180 before editing (Fig. 2.7A). They were then electroporated with a 1:1 molar combination of Rosa26- and Prdm1-targeted RNPs and incubated overnight with AAV serotype 2.5 delivering a repair template composed of a Rosa26 homology arm-flanked expression cassette. The expression cassette was composed of either green fluorescent protein (GFP) or IL-10 separated upstream from the non-coding membrane-bound region of the low affinity nerve growth factor receptor (LNGFR), chosen as a marker for cell editing and potential target for enrichment, by the polycistronic linker P2A and driven by the synthetic MND promoter.[146] B cells were washed the next day and plated on irradiated 40LB feeder cells with recombinant IL-4 for 6 days before the cells and media were harvested for analysis. Flow cytometry revealed that this dual editing approach yielded a population of non-differentiating B cells of which 5-10% also expressed detectable LNGFR (Fig. 2.7B). Although unlikely, it was possible that the observed LNGFR derived from episomal expression rather than true genomic integration. To address this, we designed a droplet digital polymerase chain reaction (ddPCR) strategy to distinguish unedited Rosa26 loci from disrupted Rosa26 loci repaired by non-homologous end-joining (NHEJ) and disrupted Rosa26 loci that incorporated an MND promoter via HDR. We confirmed that the LNGFR expression was derived from genomically integrated cassettes rather than episomal expression using this strategy, calculating HDR editing rates of 3-6%, consistent with heterozygous cell editing rates of 6-12% (Fig. 2.7C). Finally, we harvested cell supernatants and

measured secreted IL-10 via ELISA (Fig. 2.7D). While populations of unedited B cells and RNP-only edited B cells did not secrete detectable IL-10 above background, B cell populations dual-edited to disrupt Prdm1 and incorporate either GFP or IL-10 did secrete detectable IL-10. This was consistent with prior reports documenting that costimulation through CD40 and toll-like receptor 9 (TLR9) induces IL-10 expression in both murine[147] and human[148] B cells. However, the B cell populations edited to incorporate an IL-10 expression cassette secreted significantly more IL-10 than populations that incorporated a GFP cassette. These results demonstrate that Blimp1-deficient decoy B cells can be further functionalized to constitutively secrete regulatory cargo.

2.3 Discussion

Engineered plasma cells are being investigated as a potential cell-based therapy that leverages the native capacities of plasma cells to secrete large quantities of therapeutic protein and engraft long-term.[116–118,126] Importantly, B cells also manifest a unique combined ability for antigen-specific recognition and subsequent antigen presentation[128,129]. This latter capability suggests the potential to use engineered B cell therapies to directly manipulate endogenous humoral immune responses.

Consistent with this notion, adoptively transferred, naïve mature B cells expressing a defined high-affinity B cell antigen receptor are known to enter GCs and compete with endogenous B cells recognizing the same antigen for access to antigen and subsequent differentiation signals from T follicular helper cells[57,71]. We hypothesized that by utilizing CRISPR/Cas9 gene editing to knock out Blimp1, the master transcription factor for plasma cell differentiation, we could exploit affinity-based selection to flood antigen-specific GCs with non-differentiating “decoy” B cells, thereby blunting the primary endogenous humoral response to cognate antigen while leaving non-

specific responses intact. Using a combination of antigen-specific ELISA, flow cytometric analysis, and confocal microscopy, we showed not only that gene-edited primary B cells can enter and dominate GCs in an antigen-specific fashion, but that antigen-specific Blimp1-knockout decoy B cells suppress the humoral response to both cognate and cis-linked antigen. Importantly, we demonstrate that the suppression of the humoral response to linked antigen prevents the generation of functional factor VIII inhibitors in a murine model of hemophilia A, highlighting the therapeutic potential of the approach.

Taken together, these findings suggest a novel method that exploits GC biology to negatively modulate specific humoral immune responses including, for example, generation of antibody inhibitors to clinically important target antigens such as various protein therapeutics or gene therapy vectors. We also demonstrate that decoy B cells can be armed to constitutively secrete regulatory cargo, insinuating that it may be possible to generate eB_{Regs} capable of inducing antigen-specific tolerance. With optimization, gene-edited decoy B cells may provide a robust platform for precise, antigen-specific, engineered immune regulation.

2.4 Materials and Methods

Mice

B6 (C57Bl/6), CD45.1-B6 ($Ptprc^a$ $Pepc^b$/BoyJ), and MD4 mice were either purchased from the Jackson Laboratory or bred in-house. CD45.1-HemA mice (Factor VIII exon 16-knockout) on a CD45.1-B6 background[109,110] were bred and maintained within the Seattle Children's Research Institute vivarium. All mice were maintained in a specific pathogen-free environment and

protocols were approved by the Institutional Animal Care and Use Committee of Seattle Children's Research Institute.

Antigen preparation

HEL and OVA were purchased from ThermoFisher Scientific. NP-CGG, ratio >40 was purchased from Biosearch Technologies.

The gene for human FVIII C2 domain (residues 2171–2332) was subcloned into a pET28a-TEV(+) plasmid with NdeI and XhoI restriction sites, and an N-terminal His6 tag by Genscript. Wildtype C2 was then expressed in SHuffle T7 B cells (New England Biolabs) and grown in 2XYT media containing 20 mM $MgCl_2$ and 50 µg/mL Kanamycin at 30°C. Bacterial cultures were shaken at 220 rpm until OD_{600} reached 0.6-0.8, induced with 0.5 mM IPTG, and shaken for 18-20 hours at 15 °C. Bacterial cultures were pelleted by centrifugation at 7000 x g (FIBERLite F10-6x500y rotor, Thermo Fisher Scientific, Waltham, MA) for 10 minutes. Bacterial pellets were resuspended in 6 mL per g of pellet of lysis buffer (20 mM Tris pH 7.4, 300 mM NaCl, 10 mM Imidazole, 0.1% Triton X-100, and 10% glycerol) supplemented with 1 mM PMSF, 1 mg/mL chicken egg white lysozyme, and 5 µg/mL DNAse. Resuspended pellet was incubated stirring for 30 minutes at 4 °C and lysed via sonication (50% duty cycle and 30 seconds on and off cycles) for 6 minutes on ice. Whole cell lysate was clarified via centrifugation at 40,000 x g (FIBERLite F21- 8x50y rotor, Thermo Fisher Scientific, Waltham, MA) and supernatant was loaded onto a preequilibrated 5 mL HisTrap HP Nickel fast protein liquid chromatography (FPLC) column (Cytiva) attached to a AKTA prime Plus FPLC (GE Healthcare Life Sciences) at 3 mL/min. The column was washed with wash buffer (20 mM Tris pH 7.4, 300 mM NaCl, and 15 mM Imidazole) until UV_{280} reached baseline. A 12-column volume (CV) ATP wash (20 mM HEPES pH 7.4, 300 mM KCl, and 20

mM $MgCl_2$) supplemented with 5 mM ATP disodium salt heptahydrate was performed to remove contaminating chaperones. The column was washed again with wash buffer until UV_{280} reached baseline, washed with 5% elution (20 mM Tris pH 7.4, 300 mM NaCl, and 500 mM Imidazole) and 95% wash buffer, and a gradient elution (5-100% elution buffer in 100 mL at 3 mL/min) was performed. Thirty 4 mL fractions were collected and fractions containing C2 WT were pooled, cleaved with a 1:10 (w/w) ratio of TEV protease:protein, and dialyzed into 20 mM Tris pH 7.4 and 300 mM NaCl. Cleaved C2 WT was loaded onto a 5 mL HisTrap HP column and eluted with 5% elution and 95% wash buffer. Protein purity was analyzed via 12.5% SDS-PAGE. Cleaved C2 WT was concentrated using a 10 kDa MWCO spin concentrator (Amicon) to 5 mL and purified by size exclusion chromatography (Hiload 16/600 S75; Cytiva) and stored at 2 mg/mL in (20 mM HEPES pH 7.4 and 150 mM NaCl).

Maleimide-activated OVA was conjugated to sulfhydrylated HEL to generate stable HEL-OVA conjugates. OVA was maleimide-activated with a 100-fold molar excess of sulfosuccinimidyl 4-(N-maleimidomethyl)cyclohexane-1-carboxylate (sulfo-SMCC; ThermoFisher). HEL was incubated with a 7-10-fold molar excess of N-succinimidyl S-acetylthioacetate (SATA; ThermoFisher), and HEL-SATA was deacetylated in 0.5M hydroxylamine/25mM EDTA in PBS, pH 7.2-7.5. Activated proteins were then conjugated with a 4-fold molar excess of HEL to OVA before removal of unconjugated HEL and OVA monomers via size exclusion chromatography.

Maleimide-activated C2 was conjugated to sulfhydrylated HEL similarly, except C2 was activated with PEGylated SMCC ($SM(PEG)_{6;}$ ThermoFisher) and HEL was activated with PEGylated SATA ($SAT(PEG)_{4;}$ ThermoFisher) to maintain antigen solubility. HEL and C2 were conjugated at a 1:1 molar ratio.

CRISPR/Cas9 editing, culture of edited B cells, and quantification of gene editing

Spleens were harvested from 8-14 week-old B6 or MD4 donor mice and B cells were enriched using the EasySep™ Mouse B Cell Isolation Kit (StemCell) according to the manufacturer's instructions. Enriched B cells were activated for 2 days in IMDM supplemented with 55μM 2-mercaptoethanol, 10% FBS, 100 ng/mL murine multimeric CD40L (AdipoGen), 1 μg/mL rat α-mouse CD180 (BD Pharmingen), and 100 IU ml^{-1} of penicillin and 100 μg ml^{-1} of streptomycin (Gibco) at a density of 3-4 x 10^6 cells/mL. After 2 days in media at 37°C, B cells were harvested from plates, washed with MACS buffer (0.5% BSA/2mM EDTA in PBS), and counted via hemocytometer.

For *Rosa26* or *Prdm1* gene targeting, *Rosa26* or *Prdm1* sgRNA (Synthego) (Table 2.1) was complexed with Alt-R™ S.p. Cas9 Nuclease V3 (IDT) at a molar ratio of 3:1 sgRNA:Cas9 in electroporation buffer (MaxCyte) for 10-20 minutes at room temperature (RT). Electroporation reactions consisted of 1E8 cells/mL in electroporation buffer with a final Cas9 concentration of 1.25 μM. All electroporations were performed on a MaxCyte ExPERT GTx with the "B Cell 2" protocol. Following electroporation, cells were immediately diluted into B cell media (IMDM + 55μM 2-mercaptoethanol + 10% FBS) supplemented with 100 ng/mL murine multimeric CD40L, 1 μg/mL rat α-mouse CD180, 10 ng/mL murine IL-4 (PeproTech), 100 IU ml^{-1} of penicillin and 100 μg ml^{-1} of streptomycin, and 1 μg/mL HEL-OVA or HEL-C2 (where indicated) at a cell density of 3-5 x 10^6 cells/mL. Cells recovered in media at 37°C for 2 hours before adoptive transfer.

For characterization of *Prdm1* knockout efficiency, 5 x 10^4 electroporated cells were added to each of 3 wells of a 12-well plate coated with 2 x 10^5 irradiated 40LB feeder cells[138] in 4 mL B

cell media supplemented with 1 ng/mL IL-4 and Pen/Strep. After 4 days, all cells were harvested from each well, washed with MACS buffer, and transferred to a fresh 10 cm plate coated with 3 x 10^6 irradiated 40LB feeder cells in 40 mL B cell media supplemented with 1 ng/mL IL-4 and Pen/Strep. After 4 more days, all cells were harvested from the 10cm plates, incubated with biotinylated α-H-2Kd antibody (BioLegend), and 40LB feeder cells were depleted with α-biotin microbeads (Miltenyi) and LD columns (Miltenyi) according to the manufacturer's directions. Half of the remaining B cells were phenotypically characterized for expression of surface CD138 via flow cytometry. Genomic DNA was isolated from the other half of the B cells using the Zymo Research Quick-DNA Microprep Kit and gene regions surrounding Cas9 cut sites were amplified via PCR with primers manufactured by IDT and PrimeSTAR GXL DNA Polymerase (Takara Bio). Gene amplicons were cleaned with the QIAquick PCR Purification Kit, submitted to Genewiz for Sanger sequencing, and Inference of CRISPR Edits (ICE) analysis was performed to obtain indel and knockout scores by submitting .ab1 files to Synthego's online tool (https://ice.synthego.com/#/).

For dual editing, *Rosa26*, *Prdm1*, or *TRAC* sgRNA (Synthego) (Table 2.1) was complexed with Alt-R™ S.p. Cas9 Nuclease V3 (IDT) at a molar ratio of 1.23:1 sgRNA:Cas9 in P4 Primary Cell Nucleofector Solution (Lonza) for 10-20 minutes at RT. Electroporation reactions consisted of 3E7 cells/mL in P4 buffer with final sgRNA concentrations of 1.875 μM per target and final Cas9 concentrations of 3.05 μM. Electroporation was performed on a Lonza 4D-Nucleofector with the "DI-100" protocol. Following electroporation, cells were immediately diluted into B cell media supplemented with 100 ng/mL murine multimeric CD40L, 1 μg/mL rat α-mouse CD180, 10 ng/mL murine IL-4 (PeproTech), 100 IU ml^{-1} of penicillin and 100 μg ml^{-1} of streptomycin, and 20%v/v of either PBS or the appropriate AAV serotype 2.5. The next morning, B cells were harvested and

washed with MACS buffer before transferring them to 10cm plates coated with 3 x 10^6 irradiated 40LB feeder cells[138] in 40 mL B cell media supplemented with 1 ng/mL IL-4 and Pen/Strep. After 3 days, media was carefully aspirated from the 10 cm plates and replaced with fresh B cell media supplemented with IL-4 and Pen/Strep. After 3 more days, all cells were harvested from the 10cm plates and the media was set aside for IL-10 ELISAs. Half of the B cells were phenotypically characterized for expression of surface CD138 and LNGFR via flow cytometry. Genomic DNA was isolated from the other half of the B cells using the Zymo Research Quick-DNA Microprep Kit and ddPCR was performed and analyzed with a QX200 Droplet Generator and QX200 Droplet Reader (Bio-Rad) as previously described[149] using primers and guides in Table 2.2. The presence of feeders would lead to an underestimation of HDR editing. To account for this, gDNA was also harvested from a feeder-only plate and the estimated contribution of feeder-derived DNA was used to normalize calculated HDR rates.

Adoptive transfer and immunization

B cells were harvested from plates, washed with MACS buffer, and counted via hemocytometer before exchanging buffer into sterile PBS at an appropriate cell density. Cells were transferred intravenously (i.v.) in 200 µL via tail vein. Pooled B cells from 8-14 week-old mice of both sexes were transferred into age-matched male B6 and CD45.1-B6 mice in HEL-OVA immunization experiments. Pooled B cells from 8-14 week-old female mice were transferred into age-matched CD45.1-HemA mice of both sexes in HEL-C2 immunization experiments.

Where indicated, mice were immunized intraperitoneally (i.p.) with 25 µg HEL-OVA, 25 µg HEL-C2, or 100 µg NP-CGG prepared in Sigma Adjuvant System (Sigma-Aldrich) according to the manufacturer's directions.

ELISAs and Bethesda assays

For all mice except those of the HemA phenotype, serum was collected via bleeds from the submandibular or submental vein or terminally via cardiac puncture. In these experiments, blood was collected in BD Microtainer Blood Collection Tubes with clot activator and SST gel, spun at maximum speed on a benchtop microcentrifuge for 5 minutes. For experiments using HemA mice, serum was collected via retroorbital bleed with plain capillary tubes and dispensed into polypropylene microcentrifuge tubes, followed by centrifugation for 5 min at 5,000 x g. Supernatant was either used for ELISAs immediately or stored at -80°C until assayed. For measurement of total antibody secreted from cultured cells, culture supernatant was collected from centrifuged cell cultures and stored at -80°C until assayed. 96-well polystyrene plates were coated overnight at 4°C with 2 μg/mL goat α-mouse Ig (Southern Biotech), HEL, OVA, C2, or NP-BSA (ratio 1-9, Biosearch Technologies) in PBS. Wells were washed three times with 300 μL 0.05% Tween-20 in PBS (PBST) and blocked overnight with 200 μL 1% BSA, 0.05% Tween-20 in PBS at 4°C. Wells were washed three times with PBST and sevenfold serial dilutions of sera in duplicate were added to the wells with sevenfold dilutions of appropriate standards (mouse IgM, IgG, IgE, or IgA (Southern Biotech) and pooled B6 serum) in blocking buffer and the plates were incubated at RT for 90 mins. Wells were then washed six times with PBST and HRP goat α-mouse IgM, IgG, IgE, or IgA (Southern Biotech), diluted 1:2000 in blocking buffer, was added to wells and incubated at RT for 60 mins. Wells were then washed six times with PBST and treated with 100 μL TMB substrate (BD Bioscience) for 3-5 minutes before the addition of 100 μL stop solution (2N H_2SO_4). Absorbance at 450 nm was measured with a SpectraMax microplate reader (Molecular Devices). Concentrations of antibodies were calculated from standard curves generated

from diluted mouse IgM and IgG then corrected for plate-to-plate variation by normalization with the pooled B6 serum on every plate. Statistical differences in antibody in all experiments were calculated using a Kruskal-Willis test with a Dunn's test for multiple comparisons.

IL-10 ELISAs were performed with the Mouse IL-10 DuoSet ELISA (R&D Systems) according to the manufacturer's instructions. IL-10 concentrations were calculated via standard curve and blanked to control feeder wells without B cells, then normalized to cell concentration to report concentration per 1 x 10^6 B cells (edited and unedited). Statistical differences were calculated using a one-way ANOVA with a Tukey's test for multiple comparisons.

Bethesda assays were performed to examine FVIII inhibition as described previously[111,150] using a modified clotting assay with aPTT reagent and FVIII-deficient plasma. Residual activity numbers below 100 were subtracted from 100 and reported as percent inhibition of normal FVIII activity while residual activity calculated above 100 was reported as 0 percent inhibition. Statistical significance was calculated via Kruskal-Wallis test with a Dunn's multiple comparisons test.

Flow cytometry

Single-cell suspensions from spleens or cell cultures were incubated with fluorochrome-conjugated antibodies (Table 2.2) or antigen tetramer (prepared as reported previously[151]) for 20 min at RT in PBS, washed with 5 ml PBS supplemented with 2% FBS (FACS buffer), and resuspended in FACS buffer for acquisition. For experiments requiring cell counting, 50 µL of AccuCount Fluorescent Particles (Spherotech) was added to samples after final wash and used to quantify total cell numbers. Data were acquired on a LSR II or LSRFortessa and analysed using FlowJo (TreeStar).

Confocal microscopy and analysis

For confocal imaging, PFA-fixed and sectioned spleens were imaged as previously described using a Leica SP8 microscope[152]. Briefly, isolated spleens were fixed using BD Cytofix (BD Biosciences) diluted 1:3 in PBS for 24 hours at 4°C, and were then dehydrated with 30% sucrose solution for 1-3 days at 4°C. Spleens were cut longitudinally and then embedded in OCT compound (Tissue-Tek) and stored at -20°C. Spleens were sectioned on a Thermo Scientific Micron HM550 cryostat into 20µm sections and stained as previously described[152]. A Leica SP8 tiling confocal microscope equipped with a 20X 0.8NA oil objective was used for confocal image acquisition. Multiparameter confocal images were corrected for fluorophore spillover using the built-in Leica Channel Dye Separation module. Single stained controls were acquired using UltraComp eBeads (Invitrogen) that were incubated with fluorescently conjugated antibodies, mounted on slides with Fluormount-G slide mounting media (ThermoFisher), and imaged. All raw imaging data was processed, visualized, and analyzed using Imaris (Bitplane).

For analysis of germinal centers, surfaces were created on GL7 signal using the surface object creation wizard in Imaris. Surfaces were then filtered by volume and positive Bcl6 signal. In some experiments, another filter was applied for positive CD21/35 signal. Volume and CD45.2 mean intensity signal, representing relative abundance of transferred B cells, was then exported for each germinal center surface and plotted.

Data Availability.

The data that support the findings of this study are available from the corresponding author, D.J.R., upon reasonable request.

2.5 Figures

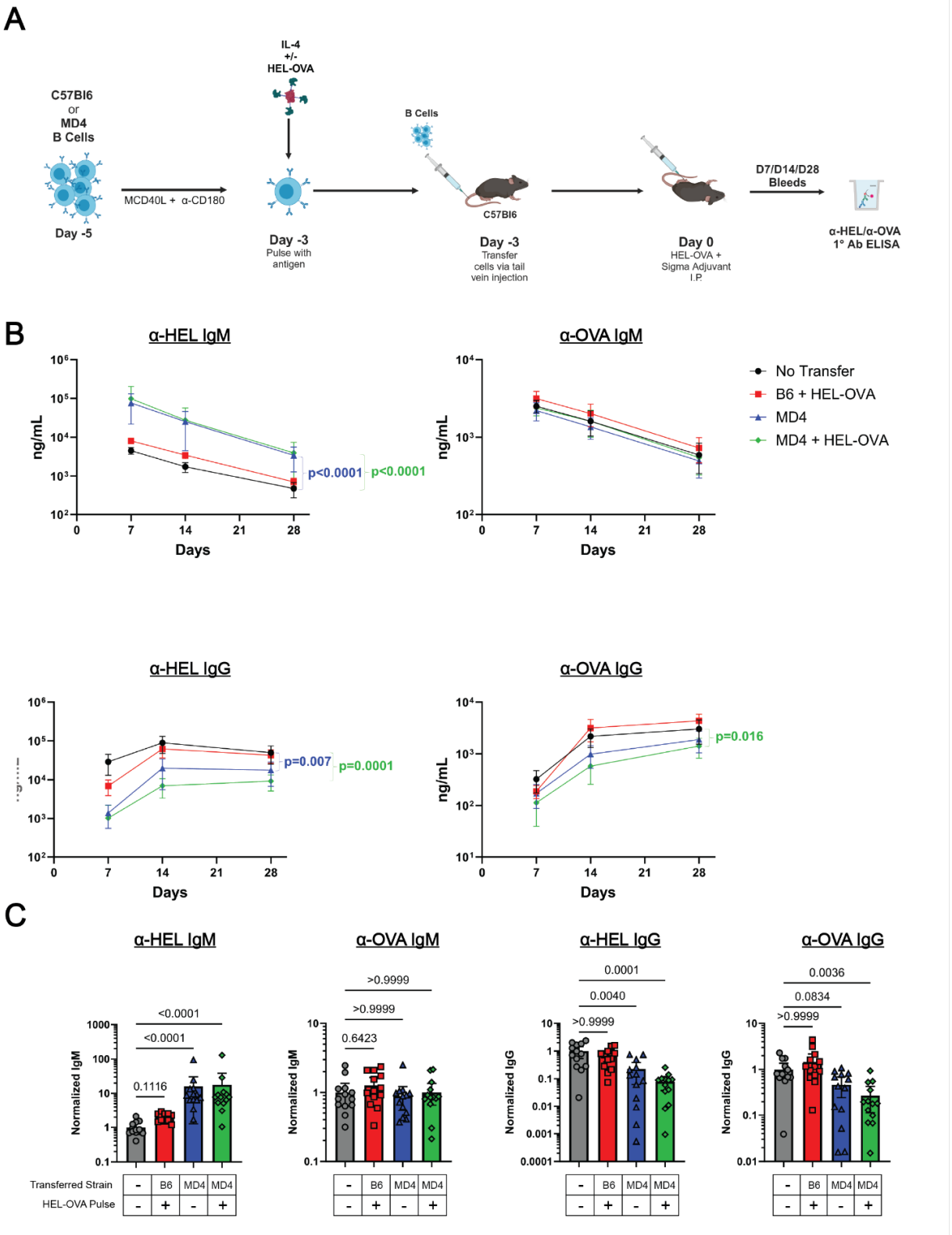
A
C57Bl6
or
MD4
B Cells
Day -5
MCD40L + α-CD180
IL-4
+/-
HEL-OVA
Day -3
Pulse with
antigen
B Cells
C57Bl6
Day -3
Transfer
cells via tail
vein injection
Day 0
HEL-OVA +
Sigma Adjuvant
I.P.
D7/D14/D28
Bleeds
α-HEL/α-OVA
1° Ab ELISA
B
α-HEL IgM
α-OVA IgM
ng/mL
Days
p<0.0001
p<0.0001
No Transfer
B6 + HEL-OVA
MD4
MD4 + HEL-OVA
α-HEL IgG
α-OVA IgG
p=0.007
p=0.0001
p=0.016
C
α-HEL IgM
α-OVA IgM
α-HEL IgG
α-OVA IgG
Normalized IgM
Normalized IgG
<0.0001
<0.0001
0.1116
>0.9999
>0.9999
0.6423
0.0001
0.0040
>0.9999
0.0036
0.0834
>0.9999
Transferred Strain
HEL-OVA Pulse
B6
MD4
MD4

Figure 2.1. Antigen-primed MD4 B cells reduce endogenous humoral responses to both cognate and linked antigen. A) Workflow for experiment. Splenic B cells were enriched from a single-cell suspension and incubated *ex vivo* in the presence of MCD40L and α-CD180 for 2 days before IL-4 was then added with or without HEL-OVA for an additional 2 hours. B cells were then washed and 1 x 10^7 were transferred via tail vein into B6 mice. These mice in addition to "No Transfer" (NT) controls were immunized 3 days later with HEL-OVA antigen in Sigma Adjuvant (IP). Mice were bled thereafter for ELISA analysis. Created with BioRender. **B)** Time course ELISA data for α-HEL and α-OVA IgM and total IgG. Data presented as mean ng/mL IgM or IgG. *p* values shown represent comparisons between the color-coded treatment condition and NT and were calculated using a Kruskal-Wallis test to analyze area under the curve values with Dunn's test for multiple comparisons. **C)** Day 14 α-HEL and α-OVA IgM and total IgG. Data presented as measured antibody normalized to the NT population average. *p* values were calculated using Kruskal-Wallis with Dunn's test for multiple comparisons. n=13 per condition from 2 experimental repeats. All error bars indicate 95% CI.

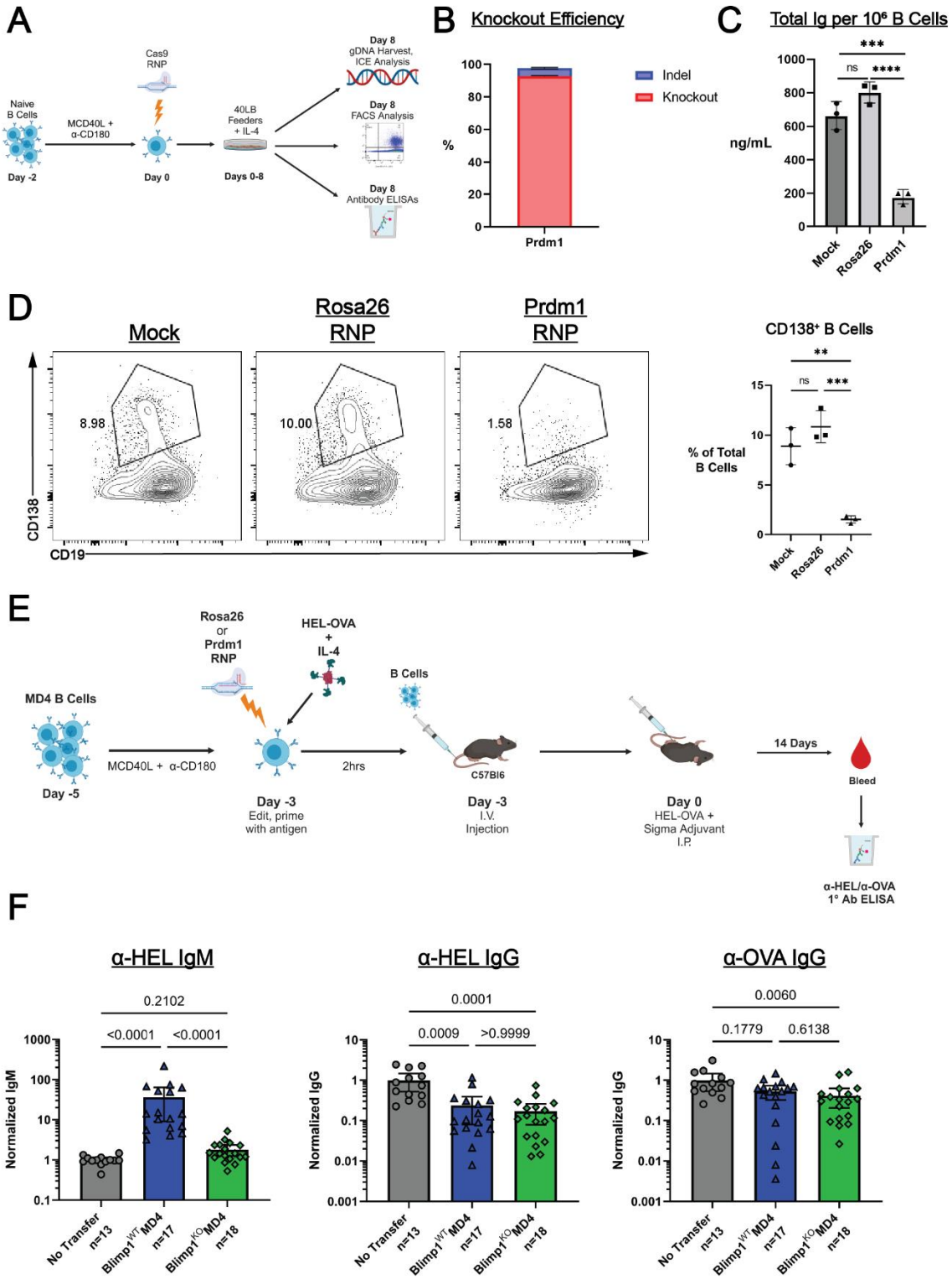
A
Naive B Cells
Day -2
MCD40L + α-CD180
Cas9 RNP
Day 0
40LB Feeders + IL-4
Days 0-8
Day 8 gDNA Harvest, ICE Analysis
Day 8 FACS Analysis
Day 8 Antibody ELISAs
B
Knockout Efficiency
%
Indel
Knockout
Prdm1
C
Total Ig per 10⁶ B Cells
ng/mL
***
ns
****
Mock
Rosa26
Prdm1
D
Mock
Rosa26 RNP
Prdm1 RNP
8.98
10.00
1.58
CD138
CD19
CD138⁺ B Cells
% of Total B Cells
**
ns
***
E
MD4 B Cells
Day -5
MCD40L + α-CD180
Rosa26 or Prdm1 RNP
HEL-OVA + IL-4
Day -3 Edit, prime with antigen
B Cells
2hrs
C57Bl6
Day -3 I.V. Injection
Day 0 HEL-OVA + Sigma Adjuvant I.P.
14 Days
Bleed
α-HEL/α-OVA 1° Ab ELISA
F
α-HEL IgM
0.2102
<0.0001
<0.0001
Normalized IgM
α-HEL IgG
0.0001
0.0009
>0.9999
Normalized IgG
α-OVA IgG
0.0060
0.1779
0.6138
Normalized IgG
No Transfer n=13
Blimp1WT MD4 n=17
Blimp1KO MD4 n=18

Figure 2.2. Antigen-primed Blimp1-deficient MD4 decoy B cells blunt specific endogenous humoral responses without secreting antibody. **A)** Experimental workflow for knocking out Blimp1. Enriched B cells are electroporated with Cas9 ribonucleoproteins (RNP) targeting either Rosa26 or Prdm1 after 2 days of stimulation *in vitro,* then cultured for 8 days on 40LB feeder cells in the presence of IL-4. Feeders are depleted and genomic DNA collected from expanded B cells for ICE analysis. B cells are analyzed for differentiation via FACS. Supernatant is collected and total Ig secretion is measured via ELISA. Generated with BioRender. **B)** Mean indel and knockout rates in the *Prdm1* gene of edited B cells at Day 8, as measured via ICE. N=3 biological replicates. **C)** Mean concentration of total Ig (combined IgM, IgG, IgA, and IgE) in supernatant of expanded B cells at Day 8, as measured by ELISA. n=3 biological replicates per condition. *p* values calculated via one-way ANOVA with a Tukey's test for multiple comparisons. **D)** Representative FACS plots (left panels) and summary data (right panel) showing $CD19^{lo}CD138^{+}$ ASC proportion within treated cell populations, gated as $Live/Dead^{-}H\text{-}2Kd^{-}$ lymphocyte singlets. n=3 biological replicates per condition. *p* values calculated via one-way ANOVA with a Tukey's test for multiple comparisons. **E)** Workflow for treating mice with CRISPR-edited B cells. Enriched B cells were electroporated with *Rosa26*- or *Prdm1*-targeted RNP and primed with IL-4 and HEL-OVA for 2 hours before adoptive transfer of 6×10^6 cells into B6 mice. Recipient and NT control mice were immunized 3 days later with HEL-OVA antigen in Sigma Adjuvant. Mice were bled thereafter for ELISA analysis. Created with BioRender. **F)** Day 14 α-HEL IgM, α-HEL IgG, and α-OVA IgG. Data presented as measured antibody normalized to the NT population average. *p* values were calculated using Kruskal-Wallis with Dunn's test for multiple comparisons. Total n per condition from 2 experimental repeats indicated on graph. All error bars indicate 95% CI.

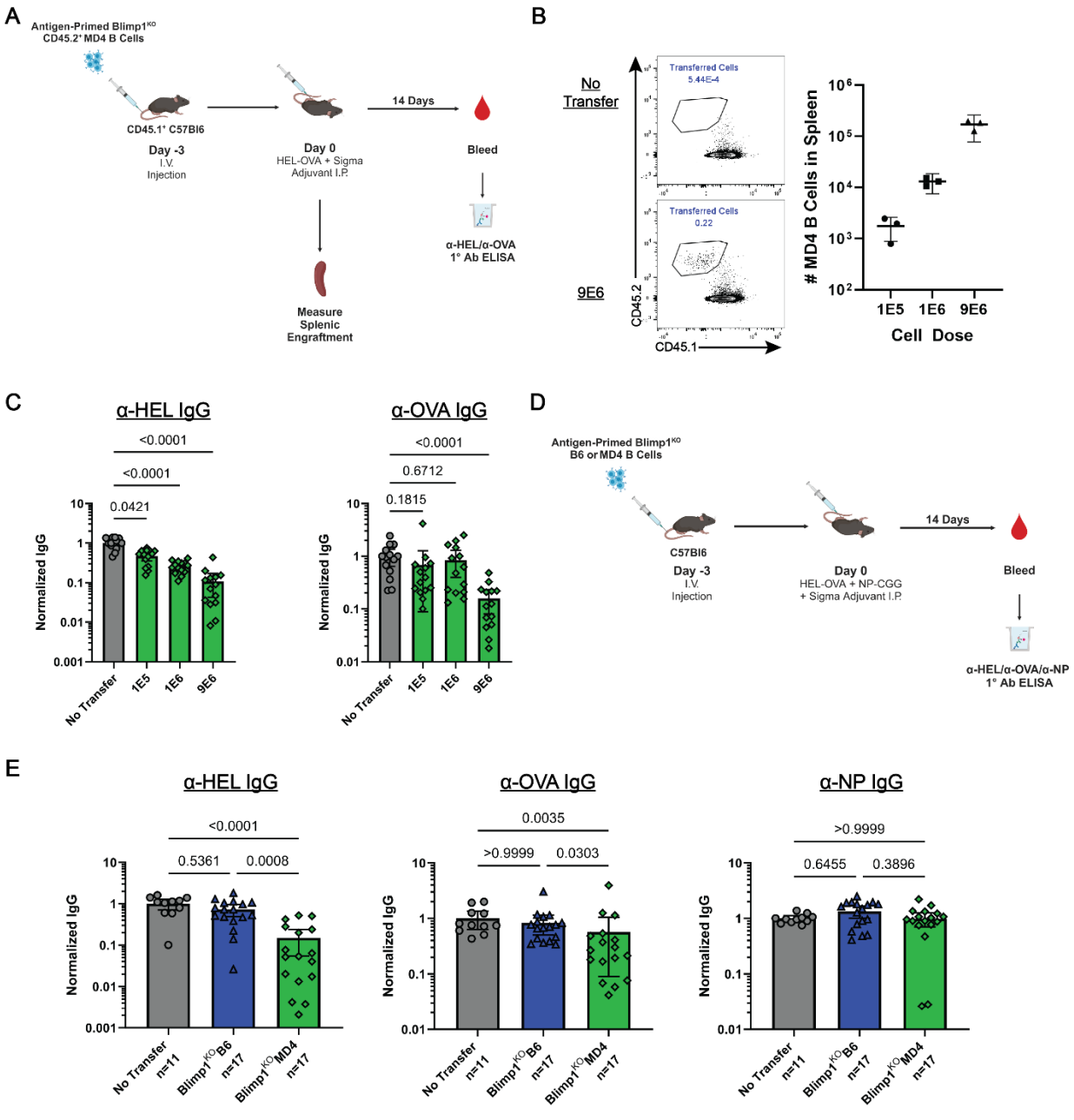
A
Antigen-Primed Blimp1KO CD45.2+ MD4 B Cells
CD45.1+ C57Bl6
Day -3
I.V. Injection
Day 0
HEL-OVA + Sigma Adjuvant I.P.
14 Days
Bleed
α-HEL/α-OVA 1° Ab ELISA
Measure Splenic Engraftment
B
No Transfer
9E6
Transferred Cells
5.44E-4
Transferred Cells
0.22
CD45.2
CD45.1
MD4 B Cells in Spleen
1E5
1E6
9E6
Cell Dose
C
α-HEL IgG
α-OVA IgG
<0.0001
<0.0001
0.0421
<0.0001
0.6712
0.1815
Normalized IgG
No Transfer
1E5
1E6
9E6
D
Antigen-Primed Blimp1KO B6 or MD4 B Cells
C57Bl6
Day -3
I.V. Injection
Day 0
HEL-OVA + NP-CGG + Sigma Adjuvant I.P.
14 Days
Bleed
α-HEL/α-OVA/α-NP 1° Ab ELISA
E
α-HEL IgG
α-OVA IgG
α-NP IgG
<0.0001
0.5361
0.0008
0.0035
>0.9999
0.0303
>0.9999
0.6455
0.3896
Normalized IgG
No Transfer n=11
Blimp1KO B6 n=17
Blimp1KO MD4 n=17

Figure 2.3. Blimp1^{KO}MD4 B cells mediate dose-dependent suppression of antigen-specific IgG responses without impacting simultaneous responses to an unrelated antigenic challenge. A) Workflow for examining the impact of cell dose on decoy-mediated suppression of antigen-specific antibody. Created with BioRender. **B)** Representative FACS plots (left) and summary data (right) showing mean engraftment of antigen-primed Blimp1^{KO}MD4 B cells across a range of adoptive cell doses, gated as Live/Dead^{-}Dump^{-}CD19^{+} lymphocyte singlets. n=3 biological replicates per condition. *p* values calculated via one-way ANOVA with a Tukey's test for multiple comparisons. **C)** Day 14 α-HEL IgG and α-OVA IgG. Data presented as measured antibody normalized to the NT population average. *p* values were calculated using Kruskal-Wallis with Dunn's test for multiple comparisons. n=13 per condition from 2 experimental repeats. **D)** Workflow for dual immunizing mice following adoptive transfer of Blimp1^{KO} B cells. Blimp1^{KO} B6 or MD4 B cells were antigen-primed and 7 x 10^6 cells were transferred into B6 mice. Recipient and NT controls were immunized 3 days later with both HEL-OVA and NP-CGG antigen in Sigma Adjuvant. Mice were bled thereafter for ELISA analysis. Created with BioRender. **E)** Day 14 α-HEL, α-OVA, and α-NP IgG. Data presented as measured antibody normalized to the NT population average. *p* values were calculated using Kruskal-Wallis with Dunn's test for multiple comparisons. Total n per condition from 2 experimental repeats indicated on graph. All error bars indicate 95% CI.

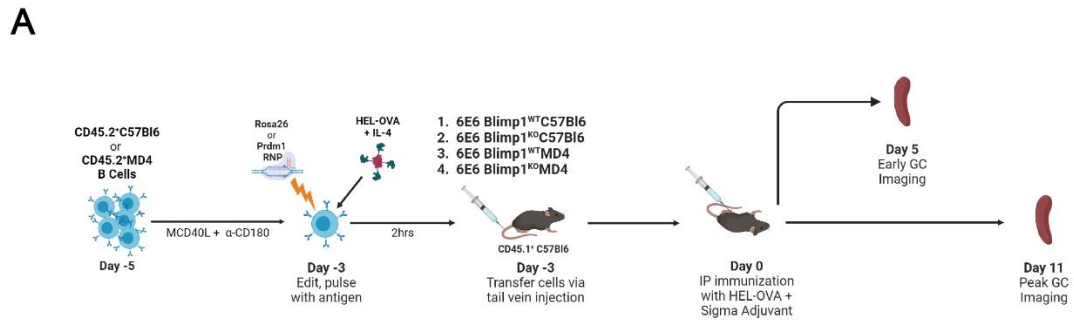
A
CD45.2+C57Bl6
or
CD45.2+MD4
B Cells
Day -5
MCD40L + α-CD180
Rosa26
or
Prdm1
RNP
HEL-OVA
+ IL-4
Day -3
Edit, pulse
with antigen
2hrs
1. 6E6 Blimp1WTC57Bl6
2. 6E6 Blimp1KOC57Bl6
3. 6E6 Blimp1WTMD4
4. 6E6 Blimp1KOMD4
CD45.1+ C57Bl6
Day -3
Transfer cells via
tail vein injection
Day 0
IP immunization
with HEL-OVA +
Sigma Adjuvant
Day 5
Early GC
Imaging
Day 11
Peak GC
Imaging

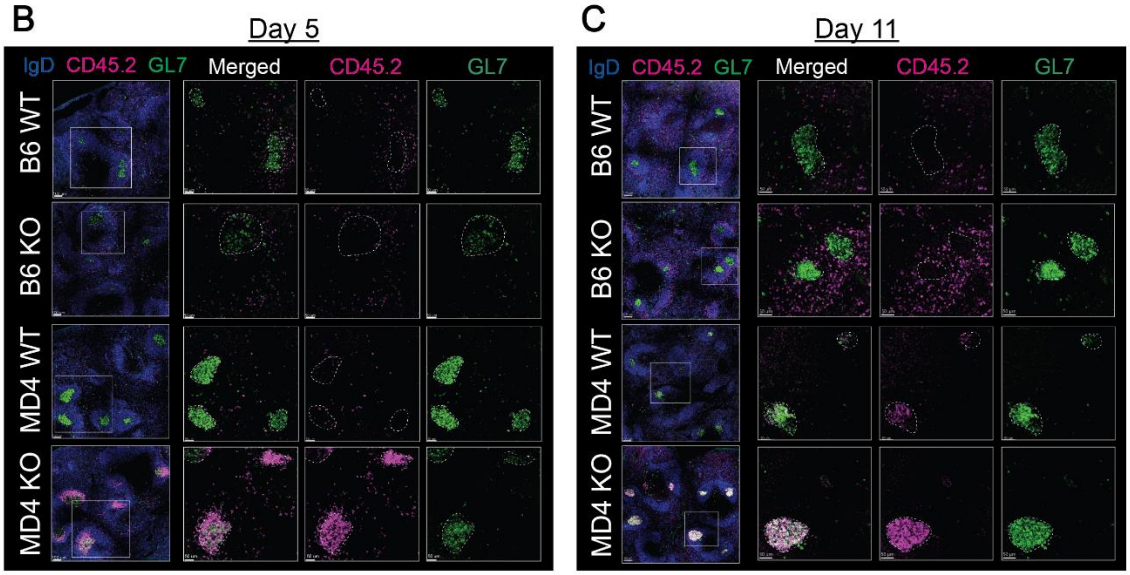
B
Day 5
IgD CD45.2 GL7 Merged CD45.2 GL7
B6 WT
B6 KO
MD4 WT
MD4 KO
C
Day 11
IgD CD45.2 GL7 Merged CD45.2 GL7
B6 WT
B6 KO
MD4 WT
MD4 KO

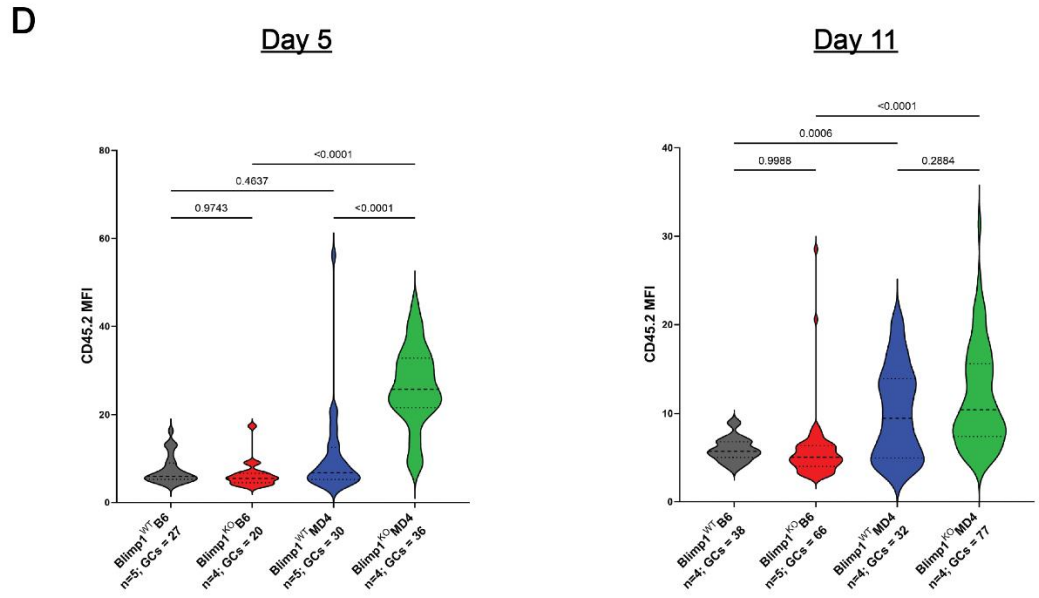
D
Day 5
CD45.2 MFI
<0.0001
0.4637
0.9743
<0.0001
BlimpWT B6
n=5; GCs = 27
BlimpKO B6
n=4; GCs = 20
BlimpWT MD4
n=5; GCs = 30
BlimpKO MD4
n=4; GCs = 36
Day 11
CD45.2 MFI
<0.0001
0.0006
0.9988
0.2884
BlimpWT B6
n=4; GCs = 38
BlimpKO B6
n=5; GCs = 66
BlimpWT MD4
n=4; GCs = 32
BlimpKO MD4
n=4; GCs = 77

Figure 2.4. Blimp1^{KO}MD4 decoy B cells dominate germinal centers. A) Workflow for microscopy experiments. CD45.2^{+}B6 or CD45.2^{+}MD4 B cells are enriched and stimulated, electroporated with either Rosa26- or Prdm1-targeted RNPs followed by antigen priming. 6 x 10^6 Blimp1^{WT}B6, Blimp1^{KO}B6, Blimp1^{WT}MD4, or Blimp1^{KO}MD4 B cells were adoptively transferred into CD45.1^{+}B6 recipient mice. Three days later recipient mice were immunized with HEL-OVA. Mice were sacrificed at Day 5 or Day 11 for GC analysis via confocal microscopy. Created with BioRender. **B)** Representative micrographs of splenic GCs in mice 5 days after immunization. **C)** Representative micrographs of splenic GCs in mice 11 days after immunization. **D)** CD45.2 mean fluorescence intensity of GCs on Day 5 (left) and Day 11 (right). *p* values were calculated using a one-way ANOVA with Šidák's test for multiple comparisons. Number of mice per condition as well as total number of GCs analyzed are indicated for each group. Representative of two experimental repeats.

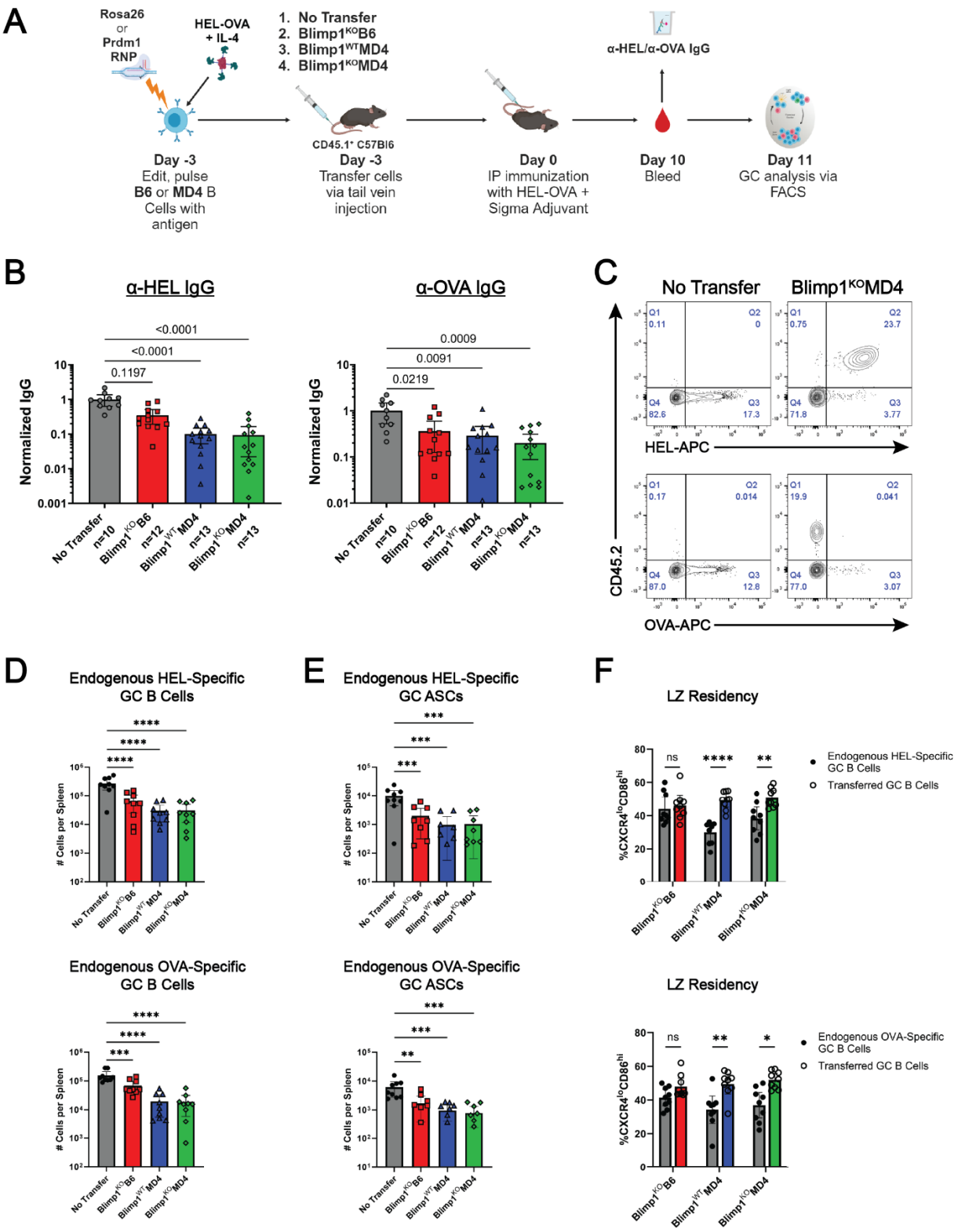
A
Rosa26
or
Prdm1
RNP
HEL-OVA
+ IL-4
1. No Transfer
2. Blimp1KOB6
3. Blimp1WTMD4
4. Blimp1KOMD4
α-HEL/α-OVA IgG
CD45.1+ C57Bl6
Day -3
Edit, pulse
B6 or MD4 B
Cells with
antigen
Day -3
Transfer cells
via tail vein
injection
Day 0
IP immunization
with HEL-OVA +
Sigma Adjuvant
Day 10
Bleed
Day 11
GC analysis via
FACS
B
α-HEL IgG
α-OVA IgG
Normalized IgG
<0.0001
<0.0001
0.1197
0.0009
0.0091
0.0219
No Transfer n=10
Blimp1KOB6 n=12
Blimp1WTMD4 n=13
Blimp1KOMD4 n=13
C
No Transfer
Blimp1KOMD4
HEL-APC
CD45.2
OVA-APC
Q1 0.11
Q2 0
Q4 82.6
Q3 17.3
Q1 0.75
Q2 23.7
Q4 71.8
Q3 3.77
Q1 0.17
Q2 0.014
Q4 87.0
Q3 12.8
Q1 19.9
Q2 0.041
Q4 77.0
Q3 3.07
D
Endogenous HEL-Specific
GC B Cells
Endogenous OVA-Specific
GC B Cells
Cells per Spleen
E
Endogenous HEL-Specific
GC ASCs
Endogenous OVA-Specific
GC ASCs
F
LZ Residency
%CXCR4loCD86hi
ns
Endogenous HEL-Specific
GC B Cells
Transferred GC B Cells
LZ Residency
Endogenous OVA-Specific
GC B Cells
Transferred GC B Cells

Figure 2.5. Blimp1^{KO}MD4 decoy B cells outcompete endogenous B cells for germinal center entry and access to the light zone. A) Workflow for GC analysis experiments. CD45.2^{+}B6 or CD45.2^{+}MD4 B cells were enriched. stimulated, then electroporated with either *Rosa26*- or *Prdm1*-targeted RNPs prior to 2-hour antigen priming. 6 x 10^{6} Blimp1^{KO}B6, Blimp1^{WT}MD4, or Blimp1^{KO}MD4 B cells were adoptively transferred into CD45.1^{+}B6 recipient mice. Three days later recipient mice were immunized with HEL-OVA. Mice were bled for ELISA analysis 10 days later and sacrificed 1 day later for GC analysis. Created with BioRender. **B)** Day 10 α-HEL and α-OVA IgG. Data presented as measured antibody normalized to the NT population average. *p* values were calculated using Kruskal-Wallis with Dunn's test for multiple comparisons. Total n per condition from 2 experimental repeats indicated on graph. **C)** Representative FACS plots showing adoptively transferred antigen-specific vs. endogenous GC B cells. Gated as Live/Dead^{-} Dump^{-}CD19^{+}PNA^{+}CD38^{-} lymphocyte singlets (see also Supplementary Figure 4). **D)** Absolute counts per spleen of endogenous HEL-specific (top) or OVA-specific (bottom) GC B cells across treatment conditions. *p* values were calculated using one-way ANOVA with Tukey's test for multiple comparisons. **E)** Absolute counts per spleen of endogenous HEL-specific (top) or OVA-specific (bottom) GC ASCs, defined as the CD138^{+} subset of **(D)**, across treatment conditions. *p* values were calculated using one-way ANOVA with Tukey's test for multiple comparisons. **F)** Light zone residency (defined as GC B cells in the CXCR4^{lo}CD86^{hi} subset) of transferred cells vs. endogenous HEL-specific (top) or OVA-specific (bottom) GC B cells. *p* values were calculated using a repeated measures one-way ANOVA with Šidák's test for multiple comparisons. n=9 per condition from 2 experimental repeats for D-F. All error bars indicate 95% CI. (*p<0.05; **p<0.01; ***p<0.001; ****p<0.0001)

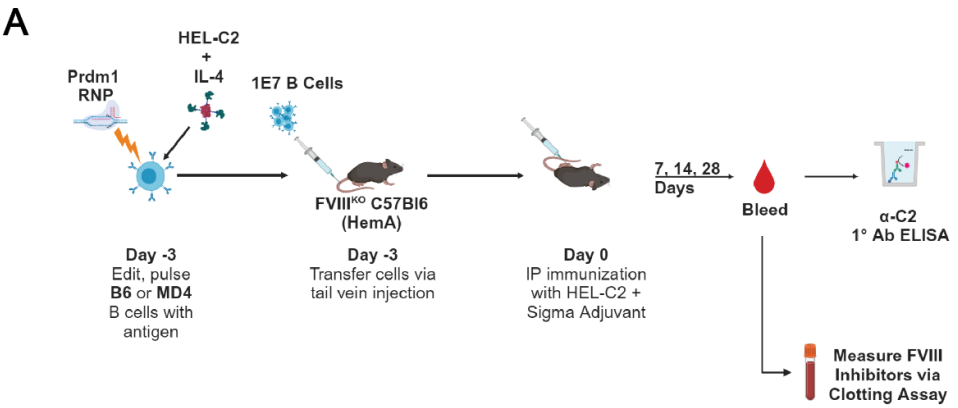
A
HEL-C2
+
IL-4
Prdm1
RNP
1E7 B Cells
FVIII^KO C57Bl6
(HemA)
7, 14, 28
Days
Bleed
α-C2
1° Ab ELISA
Day -3
Edit, pulse
B6 or MD4
B cells with
antigen
Day -3
Transfer cells via
tail vein injection
Day 0
IP immunization
with HEL-C2 +
Sigma Adjuvant
Measure FVIII
Inhibitors via
Clotting Assay

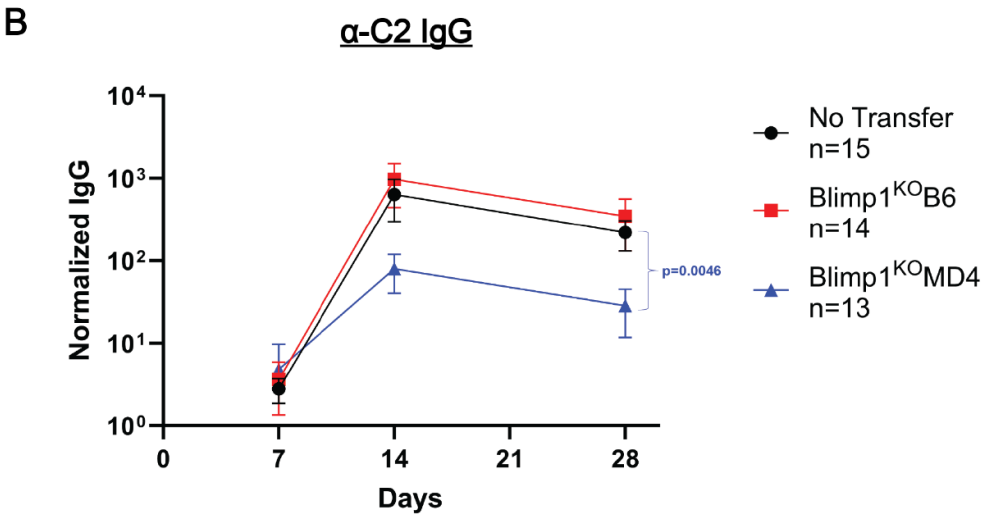
B
α-C2 IgG
Normalized IgG
10^4
10^3
10^2
10^1
10^0
0
7
14
21
28
Days
p=0.0046
No Transfer
n=15
Blimp1^KOB6
n=14
Blimp1^KOMD4
n=13

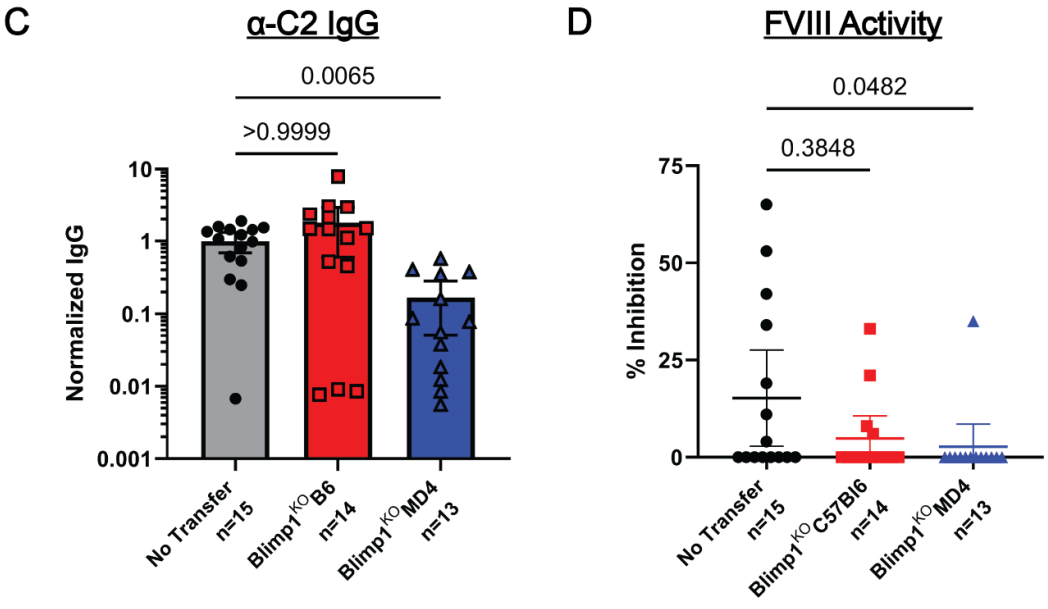
C
α-C2 IgG
0.0065
>0.9999
Normalized IgG
10
1
0.1
0.01
0.001
No Transfer
n=15
Blimp1^KOB6
n=14
Blimp1^KOMD4
n=13
D
FVIII Activity
0.0482
0.3848
% Inhibition
75
50
25
0
No Transfer
n=15
Blimp1^KOC57Bl6
n=14
Blimp1^KOMD4
n=13

Figure 2.6. Antigen-primed Blimp1^{KO}MD4 decoy B cells suppress the generation of C2-specific IgG and reduce the incidence of functional FVIII inhibition. A) Workflow for experiment. Blimp1^{KO}B6 or Blimp1^{KO}MD4 B cells were primed with HEL-C2 conjugate antigen and 10^7 cells were transferred via tail vein into HemA mice. Recipient mice were immunized i.p. three days later with the HEL-C2 antigen. Mice were bled at days 7, 14, and 28 and their serum tested for α-C2 IgG via ELISA and functional FVIII inhibitors via clotting assay. **B)** Time course ELISA data for α-C2 IgG. Data presented as mean fold difference in antibody relative to pooled serum from unimmunized HemA mice. *p* value shown represents comparison between the Blimp1^{KO}MD4 and NT conditions and was calculated using a Kruskal-Wallis test to analyze area under the curve values with Dunn's test for multiple comparisons. **C)** Day 28 α-C2 IgG. Data presented as measured antibody normalized to the NT population average. *p* values were calculated using Kruskal-Wallis with Dunn's test for multiple comparisons. Total n per condition from 2 experimental repeats indicated on graph. **D)** Day 28 FVIII inhibition as measured via Bethesda clotting assay. Data presented as % inhibition of FVIII-mediated clotting relative to control. *p* values were calculated using Kruskal-Wallis with Dunn's test for multiple comparisons. Total n per condition from 2 experimental repeats indicated on graph. All error bars indicate 95% CI.

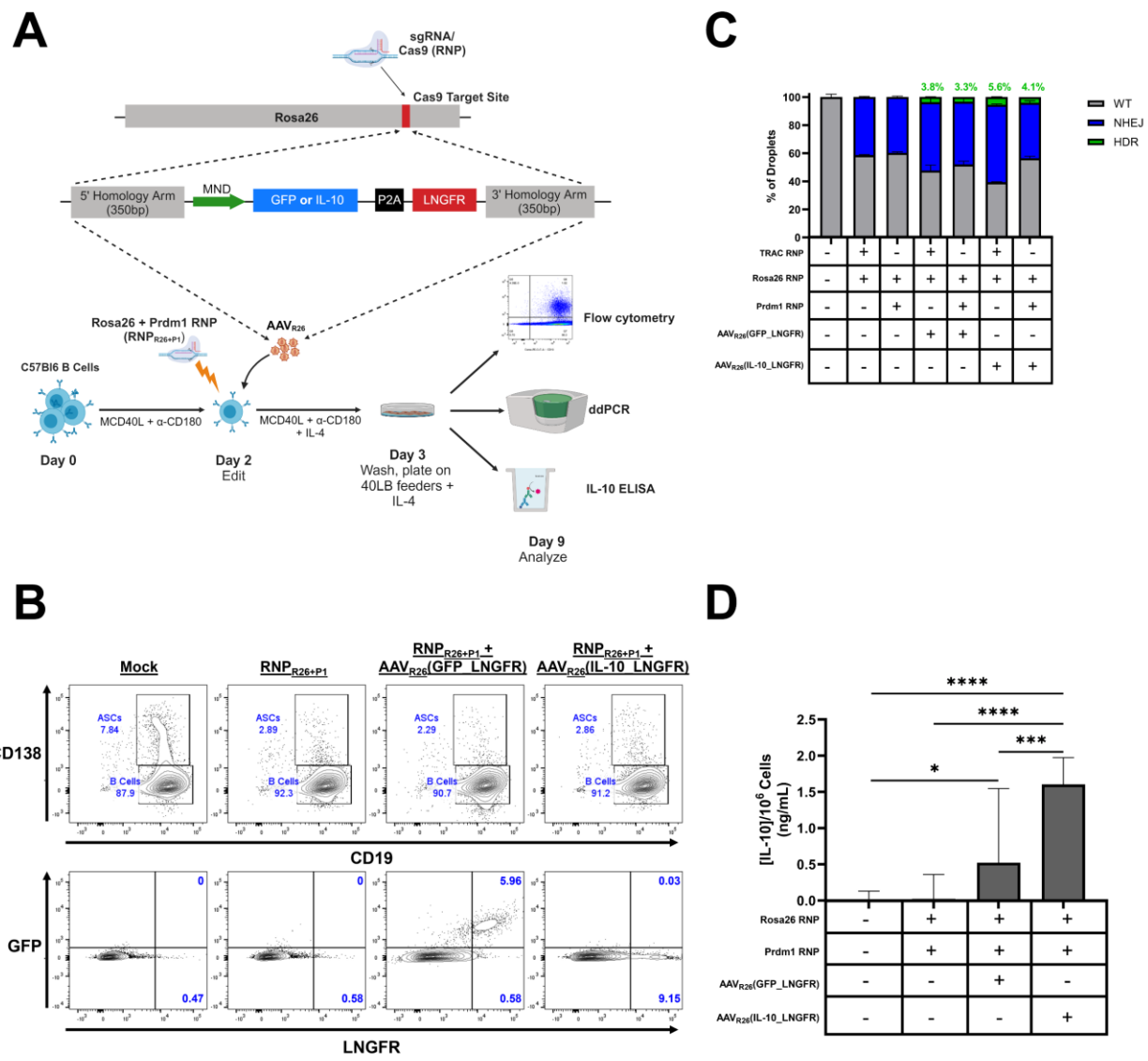
A
sgRNA/
Cas9 (RNP)
Cas9 Target Site
Rosa26
5' Homology Arm
(350bp)
MND
GFP or IL-10
P2A
LNGFR
3' Homology Arm
(350bp)
Rosa26 + Prdm1 RNP
(RNP R26+P1)
AAV R26
C57Bl6 B Cells
MCD40L + α-CD180
MCD40L + α-CD180
+ IL-4
Day 0
Day 2
Edit
Day 3
Wash, plate on
40LB feeders +
IL-4
Flow cytometry
ddPCR
IL-10 ELISA
Day 9
Analyze
C
% of Droplets
3.8%
3.3%
5.6%
4.1%
WT
NHEJ
HDR
TRAC RNP
Rosa26 RNP
Prdm1 RNP
AAV R26(GFP_LNGFR)
AAV R26(IL-10_LNGFR)
B
Mock
RNP R26+P1
RNP R26+P1 +
AAV R26(GFP_LNGFR)
RNP R26+P1 +
AAV R26(IL-10_LNGFR)
CD138
CD19
GFP
LNGFR
ASCs
7.84
B Cells
87.9
ASCs
2.89
B Cells
92.3
ASCs
2.29
B Cells
90.7
ASCs
2.86
B Cells
91.2
0
0.47
0
0.58
5.96
0.58
0.03
9.15
D
[IL-10]/10^6 Cells
(ng/mL)
****
****
***
*
Rosa26 RNP
Prdm1 RNP
AAV R26(GFP_LNGFR)
AAV R26(IL-10_LNGFR)

Figure 2.7. Dual-edited primary murine B cells constitutively secrete IL-10 without differentiating. **A)** Experimental workflow for dual-editing B cells. Enriched B cells are electroporated with RNPs targeting both *Rosa26* and *Prdm1* after 2 days of stimulation *in vitro,* then cultured for 6 days on 40LB feeder cells in the presence of IL-4. B cells are analyzed for differentiation via FACS. Genomic DNA is collected from cells and HDR is calculated via ddPCR. Supernatant is collected and Il-10 secretion is measured via ELISA. Generated with BioRender. **B)** Representative FACS plots showing $CD19^{lo}CD138^{+}$ ASC proportion and $LNGFR^{+}$ Rosa26-edited proportions within treated cell populations, gated as Live/$Dead^{-}H\text{-}2Kd^{-}$ lymphocyte singlets. **C)** Mean NHEJ and HDR rates in the *Rosa26* gene of edited B cells at Day 6, as measured via ddPCR. **D)** Mean concentration of IL-10 in supernatant of expanded B cells at Day 9, as measured by ELISA. n=3 technical replicates per condition. *p* values calculated via one-way ANOVA with a Tukey's test for multiple comparisons. Data from one experiment but representative of greater than 10 experiments. All error bars indicate 95% CI.

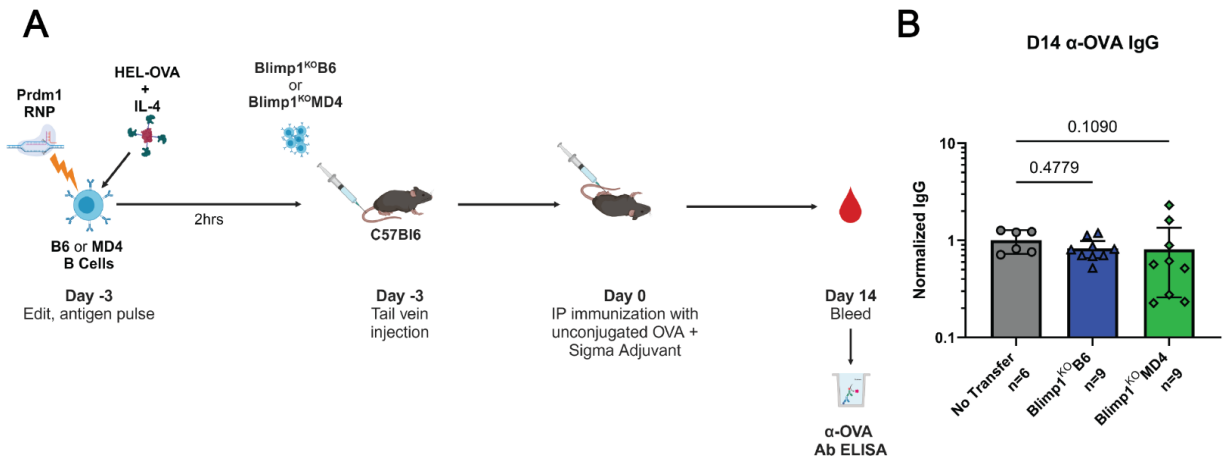

Figure 2.S1. HEL-OVA priming is insufficient for Blimp1^{KO}MD4 B cells to blunt OVA-specific humoral responses upon immunization with unconjugated OVA. A) Experimental workflow. Enriched B cells were electroporated with *Prdm1*-targeted RNP and primed with IL-4 and HEL-OVA for 2 hours before adoptive transfer of 7 x 10^6 cells into C57Bl6 mice. These mice in addition to NT controls were immunized 3 days later with unconjugated OVA antigen in Sigma Adjuvant. Mice were bled thereafter for ELISA analysis. Created with BioRender. **B)** Day 14 α-OVA IgG. Data presented as measured antibody normalized to the NT population average. *p* values were calculated using Kruskal-Wallis with Dunn's test for multiple comparisons. Total n per condition from 1 experimental repeat indicated on graph. All error bars indicate 95% CI.

A

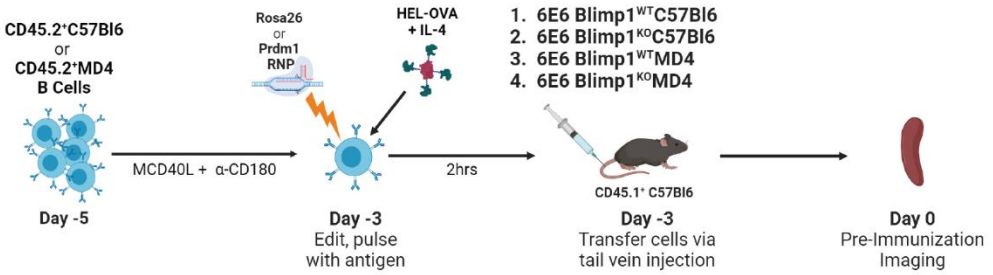
CD45.2+C57Bl6
or
CD45.2+MD4
B Cells
Day -5
MCD40L + α-CD180
Rosa26
or
Prdm1
RNP
HEL-OVA
+ IL-4
Day -3
Edit, pulse
with antigen
2hrs
1. 6E6 Blimp1WTC57Bl6
2. 6E6 Blimp1KOC57Bl6
3. 6E6 Blimp1WTMD4
4. 6E6 Blimp1KOMD4
CD45.1+ C57Bl6
Day -3
Transfer cells via
tail vein injection
Day 0
Pre-Immunization
Imaging

B

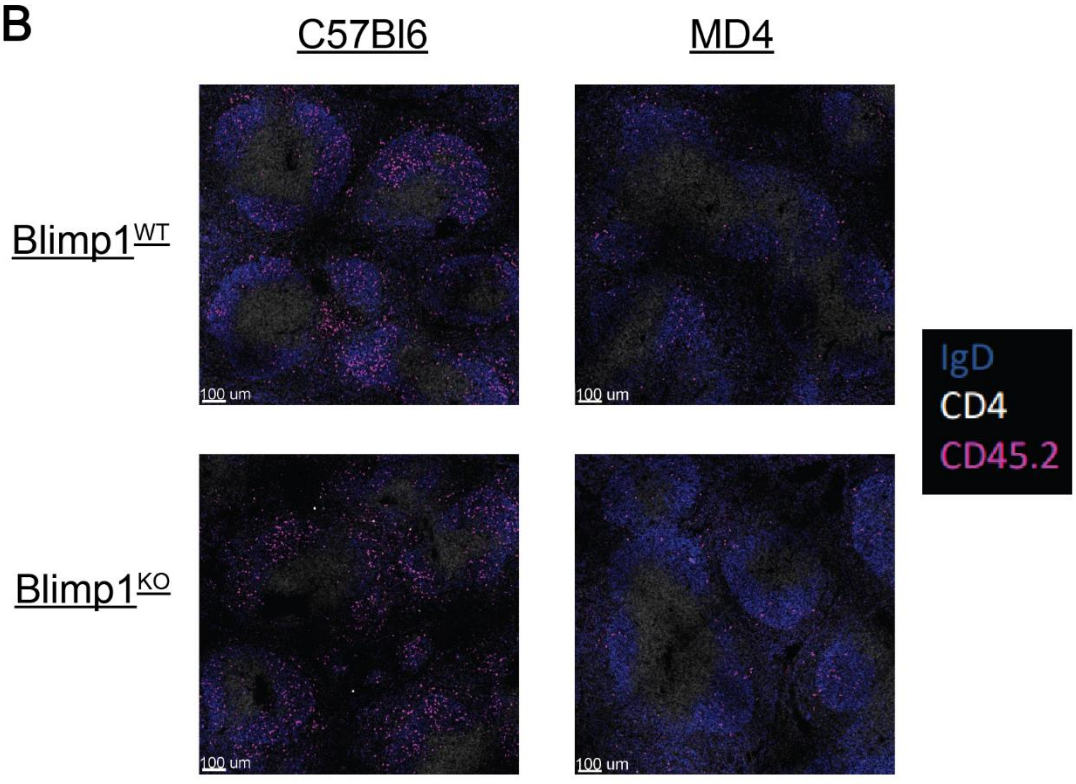
C57Bl6
MD4
Blimp1WT
Blimp1KO
100 um
100 um
100 um
100 um
IgD
CD4
CD45.2

Figure 2.S2. B cells are distributed throughout B cell follicles three days after adoptive transfer. A) Workflow for microscopy experiments. CD45.2^{+}B6 or CD45.2^{+}MD4 B cells are enriched and stimmed as before, then electroporated with either Rosa26- or Prdm1-targeted RNPs before 2-hour antigen priming. CD45.1^{+}B6 mice then received 6 x 10^{6} Blimp1^{WT}B6, Blimp1^{KO}B6, Blimp1^{WT}MD4, or Blimp1^{KO}MD4 B cells. Three days later the mice were sacrificed and their spleens analyzed via confocal microscopy. Created with BioRender. **B)** Representative confocal micrographs of spleens from mice three days after receipt of Blimp1^{WT}B6, Blimp1^{WT}MD4, Blimp1^{KO}B6, or Blimp1^{KO}MD4 B cells. B cell follicles. IgD = blue; CD4 = grey; CD45.2 = magenta

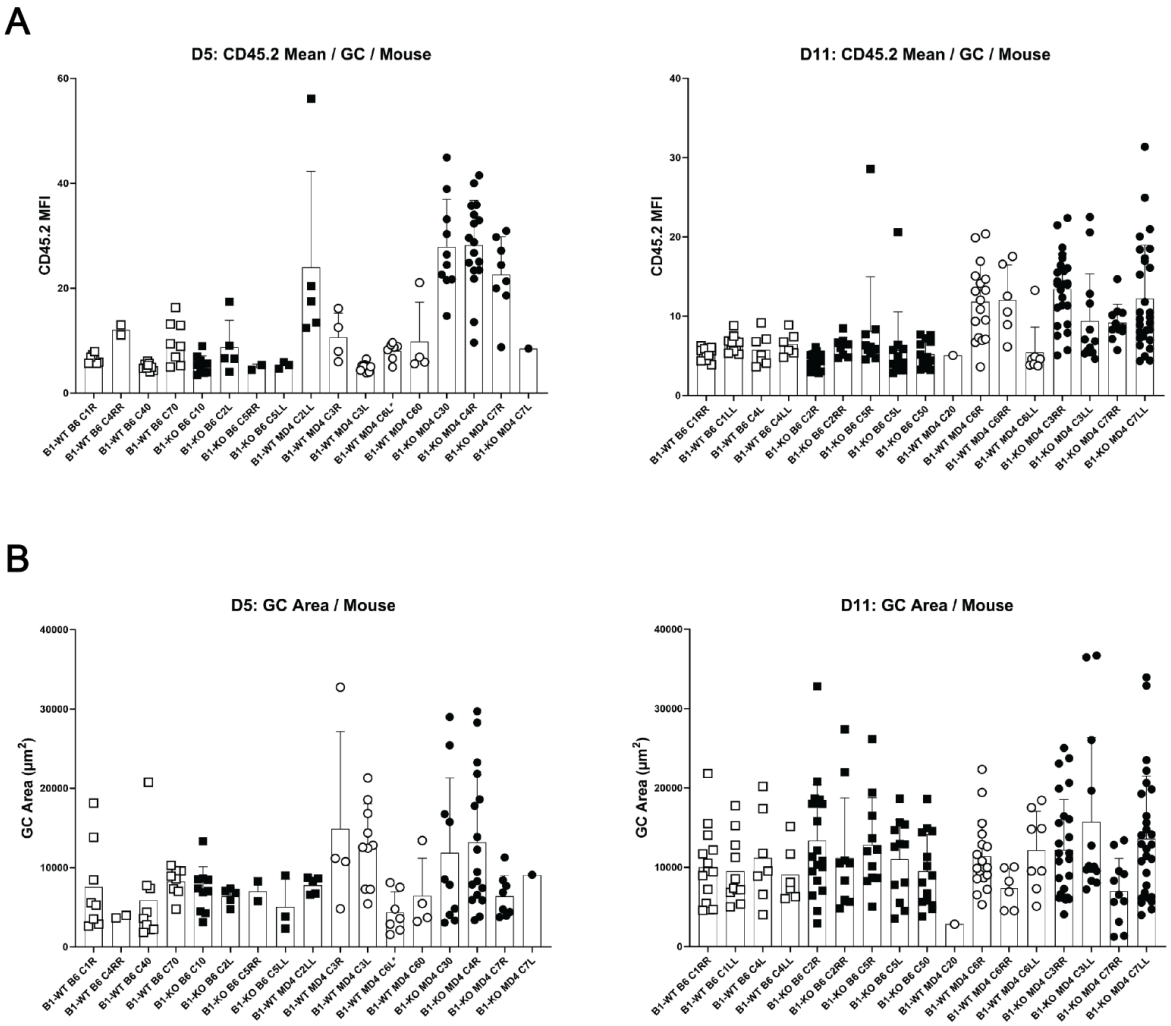

Figure 2.S3. Per-mouse quantitative analysis for confocal microscopy. A) Measured CD45.2 mean fluorescence intensity per germinal center in analyzed mice. Each bar represents a different mouse and each point a different germinal center in that mouse. **B)** Measured GC area per germinal center in analyzed mice. Each bar represents a separate mouse and each point a different germinal center in that mouse. All error bars indicate 95% CI.

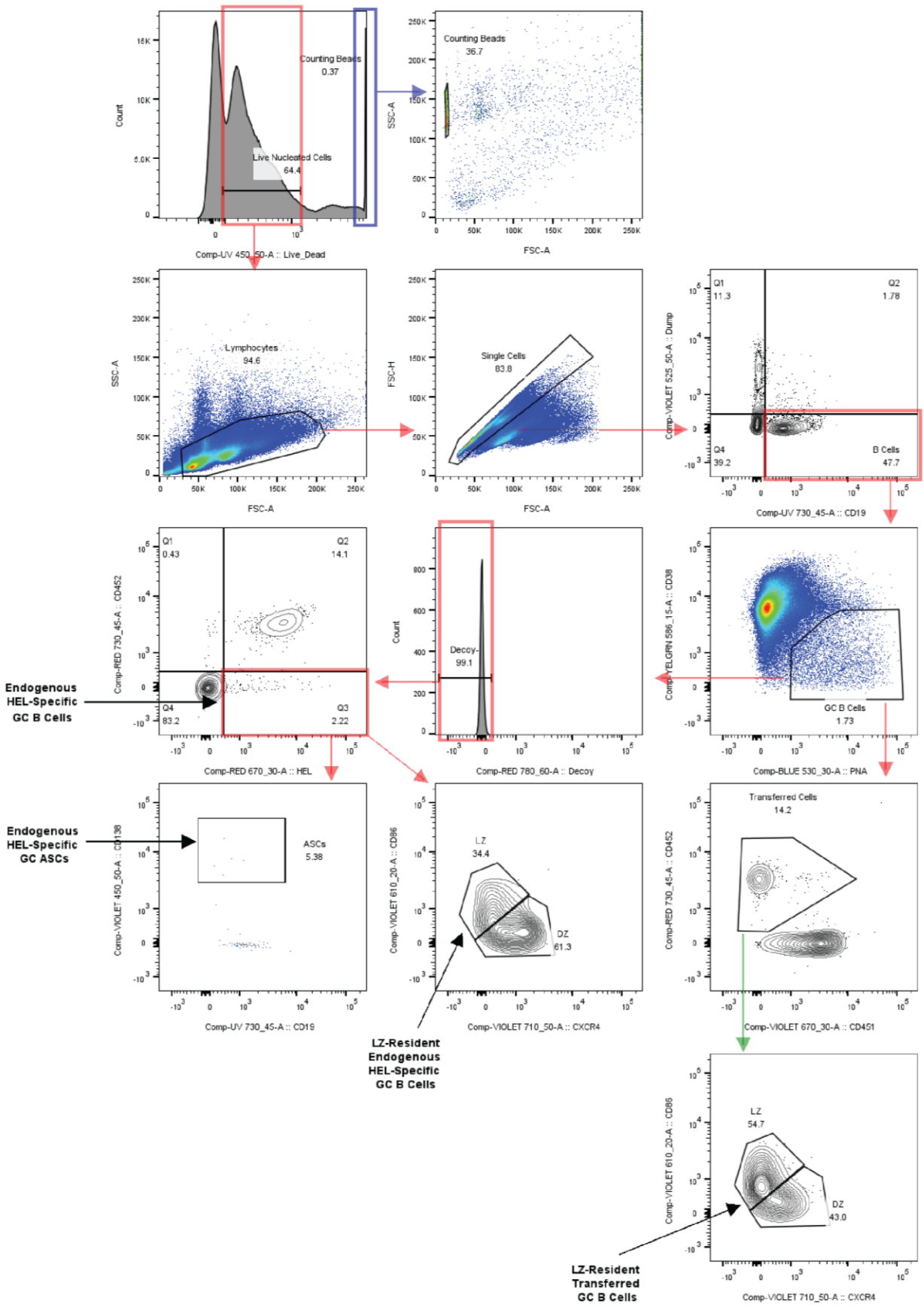
Counting Beads
0.37
Live Nucleated Cells
64.4
Count
Comp-UV 450_50-A :: Live_Dead
Counting Beads
36.7
SSC-A
FSC-A
Lymphocytes
94.6
Single Cells
83.8
FSC-H
Q1
11.3
Q2
1.78
Q4
39.2
B Cells
47.7
Comp-VIOLET 525_50-A :: Dump
Comp-UV 730_45-A :: CD19
Q1
0.43
Q2
14.1
Q4
83.2
Q3
2.22
Comp-RED 730_45-A :: CD452
Comp-RED 670_30-A :: HEL
Endogenous HEL-Specific GC B Cells
Decoy-
99.1
Comp-RED 780_60-A :: Decoy
GC B Cells
1.73
Comp-YELGRN 586_15-A :: CD38
Comp-BLUE 530_30-A :: PNA
ASCs
5.38
Comp-VIOLET 450_50-A :: CD138
Endogenous HEL-Specific GC ASCs
LZ
34.4
DZ
61.3
Comp-VIOLET 610_20-A :: CD86
Comp-VIOLET 710_50-A :: CXCR4
LZ-Resident Endogenous HEL-Specific GC B Cells
Transferred Cells
14.2
Comp-VIOLET 670_30-A :: CD451
LZ
54.7
DZ
43.0
LZ-Resident Transferred GC B Cells

Figure 2.S4. Germinal center B cell gating strategy. Gating strategy used for HEL-specific quantitative analyses outlined in Figure 5D-F. The same strategy was used for OVA-specific analyses, except these samples were stained with OVA-APC tetramer instead of HEL-APC tetramer. **Note:** In this figure, "Decoy" refers to the usage of a decoy tetramer used to distinguish APC-specific B cells from HEL-specific B cells.

2.6 Tables

Table 2.1. sgRNA, Primer, and Probe Sequences

Reagent	**Sequence**
Rosa26 sgRNA	GGCAGGCUUAAAGGCUAACC
Prdm1 sgRNA	GGUUAUUGGCGUGGUAAGUA
TRAC sgRNA	UCUCUCAGCUGGUACACGGC
Prdm1-F	GCTAATATTCTAGGCAGAGC
Prdm1-R	CCTTCTGATTCTCTTAGAACG
Rosa26-F *Binds to genomic Rosa26 upstream of the 5' HA sequence*	CTAGGGGTTGGATAAGCCAG
Rosa26-R *Binds to 3' HA of Rosa26 construct*	CTCTTCCCTCGTGATCTGCA
MND-R *Binds to region spanning 5'HA and the MND promoter*	GCCCATATTCTGCTGTTCCA
HDR Probe *Binds to MND*	**FAM-**TCTGTTCCTACGCGTACCTGGT**-BHQ1**
WT Probe *Binds across Rosa26 cut site*	**HEX-**ACCAGGTTAGCCTTTAAGCCTGC**-BHQ1**
mActinB-F	GTGACAAAACTCCTGAGGCCA
mActinB-R	ACGGATGTCAACGTCACACTT
Reference Probe *Binds to murine beta actin*	**HEX-**AGGTATGGAATCCTGTGGCATCCA**-BHQ1**

Table 2.2 – Flow Cytometry Reagents

Reactive Group	Conjugate	Clone	Manufacturer	Cat#
NHS ester	Alexa Fluor 350	N/A	ThermoFisher	A10168
α-mouse H-2K^{d}	Biotin	SF-1.1	BioLegend	116603
Streptavidin	PE	N/A	BD Biosciences	554061
α-mouse H-2K^{d}	Brilliant Violet 510	SF-1.1	BioLegend	116625
α-mouse CD3ε	Brilliant Violet 510	145-2C11	BioLegend	100353
α-mouse F4/80	Brilliant Violet 510	BM8	BioLegend	123135
α-mouse/human CD11b	Brilliant Violet 510	M1/70	BioLegend	101245
α-mouse NK-1.1	Brilliant Violet 510	PK136	BioLegend	108737
α-mouse CD19	Brilliant Violet 605	6D5	BioLegend	115539
α-mouse CD19	Brilliant Ultraviolet 737	1D3	BD Biosciences	612781
α-mouse CD138	Brilliant Violet 421	281-2	BD Biosciences	562610
α-mouse IgM	PerCP-eFluor 710	II/41	eBioscience	46-5790-82
α-mouse IgD	Brilliant Violet 786	11-26c.2a	BD Biosciences	563618
Peanut Agglutinin (PNA)	Fluorescein	N/A	Vector Laboratories	FL-1071
α-mouse CD38	PE	90/CD38	BD Biosciences	553764
α-mouse CXCR4	Brilliant Violet 711	L276F12	BioLegend	146517
α-mouse CD86	Brilliant Violet 605	GL-1	BioLegend	105037
α-human/mouse LNGFR	PE	REA648	Miltenyi	130-118-793
HEL	APC	N/A	In-house	N/A
OVA	APC	N/A	In-house	N/A
None (Decoy Tetramer)	APC-DyLight 755	N/A	In-house	N/A
α-mouse CD45.1	Brilliant Violet 650	A20	BD Biosciences	563754
α-mouse CD45.2	Alexa Fluor 700	104	eBioscience	50-168-96

Chapter 3: Summary and Concluding Remarks

3.1 Discussion

Antibody inhibitors are a frequent complication in the treatment of patients with inherited protein deficiency disorders;[10,15,30-32,118-124] the lack of targeted prophylactics that do not require broad immunosuppression limits the efficacy of the care available to these patients. In this study, we describe a cell-based approach for reducing antigen-specific antibody responses without the use of immunosuppression. We showed that adoptive transfer of exogenously antigen-primed, high-affinity B cells inhibited the generation of host ASCs and antibody responses specific for both cognate and cis-linked antigens. Rather than hindering this effect, Blimp1 deficiency appeared to convey an early advantage to antigen-primed "decoy" B cells for GC dominance and accomplished the same reduction in systemic antibody without undermining that reduction by differentiating and secreting decoy-encoded antibody. Decoy B cells outcompeted endogenous B cells for participation in GCs, which likely explains our observation of significant decreases in endogenous antigen-specific ASCs emerging from those GCs – all while leaving concurrent unrelated antibody responses intact. Finally, we leveraged the linked decoy effect to prevent the generation of FVIII-specific clotting inhibitors in a murine model of hemophilia A, demonstrating the therapeutic potential of this platform.

Previous studies have demonstrated that relatively lower-affinity B cells are outcompeted by high-affinity B cells for germinal center entry[57] and in adoptive transfer models, this correlates with a decrease in antigen-specific antibody produced by the lower-affinity endogenous B cells when high-affinity transgenic B cells are present.[71] However, it was unknown whether this effect could be leveraged to reduce antibody responses specific for a cis-linked antigen. Our studies demonstrate that when transgenic high-affinity B cells are primed with conjugate antigen *ex vivo*

prior to adoptive transfer, not only is this effect increased, but it extends to endogenous antibody responses specific for the linked antigen (Fig. 2.1 B,C). This critical observation, and our subsequent use in the FVIII model, suggest this cis-linked antigen approach is likely leverageable for B cell-based therapies designed to limit the humoral response to a broad range of candidate antigens.

Notably, Blimp1^{WT} MD4 B cells retained the capacity for secretion of antigen-specific antibodies following adoptive transfer. *Prdm1* was chosen as a target for gene ablation to curtail antibody secretion by transferred cells and, in parallel via limiting differentiation, to potentially enhance decoy cell antigen-presenting function.[153,154] We developed a CRISPR/Cas9 protocol to disrupt the *Prdm1* gene in activated primary B cells before adoptive transfer (Fig. 2.2 A). Mice treated with antigen-primed, Blimp1-deficient, high-affinity decoy B cells mounted significantly reduced antigen-specific antibody responses to both cognate and cis-linked antigen upon immunization (Fig. 2.2 D-F). The ability of Blimp1-deficent decoy cells to retain their suppressive activity supports the concept that the inhibitory impact of decoy B cells is driven primarily by competition for access to finite T cell help rather than by antibody feedback limiting the availability of soluble antigen potentially required for maintaining the GC response. This latter inference is supported both by previous work[57] and by our observation that the suppression of antibody specific for either cognate (HEL) or cis-linked (OVA) antigen is dose-dependent – cognate responses exquisitely so, with stepped reductions at every dose (Fig. 2.3 C). Finally, Blimp1 deficiency appeared to improve rather than handicap decoy access to antigen-specific T cells by driving early dominance of GCs (Fig 2.4 B,D).

Fig. 3.1 suggests a working model for decoy B cell function based upon the above detailed observations. Following adoptive transfer and immunization, both Blimp1-sufficient and Blimp1-

deficient MD4 decoy B cells are predicted to compete with endogenous B cells for help from pre-GC T cells and receive signals to either differentiate into short-lived plasmablasts or enter a GC. A large proportion of Blimp1^{WT}MD4 B cells likely become short-lived plasmablasts instead of entering a GC (supported by our observation of high serum levels of α-HEL IgM at Day 7 in HEL-OVA-immunized mice receiving Blimp1^{WT}MD4 B cells (Figs 2.1 B,C)), whereas the day 5 confocal microscopy suggests that Blimp1^{KO}MD4 B cells are diverted into GCs *en masse* to a greater degree than are Blimp1^{WT}MD4 (Fig. 2.4 B,D). Our microscopy findings further suggest that between days 5 and 11, the relatively fewer Blimp1^{WT}MD4 B cells that did enter GCs were also able to outcompete endogenous B cells and proliferated to the extent that domination by Blimp1^{KO} vs. Blimp1^{WT} MD4 B cells was indistinguishable at day 11. Not only did both Blimp1-sufficient and Blimp1-deficient MD4 B cells enter and seemingly dominate GCs, but their presence also correlated with a steep reduction in the number of endogenous HEL- and OVA-specific B cells and ASCs present in peak GCs (Fig. 2.5 C-E). Importantly, both Blimp1-sufficient and Blimp1-deficient MD4 B cells exhibited phenotypic features consistent with increased access to the GC light zone relative to endogenous antigen-specific B cells (Fig. 2.5 F). This likely translates to superior access to Tfh help relative to endogenous B cells and therefore decoy B cells may suppress endogenous affinity maturation, paralleling previously documented observations.[71] Overall, the reduction in endogenous antibody specific for both cognate and cis-linked antigen is likely due to a reduction in both pre- and post-GC endogenous antigen-specific ASCs, resulting from reduced competition for finite T cell help in the presence of decoy B cells.

This model also raises several unanswered questions. In addition to outcompeting endogenous B cells for access to T cell help, it is possible that decoy B cells may also directly tolerize antigen-specific T cells. However, if this were the case, we would have expected that

serum α-OVA IgG would be reduced following immunization of HEL-OVA-primed decoy-treated mice with unconjugated OVA. This was not the case (Fig. 2.S1), suggesting that ongoing acquisition of antigen and competition for T cell help is essential for decoy-mediated suppression. Additionally, other studies have found that lower-affinity B cell clones preferentially emerge from GCs as memory B cells,[155] suggesting that while decoy B cells may blunt the emergence of pre- and post-GC ASCs following primary immunization, they may not inhibit emergence of antigen-specific memory B cells. The duration of decoy-mediated suppression and whether secondary humoral responses are impacted remains to be determined. Decoy MD4 B cells are detectable in the spleens of treated mice up to 3 months post-immunization but not observed in spleens after 12 months (R.A.P., unpublished data). Although the long-term fate of decoy B cells after primary immunization is beyond the scope of this study, this would suggest that as presently conceived decoy therapy may require repeated administration.

Our combined data support the possibility for future therapeutic application. First, decoy B cells limited responses specific for cognate and cis-linked antigen but did not impact concurrent GC responses to an unrelated antigenic challenge (Fig. 2.3 E), suggesting this approach is unlikely to impact a simultaneous, but independent, infectious challenge. The therapeutic potential for decoy-mediated suppression was further demonstrated in a clinically relevant setting, as decoy B cells limited the generation of pathogenic clotting inhibitors in a murine model of hemophilia A. Upon immunization of $FVIII^{KO}$ HemA mice with an antigen comprised of HEL chemically conjugated to the immunogenic C2 domain of human FVIII (Fig. 2.6 A), nearly half of immunized control animals exhibited functional inhibition of FVIII-mediated clotting (Fig 2.6 D). Pretreatment with HEL-C2-primed MD4 decoy B cells resulted in a profound reduction of serum α-C2 IgG (Fig 2.6 B,C) and the proportion of mice that developed FVIII inhibitors dropped six-

fold (Fig 2.6 D). A prophylactic therapy that could prevent the generation of inhibitors to biologic therapies may be less time-consuming and more effective than ITI and might provide a powerful means to extend the therapeutic window of existing treatments.

The utility of the decoy B cell platform described here may be applicable to current challenges in gene therapy and, in parallel, is likely to be augmented by additional cell engineering. Future studies will investigate whether AAV-specific decoy B cells might be capable of limiting humoral response to therapeutic AAV vectors. Further, we show that it is possible to enforce constitutive IL-10 secretion from decoy B cells, foreshadowing an ability to manipulate adaptive immune responses in more nuanced ways.[88,156] We are now investigating whether we can exploit the ability of decoy B cells to invade and dominate GCs as a means to deliver other immunoregulatory cargoes such as TGFβ1[157] and T cell immunoreceptor with Ig and ITIM domains (TIGIT),[158] thereby leveraging decoy cell antigen-presenting capacity to suppress antigen-specific CD4 T cells or drive them to a regulatory phenotype.[89] Further, it is tempting to speculate that decoy B cells secreting regulatory cargo may be able to leverage their ability to impact responses specific for linked antigen to impose broader tolerance on related pathogenic T cells via an inverted form of epitope spreading.

In summary, we demonstrate that pretreatment with antigen-primed, antigen-specific, Blimp1-deficient B cells reduced serum antibody specific for both cognate and cis-linked antigen following immunization without impacting concurrent unrelated humoral responses. (Fig. 3.2) These “decoy” B cells readily entered germinal centers, reducing the number of endogenous antigen-specific B cells that emerged from these GCs as functional antibody-secreting cells. This approach has clinical implications, as decoy prophylaxis profoundly reduced the emergence of FVIII-targeted clotting inhibitors in a murine model of hemophilia A. Taken together, our studies

suggest that with further engineering and augmentation, Blimp1-knockout decoy B cells may provide a robust platform for precise, antigen-specific, engineered immune regulation.

3.2 Key Future Studies

Impact of Decoy B Cells on MBC Differentiation and Secondary Antibody Responses

Preliminary experiments in which decoy-treated mice were immunized a second time 4-8 weeks after primary immunization suggest that some degree of decoy-mediated suppression remains, though the difference is diminished (data not shown). This is not surprising, as we hypothesize that decoy B cells suppress T-dependent humoral responses by competing for access to limited T cell help rather than by competing for limited antigen. Endogenous B cells with low affinity for antigen are likely to receive a combination of weak BCR and weak CD40 signaling. Since these conditions likely favor memory B cell differentiation,[70] it is highly probable that decoy-mediated suppression allows the generation of MBCs that can be in turn induced to secrete antibody upon secondary immunization. However, these MBCs are expected to have undergone limited affinity maturation due to decoy-mediated competition for GC entry and residency (Fig. 2.5). Furthermore, some decoy B cells, unable to differentiate into ASCs, may persist as MBCs capable of competing in subsequent GCs. Future work should study the long-term fate of decoy B cells, changes in MBC differentiation by endogenous B cells in the presence of decoy competition, and the titer and affinity of secondary antibody responses.

Impact of Decoy B Cells on Antibody Affinity

While recent studies have demonstrated that class switch recombination primarily occurs outside the GC,[159] optimal affinity maturation is believed to require the dynamic competitive environment of a GC.[52] Since decoy B cells quickly dominate most GCs (Fig 2.4, 2.5), we predict that decoy prophylaxis will disproportionately impact the generation of high-affinity antibody arising from affinity-matured GC-derived ASCs. This may also result in the GC-derived MBC pool being of diminished average affinity since these may be out-competed after fewer cycles through the DZ. This is of particular importance since the translational efficacy of decoy-mediated suppression is likely to be impacted by not just the titer but also the affinity of antibody that is still produced. The impact of decoy treatment on SHM in endogenous B cells could be measured by sequencing the BCR genes of flow cytometry-sorted endogenous antigen-specific MBCs and ASCs in decoy-treated and control mice and comparing the number of mutations in the BCRs in the different experimental groups.[160] The quantity of high-affinity antibody in previously collected serum can be measured by performing a "stringent" ELISA with urea washes.[160]

Impact of Decoy B Cells on AAV Inhibitors

Despite decoy B cells' demonstrated efficacy in reducing the generation of C2-specific antibody inhibitors of FVIII (Fig 2.6), cell therapies are both expensive and invasive and so the bar for their application is high. As designed, decoy B cells may be a better-suited for preventing viral inhibitors during AAV-mediated gene therapy than for preventing FVIII inhibitors. AAV-mediated gene therapy is also expensive and invasive, but it has the limitation that it may be performed only once on a patient due to the inevitable generation of antibody-derived inhibitors and effector memory $CD4^+$ and $CD8^+$ T cells.[32,122] Although by design gene therapy is not intended to require continuous

dosing, it may be advantageous to enable some repeated dosing for patients who first received gene therapy early in life or to enable repeated low doses to minimize immunotoxicity. Engineered vector-specific decoy B cells may be an effective pre-treatment that greatly reduces the production of antibody-derived viral inhibitors. Future studies should leverage existing CRISPR/Cas9 editing strategies[117,118] to insert an AAV-specific BCR into Blimp1-deficient B cells and examine their ability to blunt the production of capsid-specific antibodies after following treatment of immune-competent mice with AAV. If there is a reduction in capsid-specific antibody in the serum of these mice, repeat dosing with AAV may be possible. Furthermore, the addition of immunomodulatory cargo such as IL-10 and TGF-β1 may augment this impact by tolerizing AAV-specific T cells.

Engineering Tolerance with Decoy-Delivered Immunomodulatory Cargo

Our studies show that high-affinity Blimp1-deficient decoy B cells are at a competitive advantage in GCs and reduce the number of endogenous antigen-specific ASCs arising from those GCs (Fig. 2.4, 2.5), suggesting that they are preferentially interacting with antigen-specific CD4 T cells. Furthermore, by preventing decoy differentiation these B cells can participate in adaptive immune responses without directly contributing to them with the secretion of antibody. It may be possible to compound the impact of decoy B cells by engineering them to deliver regulatory or cytotoxic signals to these antigen-dependent interaction. Our preliminary data show that it is possible to enforce regulatory cytokine secretion from decoy B cells by simultaneously inserting an IL-10 secretion cassette into a safe harbor locus via AAV-mediated HDR. This is particularly encouraging since all evidence suggests that regulatory phenotypes reflect a transient state of some activated B cells rather than a terminally differentiated lineage.[89,161] We are presently also developing strategies to generate decoy B cells that express TGF-β1, TIGIT, CD25, or cytotoxic

T-lymphocyte associated protein 4 (CTLA-4). It will be necessary to optimize cell editing protocols and adapt existing *in vitro* suppression assays to measure the impact of these eB_{Regs} on CD4 T cells in both antigen-specific and non-specific contexts, with a particular emphasis placed on cargos that may induce antigen-specific regulatory T cell differentiation.

Perhaps the most exciting result of this research is the extent to which high-affinity decoy B cells impacted the participation of B cells specific for linked antigen in GCs merely by distorting the competitive balance of antigen-specific B cells relative to antigen-specific CD4 T cells. Decoy B cells augmented to deliver regulatory cargo are ideally situated to combine this dominance of antigen-dependent interactions with specific CD4 T cells and linked recognition to induce tolerance to a diverse set of pathogenic epitopes. Epitope spreading is a major contributor to chronic autoimmune diseases such as rheumatoid arthritis and type I diabetes, as the destruction of tissue can lead to dysfunctional activation of previously naïve self-specific CD4 T cells by pathogenic B cells specific for some component of a multi-antigenic complex.[162] The activated self-specific CD4 T cells can then induce maturation of other pathogenic B cells, exacerbating pathology. Decoy B cells upgraded into true eB_{Regs} may be capable of inverting this dynamic, instead culling B and T cell epitopes from the immunogenic repertoire.

3.3 Figures

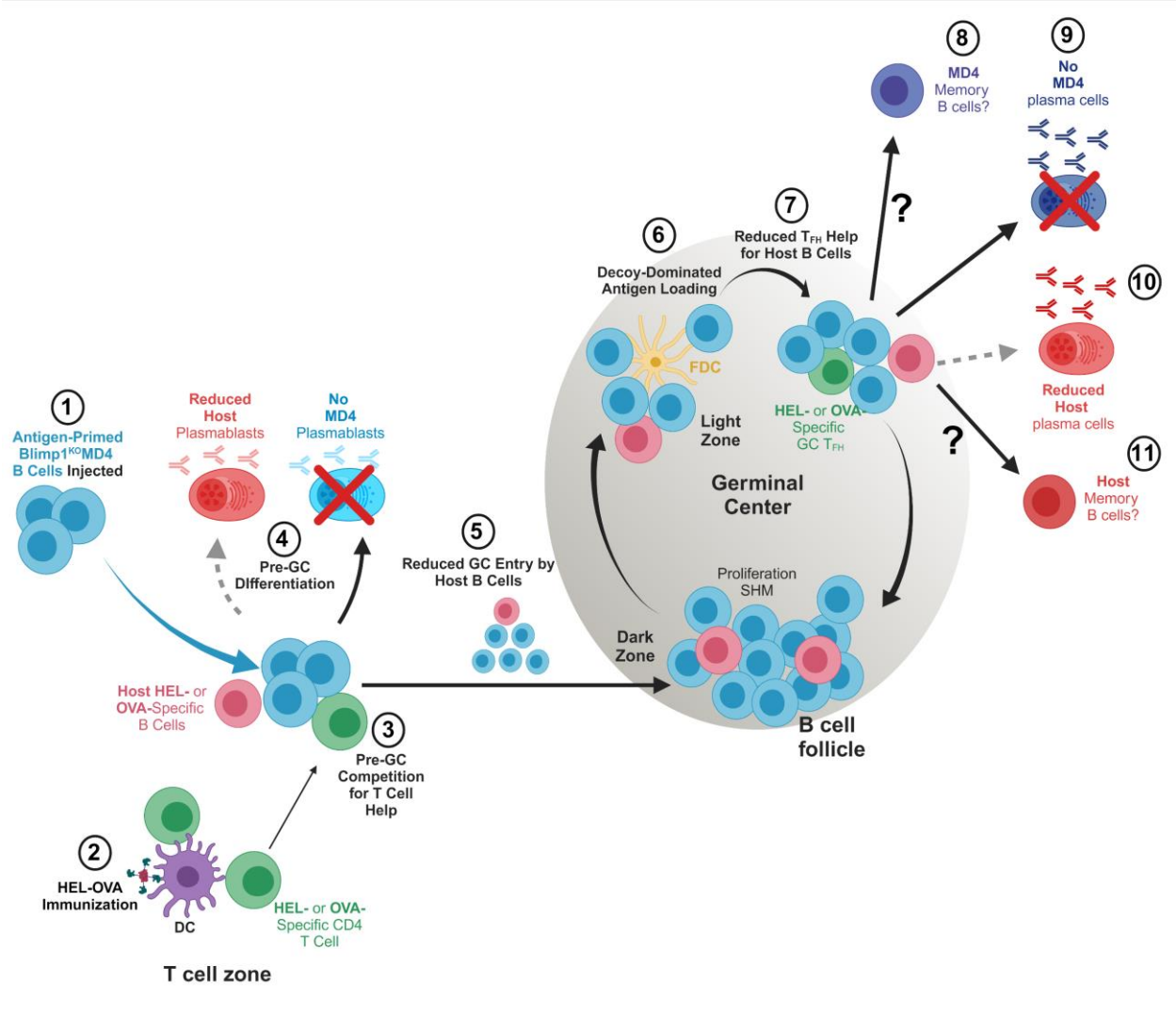
1
Antigen-Primed
Blimp1KOMD4
B Cells Injected
Reduced
Host
Plasmablasts
No
MD4
Plasmablasts
4
Pre-GC
DIfferentiation
5
Reduced GC Entry by
Host B Cells
Host HEL- or
OVA-Specific
B Cells
3
Pre-GC
Competition
for T Cell
Help
2
HEL-OVA
Immunization
DC
HEL- or OVA-
Specific CD4
T Cell
T cell zone
6
Decoy-Dominated
Antigen Loading
FDC
Light
Zone
7
Reduced TFH Help
for Host B Cells
HEL- or OVA-
Specific
GC TFH
Germinal
Center
Proliferation
SHM
Dark
Zone
B cell
follicle
8
MD4
Memory
B cells?
?
9
No
MD4
plasma cells
10
Reduced
Host
plasma cells
?
11
Host
Memory
B cells?

Fig 3.1. Proposed Model: Decoy B cells exploit GC biology to negatively modulate antigen-specific humoral responses. Following adoptive transfer, HEL-OVA-primed Blimp1^{KO}MD4 "decoy" B cells **(1)** interact with activated pre-GC HEL- and OVA-specific T cells **(2)**, competing with relatively lower affinity host HEL- and OVA-specific B cells **(3)** for access to T cell help. Due to this competition, host B cells undergo reduced pre-GC plasmablast differentiation and transferred decoy B cells do not differentiate due to Blimp1 deficiency **(4)**. Instead, decoy B cells are diverted *en masse* into GCs, also reducing the number of host B cells that enter those GCs **(5)**. Inside GCs, decoy B cells outcompete the lower-affinity host B cells for access to antigen presented on FDCs **(6)**, leading to a reduction in access by host B cells to help from antigen-specific Tfh **(7)**. By dominating GC responses, some decoy B cells may exit the GC as memory B cells **(8)** but they do not differentiate into plasma cells **(9)** due to Blimp1 deficiency. Importantly, the number of host antigen-specific plasma cells exiting GCs is reduced **(10)**. It is presently unknown how the host memory B cell compartment **(11)** or secondary responses are impacted by decoy-mediated suppression. Created with BioRender.

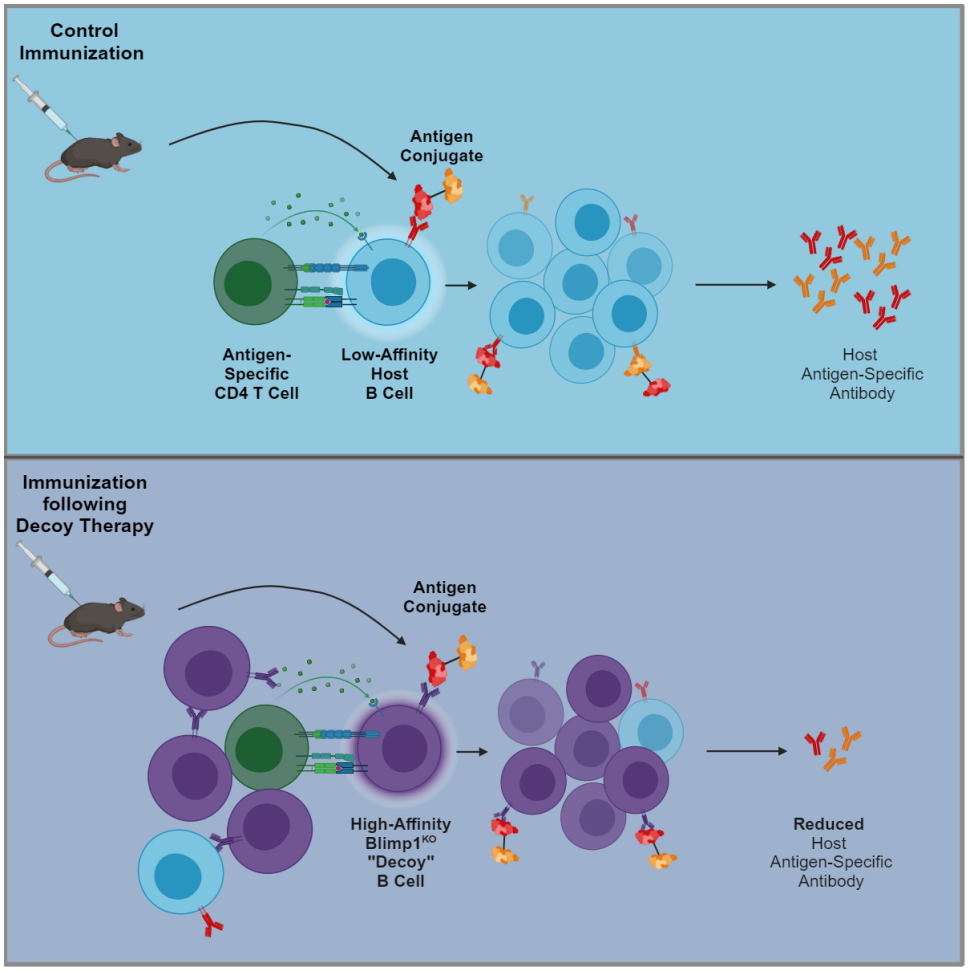

Fig 3.2. Synopsis. Antibody inhibitors remain a major obstacle to the optimal treatment of people suffering from monogenic disorders, whether they are generated against protein replacement therapies or the viral vectors used for corrective gene therapy. This study demonstrates that adoptively transferred gene-edited, antigen-specific, non-differentiating B cells serve as "decoys" that outcompete native B cells in germinal centers following exposure to foreign antigen. These decoy B cells leave unrelated immune responses intact but can selectively blunt the generation of antibodies to cis-linked antigen – an effect we exploit to block the generation of factor VIII-specific clotting inhibitors. Created with BioRender.

References

1. Briney, B., Inderbitzin, A., Joyce, C. & Burton, D. R. Commonality despite exceptional diversity in the baseline human antibody repertoire. *Nat. 2019 5667744* **566**, 393–397 (2019).
2. Hammarlund, E. *et al.* Plasma cell survival in the absence of B cell memory. *Nat. Commun. 2017 81* **8**, 1–11 (2017).
3. Sorensen, S., Per, * & Dk, P. Antidrug Antibodies Against Biological Treatments for Multiple Sclerosis. *CNS Drugs 2022 366* **36**, 569–589 (2022).
4. Fogdell-Hahn, A. Antidrug Antibodies: B Cell Immunity Against Therapy. *Scand. J. Immunol.* **82**, 184–190 (2015).
5. Hellmann, M. D. *et al.* Safety and Immunogenicity of LY3415244, a Bispecific Antibody Against TIM-3 and PD-L1, in Patients With Advanced Solid Tumors. *Clin. Cancer Res.* **27**, 2773–2781 (2021).
6. Hoyer, L. W. Hemophilia A. *N. Engl. J. Med.* **330**, 38–47 (1994).
7. Philippidis, A. BioMarin's ROCTAVIAN Wins Food and Drug Administration Approval As First Gene Therapy for Severe Hemophilia A. *Hum. Gene Ther.* **34**, 665–668 (2023).
8. Ma, A. D. & Carrizosa, D. Acquired factor VIII inhibitors: pathophysiology and treatment. *Hematol. Am. Soc. Hematol. Educ. Progr.* 432–437 (2006) doi:10.1182/ASHEDUCATION-2006.1.432.
9. Samelson-Jones, B. J. & Arruda, V. R. Translational Potential of Immune Tolerance Induction by AAV Liver-Directed Factor VIII Gene Therapy for Hemophilia A. *Front. Immunol.* **11**, (2020).
10. Shirley, J. L., de Jong, Y. P., Terhorst, C. & Herzog, R. W. Immune Responses to Viral

Gene Therapy Vectors. *Mol. Ther.* **28**, 709–722 (2020).

11. Hartley, S. B. *et al.* Elimination from peripheral lymphoid tissues of self-reactive B lymphocytes recognizing membrane-bound antigens. *Nature* **353**, 765–769 (1991).
12. Hardy, R. R. & Hayakawa, K. B cell development pathways. *Annu. Rev. Immunol.* **19**, 595–621 (2001).
13. Nemazee, D. Mechanisms of central tolerance for B cells. *Nat. Rev. Immunol. 2017 175* **17**, 281–294 (2017).
14. Samuelson Bannow, B. *et al.* Factor VIII: Long-established role in haemophilia A and emerging evidence beyond haemostasis. *Blood Rev.* **35**, 43–50 (2019).
15. Scott, D. W., Pratt, K. P. & Miao, C. H. Progress toward inducing immunologic tolerance to factor VIII. *Blood* **121**, (2013).
16. Valentino, L. A. *et al.* US Guidelines for immune tolerance induction in patients with haemophilia a and inhibitors. *Haemophilia* **21**, 559–567 (2015).
17. Khalilian, S., Motovali-Bashi, M. & Rezaie, H. Factor VIII: Perspectives on Immunogenicity and Tolerogenic Strategies for Hemophilia A Patients. *Int. J. Mol. Cell. Med.* **9**, 33 (2020).
18. Hay, C. R. M. & DiMichele, D. M. The principal results of the International Immune Tolerance Study: a randomized dose comparison. *Blood* **119**, 1335–1344 (2012).
19. Shima, M. *et al.* Factor VIII–Mimetic Function of Humanized Bispecific Antibody in Hemophilia A. *N. Engl. J. Med.* **374**, 2044–2053 (2016).
20. Teitel, J. M. Treatment and prevention of bleeding in congenital hemophilia A patients with inhibitors. *Transfus. Apher. Sci.* **57**, 466–471 (2018).
21. Palaschak, B., Herzog, R. W. & Markusic, D. M. AAV-Mediated Gene Delivery to the

Liver: Overview of Current Technologies and Methods. *Methods Mol. Biol.* **1950**, 333–360 (2019).

22. Nathwani, A. C. Gene therapy for hemophilia. *Hematology* **2022**, 569–578 (2022).
23. Patel, S. R., Lundgren, T. S., Spencer, H. T. & Doering, C. B. The Immune Response to the fVIII Gene Therapy in Preclinical Models. *Front. Immunol.* **11**, 494 (2020).
24. Finn, J. D. *et al.* Eradication of neutralizing antibodies to factor VIII in canine hemophilia A after liver gene therapy. *Blood* **116**, 5842 (2010).
25. Klamroth, R. *et al.* Global Seroprevalence of Pre-existing Immunity Against AAV5 and Other AAV Serotypes in People with Hemophilia A. *Hum. Gene Ther.* **33**, 432–441 (2022).
26. Schulz, M. *et al.* Binding and neutralizing anti-AAV antibodies: Detection and implications for rAAV-mediated gene therapy. *Mol. Ther.* **31**, 616–630 (2023).
27. Li, C. *et al.* Neutralizing antibodies against adeno-associated virus examined prospectively in pediatric patients with hemophilia. *Gene Ther. 2012 193* **19**, 288–294 (2011).
28. Mingozzi, F. & High, K. A. Immune responses to AAV vectors: overcoming barriers to successful gene therapy. *Blood* **122**, 23–36 (2013).
29. George, L. A. *et al.* Long-Term Follow-Up of the First in Human Intravascular Delivery of AAV for Gene Transfer: AAV2-hFIX16 for Severe Hemophilia B. *Mol. Ther.* **28**, 2073–2082 (2020).
30. Earley, J., Piletska, E., Ronzitti, G. & Piletsky, S. Evading and overcoming AAV neutralization in gene therapy. *Trends Biotechnol.* **41**, 836–845 (2023).
31. Kishimoto, T. K. & Samulski, R. J. Addressing high dose AAV toxicity - ‘one and done’

or ‘slower and lower’? *Expert Opin. Biol. Ther.* **22**, 1067–1071 (2022).

32. Ertl, H. C. J. Immunogenicity and toxicity of AAV gene therapy. *Front. Immunol.* **13**, 975803 (2022).

33. Prasad, S. *et al.* Immune Responses and Immunosuppressive Strategies for Adeno-Associated Virus-Based Gene Therapy for Treatment of Central Nervous System Disorders: Current Knowledge and Approaches. *Hum. Gene Ther.* **33**, 1228 (2022).

34. Mueller, C. *et al.* SOD1 Suppression with Adeno-Associated Virus and MicroRNA in Familial ALS . *N. Engl. J. Med.* **383**, 151–158 (2020).

35. Byrne, B. J. *et al.* Phase I/II trial of diaphragm delivery of recombinant adeno-associated virus acid alpha-glucosidase (rAAaV1-CMV-GAA) gene vector in patients with Pompe disease. *Hum. Gene Ther. Clin. Dev.* **25**, 134–163 (2014).

36. Corti, M. *et al.* Safety of Intradiaphragmatic Delivery of Adeno-Associated Virus-Mediated Alpha-Glucosidase (rAAV1-CMV-hGAA) Gene Therapy in Children Affected by Pompe Disease. *Hum. Gene Ther. Clin. Dev.* **28**, 208–218 (2017).

37. Bey, K. *et al.* Intra-CSF AAV9 and AAVrh10 Administration in Nonhuman Primates: Promising Routes and Vectors for Which Neurological Diseases? *Mol. Ther. Methods Clin. Dev.* **17**, 771–784 (2020).

38. Greenberg, B. *et al.* Prevalence of AAV1 neutralizing antibodies and consequences for a clinical trial of gene transfer for advanced heart failure. *Gene Ther.* **23**, 313–319 (2016).

39. Unzu, C. *et al.* Transient and intensive pharmacological immunosuppression fails to improve AAV-based liver gene transfer in non-human primates. *J. Transl. Med.* **10**, 122 (2012).

40. Meliani, A. *et al.* Antigen-selective modulation of AAV immunogenicity with tolerogenic

rapamycin nanoparticles enables successful vector re-administration. *Nat. Commun. 2018 91* **9**, 1–13 (2018).

41. Bortnick, A. & Allman, D. What Is and What Should Always Have Been: Long-lived Plasma cells Induced by T-cell Independent Antigens. *J. Immunol.* **190**, 5913 (2013).

42. Allman, D., Wilmore, J. R. & Gaudette, B. T. The continuing story of T-cell independent antibodies. *Immunol. Rev.* **288**, 128–135 (2019).

43. Di Niro, R. *et al.* Salmonella Infection Drives Promiscuous B Cell Activation Followed by Extrafollicular Affinity Maturation. *Immunity* **43**, 120–131 (2015).

44. Elsner, R. A. & Shlomchik, M. J. Germinal Center and Extrafollicular B Cell Responses in Vaccination, Immunity, and Autoimmunity. *Immunity* **53**, 1136–1150 (2020).

45. Song, W. & Craft, J. T follicular helper cell heterogeneity: Time, space, and function. *Immunol. Rev.* **288**, 85–96 (2019).

46. Okada, T. *et al.* Antigen-engaged B cells undergo chemotaxis toward the T zone and form motile conjugates with helper T cells. *PLoS Biol.* **3**, 1047–1061 (2005).

47. Qi, H., Cannons, J. L., Klauschen, F., Schwartzberg, P. L. & Germain, R. N. SAP-controlled T-B cell interactions underlie germinal centre formation. *Nature* **455**, 764–769 (2008).

48. Kelly, L. M., Pereira, J. P., Yi, T., Xu, Y. & Cyster, J. G. EBI2 guides serial movements of activated B cells and ligand activity is detectable in lymphoid and nonlymphoid tissues. *J. Immunol.* **187**, 3026–3032 (2011).

49. Taylor, J. J., Pape, K. A. & Jenkins, M. K. A germinal center-independent pathway generates unswitched memory B cells early in the primary response. *J. Exp. Med.* **209**, 597–606 (2012).

50. Paus, D. *et al.* Antigen recognition strength regulates the choice between extrafollicular plasma cell and germinal center B cell differentiation. *J. Exp. Med.* **203**, 1081–1091 (2006).

51. Shi, J. *et al.* PD-1 Controls Follicular T Helper Cell Positioning and Function. *Immunity* **49**, 264-274.e4 (2018).

52. De Silva, N. S. & Klein, U. Dynamics of B cells in germinal centres. *Nat. Rev. Immunol.* **15**, 137–148 (2015).

53. Inoue, T. & Kurosaki, T. Memory B cells. *Nat. Rev. Immunol.* **24**, 5–17 (2024).

54. MacLennan, I. C. M. Germinal centers. *Annu. Rev. Immunol.* **12**, 117–139 (1994).

55. Victora, G. D. *et al.* Germinal Center Dynamics Revealed by Multiphoton Microscopy with a Photoactivatable Fluorescent Reporter. *Cell* **143**, 592–605 (2010).

56. Jiang, W. *et al.* The receptor DEC-205 expressed by dendritic cells and thymic epithelial cells is involved in antigen processing. *Nat. 1995 3756527* **375**, 151–155 (1995).

57. Schwickert, T. A. *et al.* A dynamic T cell-limited checkpoint regulates affinity-dependent B cell entry into the germinal center. *J. Exp. Med.* **208**, 1243–1252 (2011).

58. Taylor, J. J., Pape, K. A., Steach, H. R. & Jenkins, M. K. Apoptosis and antigen affinity limit effector cell differentiation of a single naïve B cell. *Science (80-.).* **347**, 784–787 (2015).

59. Glaros, V. *et al.* Limited access to antigen drives generation of early B cell memory while restraining the plasmablast response. *Immunity* **54**, 2005-2023.e10 (2021).

60. Brynjolfsson, S. F. *et al.* Long-lived plasma cells in mice and men. *Front. Immunol.* **9**, 386243 (2018).

61. Wang, Q. *et al.* The cell cycle restricts activation-induced cytidine deaminase activity to

early G1. *J. Exp. Med.* **214**, 49–58 (2017).

62. Stewart, I., Radtke, D., Phillips, B., McGowan, S. J. & Bannard, O. Germinal Center B Cells Replace Their Antigen Receptors in Dark Zones and Fail Light Zone Entry when Immunoglobulin Gene Mutations are Damaging. *Immunity* **49**, 477-489.e7 (2018).

63. Allen, C. D. C. & Cyster, J. G. Follicular dendritic cell networks of primary follicles and germinal centers: Phenotype and function. *Semin. Immunol.* **20**, 14–25 (2008).

64. Heesters, B. A., Myers, R. C. & Carroll, M. C. Follicular dendritic cells: dynamic antigen libraries. *Nat. Rev. Immunol. 2014 147* **14**, 495–504 (2014).

65. Beamer, G. L. & Turner, J. Murine models of susceptibility to tuberculosis. *Arch. Immunol. Ther. Exp. (Warsz).* **53**, 469–83 (2005).

66. Phan, T. G. *et al.* High affinity germinal center B cells are actively selected into the plasma cell compartment. *J. Exp. Med.* **203**, 2419–2424 (2006).

67. Victora, G. D. & Nussenzweig, M. C. Germinal Centers. *https://doi.org/10.1146/annurev-immunol-120419-022408* **40**, 413–442 (2022).

68. Ise, W. *et al.* T Follicular Helper Cell-Germinal Center B Cell Interaction Strength Regulates Entry into Plasma Cell or Recycling Germinal Center Cell Fate. *Immunity* **48**, 702-715.e4 (2018).

69. Sutton, H. J. *et al.* Lack of affinity signature for germinal center cells that have initiated plasma cell differentiation. *Immunity* **57**, 245-255.e5 (2024).

70. Laidlaw, B. J. & Cyster, J. G. Transcriptional regulation of memory B cell differentiation. *Nat. Rev. Immunol.* **21**, 209–220 (2021).

71. Le, T. L., Kim, T. H. & Chaplin, D. D. Intraclonal Competition Inhibits the Formation of High-Affinity Antibody-Secreting Cells. *J. Immunol.* **181**, 6027–6037 (2008).

72. Luo, W., Weisel, F. & Shlomchik, M. J. B Cell Receptor and CD40 Signaling Are Rewired for Synergistic Induction of the c-Myc Transcription Factor in Germinal Center B Cells. *Immunity* **48**, 313-326.e5 (2018).

73. Ersching, J. *et al.* Germinal Center Selection and Affinity Maturation Require Dynamic Regulation of mTORC1 Kinase. *Immunity* **46**, 1045-1058.e6 (2017).

74. Chou, C. *et al.* The Transcription Factor AP4 Mediates Resolution of Chronic Viral Infection through Amplification of Germinal Center B Cell Responses. *Immunity* **45**, 570–582 (2016).

75. Dominguez-Sola, D. *et al.* The FOXO1 Transcription Factor Instructs the Germinal Center Dark Zone Program. *Immunity* **43**, 1064–1074 (2015).

76. Fukuda, T. *et al.* Disruption of the Bcl6 gene results in an impaired germinal center formation. *J. Exp. Med.* **186**, 439–448 (1997).

77. Huang, C. *et al.* The BCL6 RD2 domain governs commitment of activated B cells to form germinal centers. *Cell Rep.* **8**, 1497–1508 (2014).

78. Huang, C., Geng, H., Boss, I., Wang, L. & Melnick, A. Cooperative transcriptional repression by BCL6 and BACH2 in germinal center B-cell differentiation. *Blood* **123**, 1012–1020 (2014).

79. Sciammas, R. *et al.* An incoherent regulatory network architecture that orchestrates B cell diversification in response to antigen signaling. *Mol. Syst. Biol.* **7**, 495 (2011).

80. Saito, M. *et al.* A signaling pathway mediating downregulation of BCL6 in germinal center B cells is blocked by BCL6 gene alterations in B cell lymphoma. *Cancer Cell* **12**, 280–292 (2007).

81. Ochiai, K. *et al.* Transcriptional regulation of germinal center B and plasma cell fates by

dynamical control of IRF4. *Immunity* **38**, 918–929 (2013).

82. Li, X. *et al.* Cbl Ubiquitin Ligases Control B Cell Exit from the Germinal-Center Reaction. *Immunity* **48**, 530-541.e6 (2018).

83. Shaffer, A. L. *et al.* Blimp-1 orchestrates plasma cell differentiation by extinguishing the mature B cell gene expression program. *Immunity* (2002) doi:10.1016/S1074-7613(02)00335-7.

84. Oracki, S. A., Walker, J. A., Hibbs, M. L., Corcoran, L. M. & Tarlinton, D. M. *Plasma cell development and survival*. *Immunological Reviews* vol. 237 140–159 (John Wiley & Sons, Ltd, 2010).

85. Tellier, J. *et al.* Blimp-1 controls plasma cell function through the regulation of immunoglobulin secretion and the unfolded protein response. *Nat. Immunol.* (2016) doi:10.1038/ni.3348.

86. Shapiro-Shelef, M. *et al.* Blimp-1 is required for the formation of immunoglobulin secreting plasma cells and pre-plasma memory B cells. *Immunity* **19**, 607–620 (2003).

87. Chu, V. T. *et al.* Efficient CRISPR-mediated mutagenesis in primary immune cells using CrispRGold and a C57BL/6 Cas9 transgenic mouse line. *Proc. Natl. Acad. Sci. U. S. A.* **113**, 12514–12519 (2016).

88. Tedder, T. F. B10 cells: a functionally defined regulatory B cell subset. *J. Immunol.* **194**, 1395–1401 (2015).

89. Rosser, E. C. & Mauri, C. Regulatory B Cells: Origin, Phenotype, and Function. *Immunity* **42**, 607–612 (2015).

90. Skok, J., Poudrier, J. & Gray, D. Dendritic Cell-Derived IL-12 Promotes B Cell Induction of Th2 Differentiation: A Feedback Regulation of Th1 Development. *J. Immunol.* **163**,

4284–4291 (1999).

91. Moulin, V. *et al.* B lymphocytes regulate dendritic cell (DC) function in vivo: increased interleukin 12 production by DCs from B cell-deficient mice results in T helper cell type 1 deviation. *J. Exp. Med.* **192**, 475–482 (2000).

92. Sun, C. M., Deriaud, E., Leclerc, C. & Lo-Man, R. Upon TLR9 signaling, CD5+ B cells control the IL-12-dependent Th1-priming capacity of neonatal DCs. *Immunity* **22**, 467–477 (2005).

93. Zhang, X. *et al.* Type I interferons protect neonates from acute inflammation through interleukin 10-producing B cells. *J. Exp. Med.* **204**, 1107–1118 (2007).

94. Yoshizaki, A. *et al.* Regulatory B cells control T-cell autoimmunity through IL-21-dependent cognate interactions. *Nature* **491**, 264–268 (2012).

95. Evans, J. G. *et al.* Novel Suppressive Function of Transitional 2 B Cells in Experimental Arthritis. *J. Immunol.* (2007) doi:10.4049/jimmunol.178.12.7868.

96. Pers, J.-O., Le Pottier, L. & Goutsmedt, C. FRI0010 Identification of an Antigen-Specific Regulatory B Cell Subset in Humans. *Ann. Rheum. Dis.* (2015) doi:10.1136/annrheumdis-2015-eular.3923.

97. Mauri, C. & Menon, M. Human regulatory B cells in health and disease: therapeutic potential. *J Clin Invest* **127**, (2017).

98. Lighaam, L. C. *et al.* In vitro-Induced Human IL-10+ B Cells Do Not Show a Subset-Defining Marker Signature and Plastically Co-express IL-10 With Pro-Inflammatory Cytokines. *Front. Immunol.* **9**, (2018).

99. Maseda, D. *et al.* Regulatory B10 cells differentiate into antibody-secreting cells after transient IL-10 production in vivo. *J. Immunol.* **188**, 1036–1048 (2012).

100. Nutt, S. L., Hodgkin, P. D., Tarlinton, D. M. & Corcoran, L. M. The generation of antibody-secreting plasma cells. *Nat. Rev. Immunol.* **15**, 160–171 (2015).

101. Scandella, D. H. Properties of anti-factor VIII inhibitor antibodies in hemophilia A patients. *Semin. Thromb. Hemost.* **26**, 137–142 (2000).

102. Garside, P. *et al.* Visualization of specific B and T lymphocyte interactions in the lymph node. *Science (80-.).* **281**, 96–99 (1998).

103. Mason, D. Y., Jones, M. & Goodnow, C. C. Development and follicular localization of tolerant b lymphocytes in lysozyme/anti-lysozyme igm/lgd transgenic mice. *Int. Immunol.* **4**, 163–175 (1992).

104. Zhang, Y. *et al.* Germinal center B cells govern their own fate via antibody feedback. *J. Exp. Med.* **210**, 457–464 (2013).

105. Avancena, P. *et al.* The magnitude of germinal center reactions is restricted by a fixed number of preexisting niches. *Proc. Natl. Acad. Sci. U. S. A.* **118**, e2100576118 (2021).

106. Radtke, D. & Bannard, O. Expression of the plasma cell transcriptional regulator Blimp-1 by dark zone germinal center B cells during periods of proliferation. *Front. Immunol.* **10**, 435606 (2019).

107. Whelan, S. F. J. *et al.* Distinct characteristics of antibody responses against factor VIII in healthy individuals and in different cohorts of hemophilia A patients. *Blood* **121**, 1039–1048 (2013).

108. Murphy, S. L. *et al.* Diverse IgG Subclass Responses to Adeno-associated Virus Infection and Vector Administration. *J. Med. Virol.* **81**, 65 (2009).

109. Bi, L. *et al.* Targeted disruption of the mouse factor VIII gene produces a model of haemophilia A. *Nat. Genet.* **10**, 119–121 (1995).

110. Miao, C. H. *et al.* CD4+FOXP3+ regulatory T cells confer long-term regulation of factor VIII–specific immune responses in plasmid-mediated gene therapy–treated hemophilia mice. *Blood* **114**, 4034 (2009).

111. Duncan, E., Collecutt, M. & Street, A. Nijmegen-bethesda assay to measure factor VIII inhibitors. *Methods Mol. Biol.* **992**, 321–333 (2013).

112. Neta, R. & Salvin, S. B. Specific Suppression of Delayed Hypersensitivity: The Possible Presence of a Suppressor B Cell in the Regulation of Delayed Hypersensitivity. *J. Immunol.* **113**, 1716–1725 (1974).

113. Janssens, W. *et al.* Efficiency of onco-retroviral and lentiviral gene transfer into primary mouse and human B-lymphocytes is pseudotype dependent. *Hum. Gene Ther.* (2003) doi:10.1089/10430340360535814.

114. Serafini, M., Naldini, L. & Introna, M. Molecular evidence of inefficient transduction of proliferating human B lymphocytes by VSV-pseudotyped HIV-1-derived lentivectors. *Virology* (2004) doi:10.1016/j.virol.2004.04.038.

115. O'Connor, D. M. Introduction to Gene and Stem-Cell Therapy. in *Molecular and Cellular Therapies for Motor Neuron Diseases* (2017). doi:10.1016/B978-0-12-802257-3.00007-9.

116. Hung, K. L. *et al.* Engineering Protein-Secreting Plasma Cells by Homology-Directed Repair in Primary Human B Cells. *Mol. Ther.* **26**, 456–467 (2018).

117. Moffett, H. F. *et al.* B cells engineered to express pathogen-specific antibodies protect against infection. *Sci. Immunol.* **4**, (2019).

118. Voss, J. E. *et al.* Reprogramming the antigen specificity of B cells using genome-editing technologies. *Elife* **8**, (2019).

119. Walsh, C. E., Soucie, J. M. & Miller, C. H. Impact of inhibitors on hemophilia A mortality

in the United States. *Am. J. Hematol.* **90**, 400–405 (2015).

120. Leissinger, C. A. Advances in the clinical management of inhibitors in hemophilia A and B. *Semin. Hematol.* **53**, 20–27 (2016).

121. Vandamme, C., Adjali, O. & Mingozzi, F. Unraveling the Complex Story of Immune Responses to AAV Vectors Trial After Trial. *Hum. Gene Ther.* **28**, 1061–1074 (2017).

122. Verdera, H. C., Kuranda, K. & Mingozzi, F. AAV Vector Immunogenicity in Humans: A Long Journey to Successful Gene Transfer. **28**, 723–746 (2020).

123. Schep, S. J., Schutgens, R. E. G., Fischer, K. & Boes, M. L. Review of immune tolerance induction in hemophilia A. *Blood Rev.* **32**, 326–338 (2018).

124. Mingozzi, F. *et al.* Pharmacological modulation of humoral immunity in a nonhuman primate model of AAV gene transfer for hemophilia B. *Mol. Ther.* **20**, 1410–1416 (2012).

125. Yamada, K. & Herzog, R. W. When Immune Suppression Goes Wrong. *Mol. Ther.* **28**, 1381–1382 (2020).

126. Cheng, R. Y. H. *et al.* Ex vivo engineered human plasma cells exhibit robust protein secretion and long-term engraftment in vivo. *Nat. Commun.* **13**, (2022).

127. David, M. *et al.* Production of therapeutic levels of human FIX-R338L by engineered B cells using GMP-compatible medium. *Mol. Ther. Methods Clin. Dev.* **31**, 101111 (2023).

128. Arroyo, E. N. & Pepper, M. B cells are sufficient to prime the dominant CD4+ Tfh response to Plasmodium infection. *J. Exp. Med.* (2020) doi:10.1084/jem.20190849.

129. Hong, S. *et al.* B Cells Are the Dominant Antigen-Presenting Cells that Activate Naive CD4+ T Cells upon Immunization with a Virus-Derived Nanoparticle Antigen. *Immunity* (2018) doi:10.1016/j.immuni.2018.08.012.

130. Goodnow, C. C. *et al.* Altered immunoglobulin expression and functional silencing of

self-reactive B lymphocytes in transgenic mice. *Nature* **334**, 676–682 (1988).

131. Kornbluth, R. S., Stempniak, M. & Stone, G. W. Design of CD40 Agonists and their use in growing B cells for cancer immunotherapy. *Int. Rev. Immunol.* **31**, 279–288 (2012).

132. Chan, V. W. F. *et al.* The Molecular Mechanism of B Cell Activation by toll-likeReceptor Protein RP-105. *J. Exp. Med.* **188**, 93 (1998).

133. Divanovic, S. *et al.* Negative regulation of Toll-like receptor 4 signaling by the Toll-like receptor homolog RP105. *Nat. Immunol.* **6**, 571–578 (2005).

134. Chaplin, J. W., Kasahara, S., Clark, E. A. & Ledbetter, J. A. Anti-CD180 (RP105) activates B cells to rapidly produce polyclonal Ig via a T cell and MyD88-independent pathway. *J. Immunol.* **187**, 4199 (2011).

135. Wurster, A. L., Rodgers, V. L., White, M. F., Rothstein, T. L. & Grusby, M. J. Interleukin-4-mediated Protection of Primary B Cells from Apoptosis through Stat6-dependent Up-regulation of Bcl-xL. *J. Biol. Chem.* **277**, 27169–27175 (2002).

136. Granato, A., Hayashi, E. A., Baptista, B. J. A., Bellio, M. & Nobrega, A. IL-4 Regulates Bim Expression and Promotes B Cell Maturation in Synergy with BAFF Conferring Resistance to Cell Death at Negative Selection Checkpoints. *J. Immunol.* **192**, 5761–5775 (2014).

137. Klein, U. *et al.* Transcription factor IRF4 controls plasma cell differentiation and class-switch recombination. *Nat. Immunol.* (2006) doi:10.1038/ni1357.

138. Nojima, T. *et al.* In-vitro derived germinal centre B cells differentially generate memory B or plasma cells in vivo. *Nat. Commun.* **2**, (2011).

139. Conant, D. *et al.* Inference of CRISPR Edits from Sanger Trace Data. *Cris. J.* **5**, 123–130 (2022).

140. Saenko, E. L., Shima, M., Rajalakshmi, K. J. & Scandella, D. A role for the C2 domain of factor VIII in binding to von Willebrand factor. *J. Biol. Chem.* **269**, 11601–11605 (1994).

141. Saenko, E. L. & Scandella, D. The acidic region of the factor VIII light chain and the C2 domain together form the high affinity binding site for von willebrand factor. *J. Biol. Chem.* **272**, 18007–18014 (1997).

142. Nogami, K. *et al.* Factor VIII C2 domain contains the thrombin-binding site responsible for thrombin-catalyzed cleavage at Arg1689. *J. Biol. Chem.* **275**, 25774–25780 (2000).

143. Walter, J. D. *et al.* Characterization and solution structure of the factor VIII C2 domain in a ternary complex with classical and non-classical inhibitor antibodies. *J. Biol. Chem.* **288**, 9905–9914 (2013).

144. Prescott, R. *et al.* The Inhibitor Antibody Response Is More Complex in Hemophilia A Patients Than in Most Nonhemophiliacs With Factor VIII Autoantibodies. *Blood* **89**, 3663–3671 (1997).

145. Arai, M., Scandella, D. & Hoyer, L. W. Molecular basis of factor VIII inhibition by human antibodies. Antibodies that bind to the factor VIII light chain prevent the interaction of factor VIII with phospholipid. *J. Clin. Invest.* **83**, 1978–1984 (1989).

146. Honaker, Y. *et al.* Gene editing to induce FOXP3 expression in human CD4+ T cells leads to a stable regulatory phenotype and function. *Sci. Transl. Med.* **12**, 6422 (2020).

147. Miles, K. *et al.* A tolerogenic role for Toll-like receptor 9 is revealed by B-cell interaction with DNA complexes expressed on apoptotic cells. *Proc. Natl. Acad. Sci. U. S. A.* **109**, 887–892 (2012).

148. Iwata, Y. *et al.* Characterization of a rare IL-10–competent B-cell subset in humans that parallels mouse regulatory B10 cells. *Blood* **117**, 530–541 (2011).

149. Anderson, W. *et al.* PTPN22 R620W gene editing in T cells enhances low-avidity TCR responses. *Elife* **12**, (2023).

150. Chen, C. Y. *et al.* Treatment of Hemophilia A Using Factor VIII Messenger RNA Lipid Nanoparticles. *Mol. Ther. Nucleic Acids* **20**, 534–544 (2020).

151. Taylor, J. J. *et al.* Deletion and anergy of polyclonal B cells specific for ubiquitous membrane-bound self-antigen. *J. Exp. Med.* **209**, 2065 (2012).

152. Leal, J. M. *et al.* Innate cell microenvironments in lymph nodes shape the generation of T cell responses during type I inflammation. *Sci. Immunol.* **6**, (2021).

153. Silacci, P., Mottet, A., Steimle, V., Reith, W. & Mach, B. Developmental extinction of major histocompatibility complex class II gene expression in plasmocytes is mediated by silencing of the transactivator gene CIITA. *J. Exp. Med.* **180**, 1329–1336 (1994).

154. Piskurich, J. F. *et al.* BLIMP-I mediates extinction of major histocompatibility class II transactivator expression in plasma cells. *Nat. Immunol.* **1**, 526–532 (2000).

155. Viant, C. *et al.* Antibody Affinity Shapes the Choice between Memory and Germinal Center B Cell Fates. *Cell* **183**, 1298-1311.e11 (2020).

156. Cerqueira, C., Manfroi, B. & Fillatreau, S. IL-10-producing regulatory B cells and plasmocytes: Molecular mechanisms and disease relevance. *Semin. Immunol.* **44**, (2019).

157. Wallace, C. H. *et al.* B lymphocytes confer immune tolerance via cell surface GARP-TGF-β complex. *JCI Insight* **3**, (2018).

158. Xiao, S. *et al.* Checkpoint Receptor TIGIT Expressed on Tim-1+ B Cells Regulates Tissue Inflammation. *Cell Rep.* **32**, (2020).

159. Roco, J. A. *et al.* Class Switch Recombination Occurs Infrequently in GerminalCenters. *Immunity* **51**, 337 (2019).

160. Shehata, L. *et al.* Interleukin-4 downregulates transcription factor BCL6 to promote memory B cell selection in germinal centers. *Immunity* **57**, 843-858.e5 (2024).

161. Lighaam, L. C. *et al.* In vitro-induced human IL-10+ B cells do not show a subset-defining marker signature and plastically co-express IL-10 with pro-inflammatory cytokines. *Front. Immunol.* (2018) doi:10.3389/fimmu.2018.01913.

162. Cornaby, C. *et al.* B cell epitope spreading: Mechanisms and contribution to autoimmune diseases. *Immunol. Lett.* **163**, 56–68 (2015).